Imperial College London

Various facets of phases in gravitational wave physics

Aoibheann Margalit

Supervisors: Carlo Contaldi, Claudia de Rham

Thesis presented for the degree of Doctor of Philosophy

Department of Physics, Imperial College London, United Kingdom

September 2023

Abstract

This thesis contains two main results related to low-frequency gravitational waves. The first is a prescription for causality within low energy effective field theories (EFTs), specialised to gravitational theories. An EFT is a framework for parametrising macroscopic physics while remaining agnostic about the microscopic degrees of freedom. It turns out that the most generic naïvely local and covariant EFT action is not necessarily consistent with a physical UV theory, and thus imposing the causal propagation of waves can place non-trivial constraints on the EFT. Our criteria for "infrared causality" is that scattered waves do not experience a resolvable time advance relative to the geometry of the background. We apply this condition to the Gauss–Bonnet operator on black hole and pp-wave spacetimes and show that, within the EFT's regime of validity, causality is respected.

The second result relates to gravitational wave backgrounds (GWBs) within the standard cosmological model. We show that scalar perturbations to the background metric ruin any phase coherence in the GWB which may have been present at emission. The main consequence is that phase-coherent mapping methods have no foreseeable application to GWBs.

Acknowledgements

I would like to thank Claudia de Rham, who picked me up, dusted me off and set me back on track many times over the course of my PhD. Thank you for sharing your wisdom, for your support, your kindness and your bottomless patience. Thanks also to Andrew Tolley for imparting on me an appreciation for a good WKB approximation, amongst countless other insights. Thanks to Carlo Contaldi for kick-starting my PhD and for his support throughout. I would also like to express my deepest gratitude to Dan Waldram, who is a champion for student wellbeing, and who has done a great deal of good for mine. Of course, I couldn't conclude without cheers to Calvin Chen for consistently checking commas and constantly caring. Thanks to all my friends in the theory group, especially Victor and Archie, for the good times and for helping me through the bad ones. And, finally,

for Asad, I write
a haiku (my shortest yet),
just to say: thank you.

For everything.

Copyright Declaration

Declaration of Originality

I confirm that this work is my own, and that contributions from others have been appropriately referenced. A portion of the material in this thesis has appeared in the publications listed below, but this document as a whole has not been submitted for publication or for degree assessment elsewhere.

List of Publications

Chapters 2 – 4 are based on the following publications:

[1] C. Y. R. Chen, C. de Rham, **A. Margalit** and A. J. Tolley, *A cautionary case of casual causality*, JHEP **03** (2022) 025, [2112.05031].

[2] C. Y. R. Chen, C. de Rham, **A. Margalit** and A. J. Tolley, *Surfin' pp-waves with Good Vibrations: Causality in the presence of stacked shockwaves*, [2309.04534].

Chapter 5 is based on the following publication:

[3] **A. Margalit**, C. R. Contaldi and M. Pieroni, *Phase decoherence of gravitational wave backgrounds*, Phys. Rev. D **102** (2020) 083506, [2004.01727].

Contents

Chapter 1

Introduction

In this thesis we explore the information contained in the phase (specifically, the phase *shift*) of gravitational waves (GWs). GWs are perturbations to the metric of spacetime, postulated by Einstein in 1916 on formulating his theory of General Relativity (GR) [4], and directly detected by LIGO a century later [5]. The dynamics of GWs is determined by (1) the fundamental theory used to describe gravity and (2) the background spacetime on which they propagate. In chapters 2 – 4, we will show how changes to the phase of a GW in a scattering thought experiment are related to the causal properties of the underlying theory, while in chapter 5 we will see how the cosmological spacetime ruins the phase coherence of GWs with the same primordial origin.

1.1 Causality in the effective field theory of gravity

Despite the many successes of GR, big questions remain which it cannot answer, including the origin of the universe, the existence of black hole singularities and the nature of "dark" matter/energy which only interact gravitationally. The inability of GR to address these issues suggests that our understanding of gravity is incomplete. There are numerous proposals for fundamental theories of physics — such as string theory, loop quantum gravity or causal set theory — which seek to resolve such problems by postulating a specific microscopic origin for the physics at play. On large enough scales, however, any new theory of gravity must approximate GR, which is itself an experimentally watertight description of (say) solar system physics. The large-scale or low-energy *effective* description of a high-energy theory is obtained in practice by the process of "integrating out" the microscopic degrees of freedom. Their presence is then felt only through effective couplings between the macroscopic degrees of freedom which remain. In the

case of gravity, the macroscopic degrees of freedom come in the form of a metric tensor, and the effective interactions manifest as higher-order curvature operators. These quantum corrections to the classical field theory of GR are generically parametrised by the so-called effective field theory (EFT) of gravity [6–9].

The EFT of gravity is a framework for studying quantum gravity without committing to any one particular fundamental high-energy (UV) theory. The difficulty with quantising GR directly is that it is non-renormalisable — indeed, the list of EFT operators coincides with the infinite list of counter-terms which would appear when attempting to renormalise GR. The Wilson coefficients in the EFT expansion, however, are kept arbitrary to remain agnostic about their microscopic origins. The infinite number of operators may seem like a disaster for the predictability of the EFT, but at sufficiently low energies only the first few terms are ever relevant. The definition of "sufficiently low energies" is context dependent, and will be returned to many times over the course of this thesis.

This effective description of quantum gravity is not dissimilar to the effective description of Beyond Standard Model (BSM) particle physics. The Standard Model EFT (SMEFT) parametrises the interactions of unknown massive particles — heavy enough to be beyond the reach of the Large Hadron Collider (LHC) — by the set of all non-renormalisable operators built from the known SM fields [10–12]. The strength of these higher-dimension couplings is suppressed by at least the mass of the lightest unknown particle, in much the same way that the strength of the Weak Force is tempered by the heavy mass of the W-bosons. This means that BSM interactions, as parametrised by the SMEFT, are necessarily sub-dominant to the usual SM interactions at LHC energies. At these "low" energies, the SMEFT is a well-controlled series expansion which can be treated order-by-order, starting with dimension-6 operators, then dimension-8, and so on. In this way, the SMEFT captures all possible BSM interactions in one fell swoop at the price of arbitrary operator coefficients (couplings), to be fixed only by experiment (or a specific choice of BSM theory).

In the same vein, the EFT of gravity captures all possible theories of quantum gravity in its arbitrary parameters. Reasonable theories of quantum gravity could be expected to share certain physical properties: that evolution is unitary, causal, local and respects Lorentz symmetry on the very small scales. Perhaps surprisingly, it turns out that these universal principles are not necessarily manifest in the most generic EFT described by a superficially local, covariant Lagrangian. It was shown in [13] that seemingly sensible EFTs can be non-

local or acausal in certain regions of their parameter space (for the "wrong sign" choice of operators). Within that region of parameters, the EFT cannot correspond to a consistent UV theory. By weeding out the unphysical EFTs, an apparently infinite parameter space could potentially be reduced significantly [14, 15]. Understanding the space of possible physical EFTs has implications for the experimental search for deviations from GR (or the SM). On the one hand, this theoretical knowledge of the physical parameter space can be used as input for its prior probability distribution, thus impacting the reported outcome of the data analysis. On the other hand, a firm experimental measurement of an EFT coefficient in the "bad" parameter space would indicate a flaw in our assumptions about the UV physics.

One approach in this direction is known as the positivity bound programme [15–29]. The idea is to use analyticity of the UV S-matrix, in particular the positivity of certain amplitudes, to constrain the parameters in the infrared (IR). This approach has already helped constrain many of the numerous SMEFT couplings, e.g. [30]. A related, but distinct, approach is to directly require the causal propagation of fluctuations in the IR theory [1, 2, 31–39]. This is the approach we take in this thesis. Defining precisely what we mean by causality within a gravitational EFT will occupy much of our time.

Intuitively, causality is the requirement that cause comes definitively before effect. In special relativity, causality is the requirement that information cannot be transmitted outside the lightcone, or, said otherwise, that there is no superluminal signalling. Superluminal signal propagation could reverse the temporal order of cause and effect for observers in different reference frames, thus violating our intuitive notion of causality. There has been some historical confusion, however, over what exactly constitutes a signal, and its speed. While one can associate both a phase velocity ω/k and a group velocity $\partial\omega(k)/\partial k$ to a wave of frequency ω and wavenumber k, neither necessarily indicate when the wavepacket will "arrive". Indeed, superluminal *group* velocities have been experimentally observed, and do not in any way violate causality [40]. The resolution according to [41, 42] is that a signal, as opposed to any old wave, has "an element of surprise" represented by a wave *front* before which the medium is completely at rest. Only the arrival of the wave front indicates the arrival of the signal and so it is this speed which feeds into the definition of causality. The existence of a wave front requires a discontinuity, or an infinite frequency component to the signal, thus the front velocity corresponds to the phase velocity in the infinite frequency limit. In this sense, causality is a concept intrinsically tied to the UV theory, of which we are presently ignorant.

The EFT, being valid only below a certain energy, does not provide access to the high-energy limit required to define a front velocity. Moreover, in gravitational theories, speed itself is a local quantity and subject to field redefinitions. A locally superluminal low-energy sound speed at some point, in some coordinates, may not be an issue if its effects are not observable. A truer indication of causality violation at low energies is the creation of a closed time-like curve, which requires prolonged superluminality over an extended region of spacetime. For this reason, instead of a speed, we use the scattering time delay as our diagnostic for causality. The scattering time delay is defined on asymptotically flat spacetimes directly from the phase shift of a wave which has traversed the spacetime. The phase shift, in turn, is simply the eigenvalue of the S-matrix for the scattering process[1], and is therefore invariant under field redefinitions. The time delay thus serves as a reliable low-energy indicator of signal arrival.

The question now is: how is "(super)luminality" measured by the time delay? To answer this question we make two assumptions about UV physics. The first is that, in a consistent, causal UV theory, the UV modes propagate luminally. Even so, it's possible for the IR modes described by the EFT to diverge from luminality. As an example, consider Euler–Heisenberg theory, the leading low-energy EFT of quantum electrodynamics (QED) with the electron integrated out to one-loop. In 1980 Drummond and Hathrell demonstrated that, within this EFT, the photon may propagate slightly outside the lightcone of the background metric on certain curved spacetimes [43]. Of course, the photon of QED propagates luminally and this apparent change to its speed is only an artefact of the EFT truncation at finite order. We will similarly see that GWs may deviate from luminality in the EFT of gravity.

The second assumption is that gravity experienced by the UV modes is described by GR, the "zeroth" order in the EFT of gravity, just as electromagnetism experienced by UV photons is described by Maxwell's Lagrangian. In other words, the metric experienced by UV modes is the metric of GR, and their time delay is the time delay of GR. Together these two assumptions set a reference scale: luminality means a time delay equal to the time delay of GR. Violating causality is equivalent to a time delay smaller than the time delay of GR.

Does Euler–Heisenberg theory violate causality, even though QED patently doesn't? The answer is, of course, no. The tension between apparent superluminality of low-energy modes and causality of QED was examined in a series of papers by Hollowood and Shore [44–51], who showed precisely how luminality is restored in the high-frequency limit (the front velocity) when

[1]The asymptotic states for a scattering process can only be well-defined if the spacetime is asymptotically flat.

the microscopic degrees of freedom (the electron in this case) are brought back to life. More to the point, the issue was resolved entirely within the context of the EFT in [36, 52] by showing that *the apparent time advance was unresolvable within the regime of validity of the EFT*. The premise we adopt in this work is that a consistent EFT, which corresponds to a causal UV theory, will propagate low-energy modes which are either strictly slower, or unresolvably faster, than the UV modes.

1.2 Phase decoherence of the gravitational wave background

The primordial stochastic gravitational wave background (SGWB) is a conjectured all-sky GW signal originating in the early universe, very much analogous to the Cosmic Microwave Background (CMB) of photons. Such a SGWB could have been generated by any number of cataclysmic events, such as a first order electroweak phase transition, which might have occurred during the inflationary epoch [53]. Recently, the North American Nanohertz Observatory for Gravitational Waves (NANOGrav) announced evidence for the detection of such a background in their 15 year data set, and placed constraints on possible origins [54, 55]. The Laser Interferometer Space Antenna (LISA), which is planned for launch in the 2030s, may also reach the sensitivity required for the detection of a background at much higher frequencies [56]. Such observations offer invaluable insight into early universe cosmology and particle physics.

The SGWB generated by an inflationary mechanism is likely to be phase-coherent at source. In other words, there would be non-trivial angular correlations in the phase of waves from different points in the sky, just like the angular correlations in the temperature anisotropy of the CMB. Since GW observatories such as LIGO and LISA can measure the phase of the passing signal, there is the potential to map the phase of any background detected. Unfortunately, we argue in [3] that a SGWB would lose all phase coherence between emission and detection, and there is thus no foreseeable application for phase-coherent mapping of the SGWB. When it comes to background signals, the most promising avenue is incoherent mapping methods.

This phase *decoherence* is caused by scalar perturbations in the cosmological metric. By repeated scattering processes, they induce a large and effectively random phase shift along each line-of-sight in the sky. The result is that all angular correlations are wiped out for frequencies larger than 10^{-12} Hz with the source at any reasonable distance from Earth.

GWs are one of the most promising avenues for extending our understanding beyond GR and the standard cosmological model. With so many experiments coming on-line now or in the near future, it is important to understand where the relevant information could be hiding in the data. In the first part of this thesis, we argue from a theoretical standpoint that important constraints can emerge from demanding the causality of effective operators. These constraints can be used to formulate the prior probability distribution for the statistical analysis of experimental data. In the second part of this thesis, we argue that any information there once was in the phase of the SGWB will be unfortunately lost to the cosmos by the time we measure it.

1.3 Thesis overview

The next three chapters are based on the work in [1] and [2]. In chapter 2 we introduce EFT with a scalar field example. We see that integrating out microscopic degrees of freedom can modify the propagation speed of the surviving degrees of freedom. We explore the implications for causality and demonstrate how enforcing causality can constrain a-priori arbitrary coefficients in an EFT. In chapter 3 we introduce the EFT of gravity and two vacuum spacetime solutions: the Schwarzschild-like black hole and the pp-wave. We calculate the equations of motion for gravitational waves propagating on these spacetimes within the EFT. We discuss the regime of validity of a gravitational EFT and show how it manifests as bounds on the parameter space of the metric and its fluctuations. In chapter 4 we return to the notion of causality and how it applies to theories of dynamical gravity. We argue in favour of the "infrared" definition of causality over the "asymptotic" definition, using again a scalar theory as an example. We then apply this definition, in tandem with the EFT's regime of validity, to the black hole and pp-wave spacetimes in turn.

Chapter 5 is based on the work in [3]. In this chapter, we introduce the notion of a SGWB. We argue that a SGWB generated in the very early universe could be phase-coherent at emission, but that scalar perturbations in the metric of the universe will completely randomise the phase by the time of observation. We quantify this effect with an angular power spectrum for the phase shift and provide an example of the decoherence process.

1.4 Conventions

The list of conventions below is for ease of reference. There are reminders of the relevant conventions throughout the text when they first appear.

Throughout this thesis we work in units where $\hbar = c = 1$. For the first three chapters 2 – 4 we work in general D-spacetime dimensions, and for chapter 5 we work specifically in $D = 4$-dimensions.

Full spacetime: Metrics on the full spacetime are denoted by the letter g and come in the mostly-plus signature $(-, +, \dots, +)$. Components of tensors on the full spacetime are indexed with letters from the Greek alphabet $\{\alpha, \beta, \dots\}$. The covariant derivative on the full spacetime is denoted by ∇_α and the associated Laplace–Beltrami operator is $\Box = g^{\alpha\beta}\nabla_\alpha\nabla_\beta$.

Euclidean subspace: The pp-wave solution of chapters 2 – 4 has a Euclidean subspace of dimension $d = D - 2$. For the most part, we will use the usual Cartesian coordinates $\mathbf{x}$ on this subspace. Components of tensors on this subspace are indexed with letters from the middle of the Latin alphabet $\{i, j, \dots\}$, and the metric is simply the Kronecker delta δ_{ij}. The covariant derivative is just the usual partial derivative $\partial_i = \partial/\partial x^i$, the Laplacian is $\nabla_d^2 = \delta^{ij}\partial_i\partial_j$ and no distinction is made between upper and lower indices in these coordinates.

Spherical subspace: Both the black hole and the point-like pp-wave solution will have spherically symmetric subspaces. Components of tensors on the sphere are indexed with lower-case letters from the start of the Latin alphabet $\{a, b, \dots\}$. The spherical polar coordinates are written as θ^a with metric γ_{ab}. On the n-sphere, the line element is written as $\mathrm{d}\Omega_n^2 = \gamma_{ab}\mathrm{d}\theta^a\mathrm{d}\theta^b$. (For the black hole solution $n = D - 2$, whereas for the pp-wave $n = D - 3 = d - 1$.) The covariant derivative on the sphere is denoted by $\hat{D}_a$ and the associated Laplace–Beltrami operator is $\hat{\Delta}_n = \gamma^{ab}\hat{D}_a\hat{D}_b$. In spherical coordinates, the aforementioned Euclidean metric is

$$\delta_{ij}\mathrm{d}x^i\mathrm{d}x^j = \mathrm{d}r^2 + r^2\mathrm{d}\Omega_n^2, \tag{1.1}$$

with $r^2 = \mathbf{x}^2$.

Other miscellany: The black hole solution has a 2-dimensional orbit space with indices on this orbit space (where rarely needed) denoted by upper-case letters from the start of the Latin alphabet $\{A, B, \dots\}$. On the pp-wave background, it will be useful to have a unique symbol for the Laplace–Beltrami operator as it would act on a scalar: $\tilde{\Box}$. A "prime" always indicates a derivative with respect to the sole argument of the function it acts on.

Chapter 2

Toy example: scalar EFT

Consider a universe with two occupants: omnipotent being (OB) and low energy observer (LEO). OB has perfect knowledge of the particle content of their universe (up to, say, the Planck mass $M_{\rm Pl}$) and can predict the outcome of any experiment with arbitrary precision. LEO, on the other hand, sees only one (real) light scalar field ϕ. As far as LEO is concerned, he is made up of a condensate of this scalar field, as is his planet, his planet's star and everything else around them. LEO builds a particle accelerator and collides the smallest units of the scalar condensate he can isolate. However, in all the experiments LEO is capable of, the collisions only result in more scalars. Sometimes two become three, sometimes four, sometimes even more, albeit at a lower rate. LEO is forced to conclude that the universe is effectively described by the following schematic action, called the scalar EFT,

$$S_{\rm EFT} = \int \mathrm{d}^D x \left[-\frac{1}{2} (\partial\phi)^2 + \Lambda^D \sum_{m\geq 0, n\geq 2} c_{mn} \left(\frac{\partial}{\Lambda}\right)^m \left(\frac{\phi}{\Lambda^{(D-2)/2}}\right)^n \right], \tag{2.1}$$

where Λ is some "cut-off" energy scale just beyond his reach and the $\{c_{mn}\}$ are called "Wilson coefficients".

Unfortunately, just the relevant operators alone are not enough to explain the results of all LEO's experiments. This suggests there are some microscopic degrees of freedom at play beyond just the single scalar LEO observes. Of course, OB knows all about these microscopic degrees of freedom but she likes to keep that information to herself. Meanwhile, LEO is faced with the daunting prospect of performing an infinite number of experiments to measure an infinite number of Wilson coefficients $\{c_{mn}\}$. By observing symmetries in his universe (e.g. scalar shift symmetry, $\mathbb{Z}_2$-symmetry, etc.) LEO can set to zero any coefficients of operators which don't

comply with those symmetries. Still, it may seem like such a Wilsonian effective action lacks any predictive power. However, LEO's saving grace is that as long as he remains at low energies, the higher-order terms in the series must be suppressed by the ratio of the field energy (powers of ϕ and its derivatives) to the cut-off scale. That is, only the first few terms in this series are usually important.

On the other hand, OB could simply calculate the value of each c_{mn} to arbitrary precision given her knowledge of the UV theory which describes the microscopic degrees of freedom, and which is inaccessible to LEO. For example, consider that up to the energy scale $\Lambda_* \gg \Lambda$, there is only one additional (real) scalar field H of mass M (where $\Lambda \ll M \ll \Lambda_*$) with the following coupling[1] to the massless ϕ,

$$S_* = \int \mathrm{d}^D x \left[-\frac{1}{2} (\partial\phi)^2 - \frac{1}{2} (\partial H)^2 - \frac{1}{2} M^2 H^2 + \frac{\lambda}{\Lambda_*^{(D-2)/2}} H (\partial\phi)^2 \right]. \tag{2.2}$$

To understand the world as LEO sees it, and make predictions for the outcome of his experiments, OB would integrate out the heavy field H at tree-level to obtain just an action for ϕ,

$$S_* \xrightarrow{\int \mathcal{D}H} \int \mathrm{d}^D x \left[-\frac{1}{2} (\partial\phi)^2 + \frac{1}{2} \frac{\lambda^2}{\Lambda_*^{D-2}} (\partial\phi)^2 \frac{1}{M^2 - \Box} (\partial\phi)^2 \right]. \tag{2.3}$$

To leading order in low energies, that is $k^2 \sim \Box \ll M^2$, this action reduces to the so-called Goldstone scalar (GS) action,

$$S_{\mathrm{GS}} = \int \mathrm{d}^D x \left[-\frac{1}{2} (\partial\phi)^2 + \frac{c_{\mathrm{GS}}}{\Lambda^D} (\partial\phi)^4 + \dots \right], \tag{2.4}$$

where

$$c_{\mathrm{GS}} = \frac{\lambda^2}{2}, \tag{2.5a}$$

$$\Lambda^D = M^2 \Lambda_*^{D-2}, \tag{2.5b}$$

as illustrated in the schematic Feynman diagrams of figure 2.1 and discussed, for example, in [57]. As well as the Goldstone term, (2.3) contains additional irrelevant operators which we are neglecting because they are suppressed by powers of k^2/M^2 compared to the Goldstone

[1] The action S_* in (2.2) is really itself still an effective action, valid up until the new, higher cut-off scale Λ_*. It represents a "partial" UV-completion, introducing some new microscopic degree of freedom, but not enough to make the action fully renormalisable.

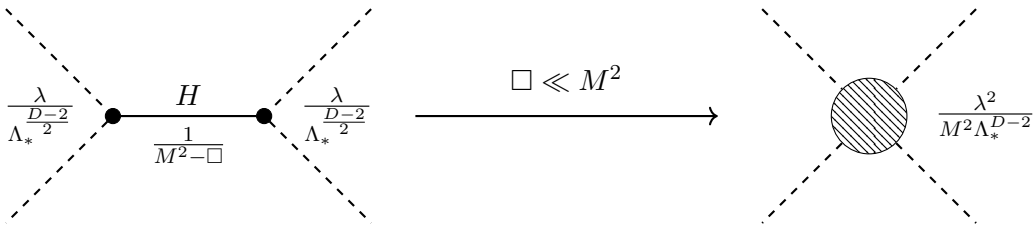

Figure 2.1: At energies much below the mass of the H-field, the tree-level interaction illustrated on the left is reduced to the effective contact interaction illustrated on the right. The dashed lines are instances of the light scalar field ϕ and the solid internal line in the left diagram represents the heavy field H.

operator. This is the type of mechanism which gives rise, in concrete terms, to the suppression of higher-order operators in LEO's effective action (2.1).

This example should make apparent that the values of the Wilson coefficients, which LEO tries to measure in the low-energy (or infrared/IR) regime, depend on high-energy (or ultraviolet/UV) details, which only OB knows. In this case, the coefficient of the $(\partial\phi)^4$-term is related to the coupling of ϕ to the heavy H. In particular, as long as that coupling is real-valued $\lambda \in \mathbb{R}$, OB's calculation shows that the corresponding Wilson coefficient is positive, $c_{\rm GS} > 0$.

From LEO's perspective, the action in (2.2) is just one example of a possible UV-completion of the low-energy Goldstone action (2.4). Generically, UV theories with a light scalar field in their spectrum will turn up a Goldstone-term in their low-energy effective description. While OB knows that the Wilson coefficient of the Goldstone operator $c_{\rm GS}$ takes the value (2.5a) in their universe, LEO in his ignorance must treat $c_{\rm GS}$ as arbitrary. However, it is possible for LEO to gain some information about the Wilson coefficients if he makes some assumptions about physics in the UV. By applying principles of causality, unitarity and S-matrix analyticity, LEO could, for example, deduce that there are no consistent UV-theories which would generate an IR action with $c_{\rm GS} < 0$, as shown in [13]. That is, all possible physical theories must have $c_{\rm GS} > 0$. The specific example of OB's universe discussed above is just one realisation of this general property of UV-theories. There is a whole host of so-called "positivity bounds" (for example, [16–29], amongst many others) which use physical assumptions about an UV S-matrix to bound coefficients in an IR Wilsonian action.

In this thesis, we use the principle of causality to try constrain the a-priori arbitrary coefficients of an EFT. The presence of effective operators in an action can modify the speed of wave propagation and, depending on the magnitude of the modification, lead to the possibility of

faster-than-light signalling. While diagnosing acausality is a relatively straightforward procedure for non-gravitational theories, there is additional nuance in theories with dynamical gravity where geometry plays a significant role in a wave's propagation. This will be discussed extensively in chapter 4. In this chapter, we use two scalar field examples to establish the basic machinery necessary to investigate causality. For the first example, we will reproduce the result $c_{\rm GS} > 0$ for the Goldstone scalar. For the second example, we will consider a different type of effective operator known as the quartic Galileon (QG) and show that its coefficient must be negative $c_{\rm QG} < 0$ to preserve causality. Said otherwise, for this chapter, we share LEO's perspective that the universe is described by a scalar field action like (2.1) and try to gain access to some of OB's knowledge about the Wilson coefficients contained therein.

2.1 The Goldstone scalar

Consider the Goldstone action (2.4) on Minkowski spacetime. This action represents the leading-order EFT for a field with shift symmetry $\phi \to \phi +$constant and $\mathbb{Z}_2$-symmetry $\phi \to -\phi$. Causality will be determined by the propagation of wave perturbations in this theory, so first we determine their equation of motion. In vacuum, the field equation for the Goldstone scalar is

$$\Box\phi - \frac{4c_{\rm GS}}{\Lambda^D}\left(\Box\phi\nabla_\alpha\phi\nabla^\alpha\phi + 2\nabla_\alpha\nabla_\beta\phi\nabla^\alpha\phi\nabla^\beta\phi\right) = 0, \tag{2.6}$$

where ∇_α is the covariant derivative and $\Box = \nabla_\alpha\nabla^\alpha$ is the d'Alembertian on Minkowski spacetime. We will assume that there is a background field sourced by a static point source at the origin. This choice is meant to emulate the spherical symmetry of the black hole background we will consider for gravitational theories in chapters 3 and 4. In spherical coordinates, we may solve (2.6) for the background field $\bar{\phi} = \bar{\phi}(r)$ perturbatively to $\mathcal{O}(\Lambda^{-D})$,

$$\bar{\phi} = \frac{\alpha}{r^{D-3}} + \frac{4(D-3)^3}{3D-7}\frac{c_{\rm GS}}{\Lambda^D}\frac{\alpha^3}{r^{3D-7}}, \tag{2.7}$$

where $r^2 = \mathbf{x}^2$ is the radial coordinate and α is a constant. Recall that we are considering the Goldstone action (2.4) as an effective theory, meaning it represents only the leading-order terms in an infinite series expansion (of e.g. the right hand side of (2.3) expanded in powers of k^2/M^2). As such, terms of higher order than Λ^{-D} are a) suppressed compared to those written and b) would contribute at the same order as terms we have implicitly neglected in the action (2.4). In

this EFT picture, we will only ever work up to $\mathcal{O}(\Lambda^{-D})$ as a matter of consistency. In fact, the requirement that the Goldstone term truly dominates in this expansion will define the "EFT regime of validity" in section 2.1.3.

For now, consider the dynamics of scalar fluctuations on this background $\phi = \bar{\phi} + \delta\phi$. Denoting by $\bar{\phi}_0 = \alpha/r^{D-3}$ the leading-order behaviour of the background field, the equation of motion for the fluctuations up to $\mathcal{O}(\Lambda^{-D})$ is

$$\Box\delta\phi - \frac{8c_{\rm GS}}{\Lambda^D}\left(\nabla_\alpha\nabla_\beta\delta\phi\nabla^\alpha\bar{\phi}_0\nabla^\beta\bar{\phi}_0 + 2\nabla_\alpha\nabla_\beta\bar{\phi}_0\nabla^\alpha\bar{\phi}_0\nabla^\beta\delta\phi\right) = 0, \tag{2.8}$$

where we have already made use of the fact that $\Box\phi \approx 0$ to remove such terms perturbatively. We make a wave ansatz for $\delta\phi$ and decompose it in a basis of spherical harmonics

$$\delta\phi(t, r, \Omega_{D-2}) = e^{-i\omega t}\sum_{l=0}^{\infty}\delta\phi_l(r)Y_l(\Omega_{D-2}) \tag{2.9}$$

where ω is its frequency and Y_l are scalar spherical harmonics, eigenfunctions of the Laplace–Beltrami operator $\hat{\Delta}_{D-2}$ on the $(D-2)$-sphere with discrete eigenvalues,

$$\left(\hat{\Delta}_{D-2} + \kappa_S^2\right)Y_l = 0, \tag{2.10a}$$

$$\kappa_S^2 = l(l+D-3), \quad l = 0, 1, 2, \ldots. \tag{2.10b}$$

Due to the spherical symmetry of the background, each partial wave $\delta\phi_l$ will evolve independently. Defining

$$\chi_l = r^{\frac{D-2}{2}}\left[1 - \frac{6c_{\rm GS}}{\Lambda^D}\frac{\alpha^2}{r^{2(D-2)}}\right]\delta\phi_l \tag{2.11}$$

we obtain a wave equation of the form

$$\frac{\mathrm{d}^2\chi_l}{\mathrm{d}r^2} + W_{\rm GS}(r)\chi_l(r) = 0, \tag{2.12}$$

where

$$\begin{aligned} W_{\rm GS}(r) = \omega^2\left(1 + \frac{8c_{\rm GS}}{\Lambda^D}\frac{\alpha^2}{r^{2(D-2)}}\right) - \frac{\kappa_S^2}{r^2}\left(1 + \frac{8c_{\rm GS}}{\Lambda^D}\frac{\alpha^2}{r^{2(D-2)}}\right) \\ + \frac{1-(D-3)^2}{4}\frac{1}{r^2} + 12(D-1)(D-2)\frac{c_{\rm GS}}{\Lambda^D}\frac{\alpha^2}{r^{2(D-1)}} \end{aligned} \tag{2.13}$$

is related to the effective potential for a wave of frequency ω, as in (2.17).

2.1.1 First look at causality

From the wave equation (2.12) we can identify the angular and radial speeds of the Goldstone scalar,

$$v_\Omega^2 = 1, \tag{2.14a}$$

$$v_r^2 = 1 - \frac{8c_{\rm GS}}{\Lambda^D}\frac{\alpha^2}{r^{2(D-2)}}. \tag{2.14b}$$

These represent the low-energy sound speed of scalar perturbations on the background $\bar{\phi}$ in the EFT with action (2.4). Note that the speed is different from the speed of ϕ-perturbations in the partial UV-completion (2.2) of the same theory. It was explained in [57] how the sound speed may return to luminality ($v = 1$) in the UV even it differs from luminality ($v \neq 1$) in the IR. In truth, expressions like those in (2.14) are simply leading-order in our low-energy expansion. In this case, the leading-order sound speed just happens to be constant-in-momentum for the low-energy states described by the EFT. In the context of the two-field partial UV-completion (2.2), "low-energy" means $k \ll M$. For that example, corrections to the dispersion relation appear at higher-order in k^2/M^2, and return the speed to luminality as $k \to M$.

We can see from (2.14) that if $c_{\rm GS} < 0$, the low-energy radial speed is superluminal — that is, greater than the speed of light or other massless particles. The possibility of faster-than-light signalling seems to align with our expectation from [13] that $c_{\rm GS} < 0$ is a bad Wilson coefficient. In field theory, however, causality is determined by the front velocity (and not phase nor group velocities) of the propagating waves. The front velocity is the same as the phase velocity of the high-frequency (beyond the EFT regime of validity) modes. In other words, local superluminality at low energies by itself does not necessarily indicate a bona fide violation of causality. Unfortunately, without OB's access to the UV-theory, LEO does not know how the sound speed behaves at higher energies. He must use the information available to him at low energies to diagnose possible acausality in his proposed theory.

From LEO's perspective, what would be in direct tension with causality (even at low energies) is the potential for closed time-like curves created by prolonged superluminality over some trajectory. To account for the cumulative effects of superluminality, we instead calculate the scattering time delay by integrating over the full trajectory of a scattering wave. The time delay ΔT is the difference in time taken to travel between asymptotic infinities on a background (in this case, the background Goldstone field $\bar{\phi}$ sourced by a point at the origin) compared to in

a complete vacuum (that is, $\alpha = 0$). As we can see from (2.14), the radial speed of Goldstone fluctuations is luminal in vacuum. For that reason, any $\Delta T < 0$ is called a time *advance* and corresponds to superluminality-on-average, or net propagation outside the lightcone, over the full trajectory.

There is a second reason that bare local superluminality in the IR may not indicate a violation of causality. Goldstone fluctuations represent quantum particles whose properties (including speed) can only be resolved within the limitations set by Heisenberg's uncertainty principle. In particular, this means the arrival time of a wave bears a fundamental uncertainty which is inversely proportional to its energy. Working in units where $\hbar = 1$, we say that a time delay/advance for a wave of frequency ω can only be resolved if

$$\omega|\Delta T| \geq 1. \tag{2.15}$$

If an apparent time advance cannot be resolved under this optical resolution scale, it cannot truly be considered a violation of causality. In that sense, a small amount of superluminality is not a problem for causality as long as it cannot lead to observable effects. As we will see in section 2.1.3, there is a chance for the magnitude of ΔT to be bounded within the EFT's regime of validity. More on this later.

With this reasoning in mind, our condition for causality has two parts. First, if the time delay is strictly positive $\Delta T > 0$, then the wave propagation is causal. Second, if the time delay is negative $\Delta T < 0$ (i.e. a time advance), but not resolvable in magnitude, then we still say the wave propagation is causal, or at least that there is no resolvable violation of causality. Summed up in one statement, causality means

$$\Delta T \gtrsim -\omega^{-1}. \tag{2.16}$$

We will sometimes refer this type of bound as "weak positivity" of the time delay. The implicit assumption in this definition is that high-energy modes travel luminally (as if in vacuum), and thereby set the front velocity to luminality. A resolvable time advance corresponds to travelling faster than this front velocity and, in doing so, violating the field-theory notion of causality.

2.1.2 Scattering time delay

To calculate the time delay, consider an experiment where a wavepacket of frequency ω and partial wave number[2] l scatters off an effective potential V_{eff} defined via the wave equation (2.12) with

$$W_{\text{GS}}(r) = \omega^2 - V_{\text{eff}}(r). \tag{2.17}$$

In vacuum ($\alpha = 0$), the effective potential is an artefact of the spherical-coordinate choice and given by

$$V_{\text{eff}} = \frac{\omega^2 b^2}{r^2} - \frac{1}{4r^2}, \tag{2.18}$$

where we have defined the classical impact parameter as

$$b = \frac{1}{\omega}\left(l + \frac{D-3}{2}\right). \tag{2.19}$$

For large-l, the impact parameter is a good approximation to the distance of closest approach to the origin[3]. In the presence of a source, the effective potential for the Goldstone particle is given by the definition in (2.17) with the expression for W_{GS} in (2.13). The situation is illustrated in figure 2.2.

Deviation from the vacuum trajectory gives rise to an Eisenbud–Wigner time delay [59–62]. For a fixed partial wave number l, the time delay is related to the scattering phase shift δ_l as

$$\Delta T = 2\frac{\partial \delta_l}{\partial \omega}. \tag{2.20}$$

The phase shift, in turn, can be estimated by matching a Wentzel–Kramers–Brillouin (WKB) ansatz for the field solution $\chi_l(r)$ onto the known asymptotic form for a field scattered in a central potential. The full derivation of an expression for the asymptotic phase shift is provided in appendix A, with just the main steps outlined below.

The wave equation (2.12) has a turning point where $W_{\text{GS}}(r_t) = 0$, a point where the kinetic and potential energy of the system are balanced. Away from this point, the WKB approximation

[2] Recall l is an integer labelling the eigenspectrum of the Laplace–Beltrami operator on the sphere with eigenvalues $-\kappa_S^2 = -l(l + D - 3)$.

[3] There is another choice of coordinate, the Langer coordinate $r = e^{\rho}$, which is better suited to analysis of the scattering problem in a central potential [58]. With the appropriate Langer field redefinition, b would be exactly the point of closest approach. However, in the eikonal (large-l) limit the difference is immaterial and hence neglected.

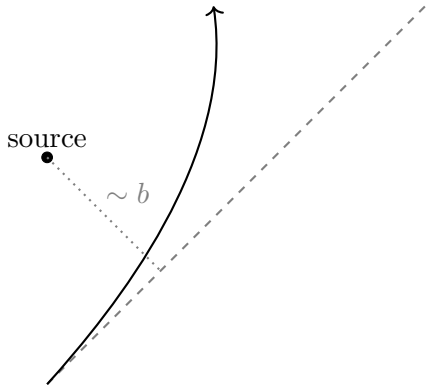

Figure 2.2: The scattering of a χ-particle due to an effective potential V_{eff} set up by a source at the origin. The dashed line represents the particle's would-be trajectory in vacuum. The distance of closest approach to the origin is called the impact parameter b. The solid line shows how the particle deviates from this trajectory in a non-zero potential.

can be used to solve for $\chi_l(r)$. Below the turning point, the potential energy exceeds the kinetic so this region is classically forbidden and we must choose the decaying branch of the WKB solution. Using the WKB connection formulae, we then find that the solution above the turning point is

$$\chi_l(r > r_t) \approx \frac{2\bar{\chi}}{W_{\text{GS}}^{\frac{1}{4}}} \sin\left[\int_{r_t}^{r} \mathrm{d}\tilde{r}\sqrt{W_{\text{GS}}(\tilde{r})} + \frac{\pi}{4}\right], \tag{2.21}$$

where $\bar{\chi}$ is a constant amplitude. Now, the known asymptotic form of a wave propagating in a central potential is

$$\chi_l \overset{r\to\infty}{\sim} \left(e^{2i\delta_l}e^{i\omega r} + e^{i\pi l}e^{i\pi(D-2)/2}e^{-i\omega r}\right), \tag{2.22}$$

where δ_l is the l-dependent asymptotic phase shift. By matching the WKB solution onto this asymptotic form, we obtain a formula for the scattering phase shift:

$$\delta_l(\omega) = \int_{r_t}^{\infty}\left(\sqrt{W_{\text{GS}}(r)} - \omega\right)\mathrm{d}r - \omega r_t + \frac{\pi}{2}\left(l + \frac{D-3}{2}\right). \tag{2.23}$$

The various regions and matching points relevant to the WKB solution are illustrated in figure 2.3.

In the large-l eikonal limit, the expression for the phase shift can be simplified further by

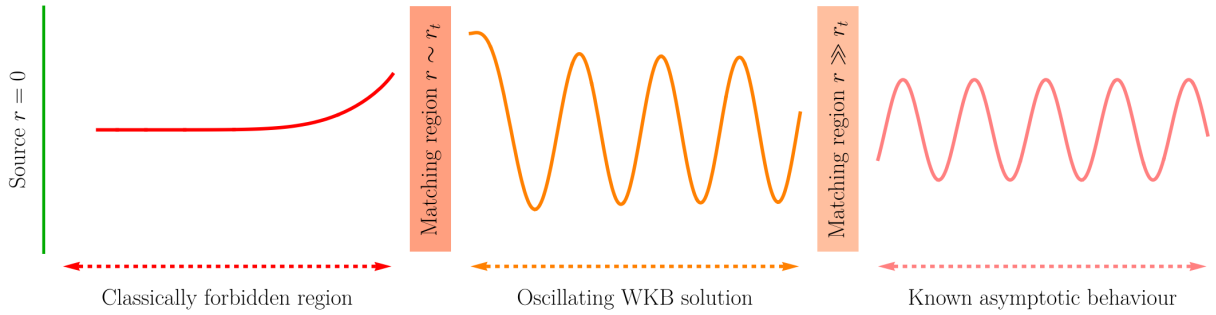

Figure 2.3: WKB solution to (2.12) for χ-field. The region below the turning point ($r < r_t$) is classically forbidden, so the field must decay exponentially. The behaviour above the turning point ($r > r_t$) is determined by the WKB connection formula. Lastly, the asymptotic behaviour ($r \gg r_t$) is known independently and matching it onto the WKB solution allows us to the determine the asymptotic phase shift.

splitting the function $W_{\rm GS}$ in two parts:

$$W_{\rm GS} = \underbrace{\omega^2\left(1-\frac{b^2}{r^2}\right)}_{W_{\rm coord}} + \underbrace{\frac{8c_{\rm GS}}{\Lambda^D}\frac{\alpha^2}{r^{2(D-2)}}\omega^2\left(1-\frac{b^2}{r^2}\right)}_{W_{\rm EFT}} + \mathcal{O}(l^0), \tag{2.24}$$

where terms which have been neglected are lower order in l. The $W_{\rm coord}$-term would be present even in completely vanilla, flat, vacuum spacetime, without any scalar background as discussed for the effective potential above. The label "coord" indicates that it arises due to the spherical coordinate choice. The second part $W_{\rm EFT}$ is due to the effective Goldstone operator in the action (2.4). By treating $W_{\rm EFT}$ as a perturbation, we show in appendix A.2 that the phase shift reduces to simply

$$\begin{aligned}\delta_l &= \frac{1}{2\omega}\int_b^\infty {\rm d}r \frac{W_{\rm EFT}(r)}{\sqrt{1-b^2/r^2}} \\ &= \frac{\sqrt{\pi}\Gamma\left(D-\frac{5}{2}\right)}{\Gamma(D-1)}\frac{c_{\rm GS}\alpha^2}{\Lambda^D}\frac{\omega}{b^{2D-5}}.\end{aligned} \tag{2.25}$$

Using the relationship between b and l (2.19) to hold l fixed, we find the time delay of a scattering Goldstone particle on a non-trivial background field $\bar{\phi}$ is

$$\Delta T_{\rm GS} = \frac{4\sqrt{\pi}\Gamma\left(D-\frac{5}{2}\right)}{\Gamma(D-1)}\frac{c_{\rm GS}\alpha^2}{\Lambda^D b^{2D-5}}. \tag{2.26}$$

The sign of $\Delta T_{\rm GS}$ is negative if $c_{\rm GS}$ is negative. In other words, for an EFT with $c_{\rm GS} < 0$, a

Goldstone particle scattering off a central potential experiences a time advance. This is consistent with our earlier result that the local sound speed of the Goldstone particle is superluminal if $c_{\rm GS}$ is negative. However, we cannot yet in good conscience conclude that the Goldstone EFT is acausal for $c_{\rm GS} < 0$. It remains to be seen whether this apparent violation of causality is, in fact, resolvable for states within the EFT.

2.1.3 Regime of validity and resolvability

Recall, the apparent time advance uncovered above can only be resolved if its magnitude exceeds the optical resolution scale: $|\Delta T_{\rm GS}| > \omega^{-1}$. A-priori it may seem like the quantity $\omega|\Delta T_{\rm GS}|$ could be made as large as we like either by increasing the background field strength (as measured by α), increasing the wave frequency ω or decreasing the impact parameter b. However, any of these processes would increase the total energy of the system and the EFT action (2.4) is only valid at sufficiently low energies. At higher and higher energies, more and more terms in the generic series expansion (2.1) could enter in the description of scalar physics. The parameter regime in which this expansion is under control, thereby ensuring that the Goldstone term is the single most important term in the expansion, is called the EFT's *regime of validity*. It is incumbent on us to check whether a resolvable time advance can be generated while remaining within that regime of validity. Outside of the regime of validity, any supposed violation of causality should not be taken seriously anyway since the Goldstone EFT would become a bad description of physics.

In practical terms, the regime of validity for a generic scalar EFT is determined by bounding the magnitude of effective operators in the EFT expansion. Schematically, it means

$$\left(\frac{\partial}{\Lambda}\right)^m \left(\frac{\phi}{\Lambda^{(D-2)/2}}\right)^n \ll 1. \tag{2.27}$$

Here, the ϕ-field comprises of both the background and its fluctuations: $\phi = \bar{\phi} + \delta\phi$. Taking the $m \to \infty$ limit of this expression returns the condition that $\partial \ll \Lambda$. In terms of true Lorentz scalar quantities, we understand such a bound to mean

$$\Box \cdot \text{scalar} \ll \Lambda^2 \cdot \text{scalar}. \tag{2.28}$$

There are three possibilities for the stand-in "scalar". Firstly, when "scalar" is a background quantity (such as $\bar{\phi}^2$), this corresponds to a distance resolution scale inversely proportional to the EFT cut-off. In spherical coordinates that means $r \gg \Lambda^{-1}$. Applying this to the impact

parameter, we see why it cannot be made arbitrarily small: $b \gg \Lambda^{-1}$. Secondly, when "scalar" is a fluctuation $\delta\phi$, we don't obtain any new useful bound because $\Box\delta\phi \approx 0$ up to Λ suppressed corrections. Thirdly, when "scalar" is a mix of background and fluctuation (e.g. the product $\bar{\phi}\delta\phi$), we obtain a bound of the form $k \cdot \partial\bar{\phi} \ll \Lambda^2\bar{\phi}$ where $(k^\alpha) = (\omega, \mathbf{k})$ is the momentum vector for the perturbations. In practice, this represents a bound on the frequency: $\omega \ll \Lambda^2 b$.

Similarly, we should take the $n \to \infty$ limit. However, since our EFT should have shift symmetry, we can't take this limit independently of $m \to \infty$ because only the shift-symmetric terms are non-zero. We should first set $m = n$,

$$(\partial\phi)^n \ll \Lambda^{nD/2}, \tag{2.29}$$

and then take the limit $n \to \infty$. On the background field this amounts to a bound of the form $(\partial\bar{\phi})^2 \ll \Lambda^D$ or, evaluated at $r = b$, that is $\alpha^2/b^{2(D-2)} \ll \Lambda^D$.

Lastly, we have contractions of the form

$$\left(\frac{k \cdot \partial}{\Lambda^2}\right)^m \left(\frac{\bar{\phi}}{\Lambda^{(D-2)/2}}\right)^n \ll 1. \tag{2.30}$$

The bounds arising from the $m \to \infty$ and $n \to \infty$ limits of this expression have already been accounted for above. In between those limits we have e.g.

$$k^\alpha k^\beta \partial_\alpha \partial_\beta \bar{\phi} \ll \Lambda^{(D+6)/2}, \tag{2.31}$$

or

$$\omega^2 \ll \frac{\Lambda^{(D+6)/2} b^{D-1}}{\alpha}. \tag{2.32}$$

It is no use contracting two momentum vectors with each other for the aforementioned reason that $\Box\delta\phi \approx 0$ up to cut-off-suppressed corrections. So, this concludes our search for the EFT's regime of validity.

To summarise, the regime of validity for the Goldstone EFT amounts to the following four bounds on the parameters of the theory:

$$b \gg \Lambda^{-1} \tag{2.33a}$$

$$\omega \ll \Lambda^2 b \tag{2.33b}$$

$$\frac{\alpha^2}{b^{2(D-2)}} \ll \Lambda^D \tag{2.33c}$$

$$\omega^2 \ll \frac{\Lambda^{(D+6)/2} b^{D-1}}{\alpha} \tag{2.33d}$$

Arguments similar to above will be repeated again in section 3.3 to establish the regime of validity of gravitational EFTs on specific spacetime backgrounds. Despite the differences between scalar theories in Minkowski spacetime and tensor theories on curved spacetimes, the basic story told by the regime of validity remains always the same. For the EFT to remain a good description of physics, one cannot use it to probe energies that are too high, distances that are too small or fields that are too strong.

With the Goldstone's regime of validity (2.33) in hand, we can now return to the question of whether the apparent time advance (2.26) for $c_{\rm GS} < 0$ is resolvable. Ignoring numerical factors, we have:

$$\omega|\Delta T_{\rm GS}| \sim |c_{\rm GS}| \frac{\omega\alpha^2}{\Lambda^D b^{2D-5}} \ll |c_{\rm GS}|\omega b \ll |c_{\rm GS}| b^2\Lambda^2, \tag{2.34}$$

where we first employed (2.33c) and then (2.33b). There is no limit on the size of the right-hand-side of this inequality since there is no limit on how big $b\Lambda$ can be. Therefore, we conclude that there is nothing stopping us from making a resolvably large time advance in an EFT with $c_{\rm GS} < 0$. Finally, we may in good conscience declare that such a theory violates causality. As a consequence, we know there is no consistent UV-completion for that EFT. We will see in chapter 4 examples of a time advance which *cannot* be made resolvably large within the EFT's regime of validity and thus does not constrain the corresponding Wilson coefficient in a significant way.

To recap: in this section, we started from the low-energy perspective that the shift-symmetric scalar universe is described by (2.4) with a completely arbitrary Wilson coefficient $c_{\rm GS}$. We then calculated the time delay $\Delta T_{\rm GS}$ experienced by a particle of this theory in a hypothetical scattering experiment. We saw that if $c_{\rm GS} < 0$, the particle would experience a time *advance*, i.e. travel superluminally in aggregate. We then determined the shift-symmetric scalar EFT's regime of validity (2.33) in order to check whether this time advance could become resolvably large (in the sense of Heisenberg's uncertainty principle) for a particle state within the EFT. Having shown that it could be very large indeed, we conclude that $c_{\rm GS} < 0$ corresponds to an acausal theory which cannot have a consistent UV-completion. On the other hand, the EFT with a positive $c_{\rm GS}$ exhibits no such acausality and can be consistently UV-completed, as for example in (2.2).

2.2 The quartic Galileon

For our second example, we will consider the Galileon action [63] which is defined by its invariance under the (global) non-linearly realised Galilean symmetry

$$\phi \to \phi + c + b_\alpha x^\alpha. \tag{2.35}$$

In D-spacetime dimensions it is given by [64]

$$S = \int \mathrm{d}^D x \sum_{n=2}^{D+1} c_n \mathcal{L}_n \left[\phi(x)\right], \tag{2.36}$$

where

$$\mathcal{L}_n \left[\phi\right] = \phi\, \varepsilon^{\alpha_1\alpha_2\ldots\alpha_D} \varepsilon^{\beta_1\beta_2\ldots\beta_D} \prod_{i=1}^{n-1} K_{\alpha_i\beta_i} \prod_{j=n}^{D} g_{\alpha_j\beta_j}, \tag{2.37}$$

ε is the Levi–Civita symbol, g is the Minkowski metric and

$$K_{\alpha\beta} = \partial_\alpha \partial_\beta \phi. \tag{2.38}$$

The Galileon action has several special properties. Firstly, despite the fact that the action contains higher-derivative operators, the resulting equations of motion are only second-order. In other words, this action describes a single real scalar with no additional ghostly degrees of freedom. In fact, it happens to describe the scalar polarisation contained in deRham–Gabadadze–Tolley (dRGT) massive gravity [65–67]. Moreover, for a particular choice of coefficients $\{c_n\}$, the action (2.36) is dual to a free scalar field theory [64].

Similar to the Goldstone, it is known that Galileons can exhibit superluminality depending on the sign of their coefficients [68–70]. In this section, we will reproduce the requirement that the coefficient of the quartic term must be negative to preserve causality, using the same methods described above for the Goldstone scalar.

Specialising to the quartic Galileon, the action is

$$S_{\mathrm{QG}} = \int \mathrm{d}^D x \left[-\frac{1}{2}\left(\partial\phi\right)^2 + \frac{c_{\mathrm{QG}}}{\Lambda^{D+2}}\left(\partial\phi\right)^2 \left([K^2] - [K]^2\right)\right], \tag{2.39}$$

where $[K] = K^\alpha{}_\alpha$. The QG action may be considered the leading-order terms in an effective field theory with both $\mathbb{Z}_2$-symmetry and Galilean symmetry (2.35). Since we are considering it as an

EFT, we have split the coefficient of the QG term into a dimensionless Wilson coefficient $c_{\rm QG}$ and a cut-off energy scale, again called Λ. The aim of this section is to show that only $c_{\rm QG} < 0$ could possibly be compatible with a consistent UV theory.

The field equation for ϕ in vacuum is

$$[K] + \frac{2c_{\rm QG}}{\Lambda^{D+2}}\left([K]^3 + 2[K^3] - 3[K][K^2]\right) = 0. \tag{2.40}$$

Once again, we will consider a point source at the origin so that the background field solution has spherical symmetry. Perturbatively to $\mathcal{O}(\Lambda^{-(D+2)})$, the background field is

$$\bar{\phi} = \frac{\alpha}{r^{D-3}} - \frac{2(D-2)(D-3)^4}{(3D-5)}\frac{c_{\rm QG}}{\Lambda^{D+2}}\frac{\alpha^3}{r^{3D-5}}, \tag{2.41}$$

and the equation of motion for the fluctuations is

$$\Box\delta\phi + \frac{12c_{\rm QG}}{\Lambda^{D+2}}\nabla_\alpha\nabla_\beta\delta\phi\nabla^\beta\nabla^\gamma\bar{\phi}_0\nabla_\gamma\nabla^\alpha\bar{\phi}_0 = 0. \tag{2.42}$$

As before, we can expand $\delta\phi$ in a basis of spherical harmonics (2.9) and, due to the symmetry of the background, each partial wave will evolve independently. Defining

$$\chi_l = r^{\frac{D-2}{2}}\left[1 + 3(D-2)(D-3)^3\frac{c_{\rm QG}}{\Lambda^{D+2}}\frac{\alpha^2}{r^{2(D-1)}}\right]\delta\phi_l \tag{2.43}$$

we obtain the wave equation

$$\frac{{\rm d}^2\chi_l}{{\rm d}r^2} + W_{\rm QG}(r)\chi_l(r) = 0, \tag{2.44}$$

where

$$\begin{aligned} W_{\rm QG}(r) = \omega^2&\left(1 - 12(D-2)^2(D-3)^2\frac{c_{\rm QG}}{\Lambda^{D+2}}\frac{\alpha^2}{r^{2(D-1)}}\right)\\ &- \frac{\kappa_S^2}{r^2}\left(1 - 12(D-1)(D-3)^3\frac{c_{\rm QG}}{\Lambda^{D+2}}\frac{\alpha^2}{r^{2(D-1)}}\right)\\ &+ \frac{1-(D-3)^2}{4}\frac{1}{r^2} - 6(D+1)(D-1)(D-2)(D-3)^3\frac{c_{\rm QG}}{\Lambda^{D+2}}\frac{\alpha^2}{r^{2D}} \end{aligned} \tag{2.45}$$

determines the effective potential.

2.2.1 Speed and time delay

In this example, both the radial and angular speeds of the QG particles differ from luminality. They are given by

$$v_\Omega^2 = 1 + 12(D-3)^2\left(D^2+1\right)\frac{c_{\rm QG}}{\Lambda^{D+2}}\frac{\alpha^2}{r^{2(D-1)}}, \tag{2.46a}$$

$$v_r^2 = 1 + 12(D-2)^2(D-3)^2\frac{c_{\rm QG}}{\Lambda^{D+2}}\frac{\alpha^2}{r^{2(D-1)}}. \tag{2.46b}$$

Both speeds are superluminal for $c_{\rm QG} > 0$ and subluminal for $c_{\rm QG} < 0$ (assuming $D \geq 4$). This seems to be consistent with our expectation from the literature that the quartic Galileon term is acausal for $c_{\rm QG} > 0$.

The time delay can be calculated in the exact same manner as for the Goldstone scalar to get

$$\Delta T_{\rm QG} = -6\sqrt{\pi}(D-1)^2(D-3)^2\frac{\Gamma\left(D-\frac{3}{2}\right)}{\Gamma(D-1)}\frac{c_{\rm QG}}{\Lambda^{D+2}}\frac{\alpha^2}{b^{2D-3}}. \tag{2.47}$$

From here we see that $c_{\rm QG} > 0$ leads to a time advance, again in line with expectations. To close the case on the positive-sign quartic Galileon, it remains to check whether this time advance can be made resolvably large within the EFT regime of validity.

2.2.2 Regime of validity and resolvability

The arguments which established the Goldstone regime of validity apply almost identically to the quartic Galileon. The only slight difference is that the average operator in the Galileon EFT has a higher ratio of derivatives-to-fields due to the additional Galilean shift symmetry. More precisely, there are at least $2(n-1)$ derivatives for every ϕ in an operator with Galilean symmetry:

$$\left(\frac{\partial}{\Lambda}\right)^{2(n-1)+m}\left(\frac{\phi}{\Lambda^{(D-2)/2}}\right)^n \ll 1. \tag{2.48}$$

As before, the $m \to \infty$ limit of this expression provide the bounds $b\Lambda \gg 1$ and $\omega \ll \Lambda^2 b$. However, now the $n \to \infty$ limit, evaluated on the background field $\bar{\phi}$, amounts to

$$\frac{\alpha}{b^{D-1}} \ll \Lambda^{(D+2)/2}, \tag{2.49}$$

(c.f. (2.33c)).

Imposing this condition on the time delay we have:

$$\omega\left|\Delta T_{\rm QG}\right| \sim \left|c_{\rm QG}\right|\frac{\omega\alpha^2}{\Lambda^{D+2}b^{2D-3}} \ll \left|c_{\rm QG}\right|\omega b \ll \left|c_{\rm QG}\right|b^2\Lambda^2, \tag{2.50}$$

where in the last step we also imposed $\omega \ll \Lambda^2 b$. Again, there is no limit on how big $b\Lambda$ can be and thus no limit (from the point of view of EFT validity) on how big $\omega\left|\Delta T_{\rm QG}\right|$ could be. That is to say, a resolvably large time advance could be generated in an EFT with $c_{\rm QG} > 0$ and violate causality. This conclusion is in good agreement with known results that the positive-sign quartic Galileon is an unphysical theory.

2.3 Chapter summary

In this chapter, we motivated effective field theory as a low-energy/IR description of (possibly unknown) high-energy/UV physics. We saw an explicit example how a heavy mode (scalar H) could be integrated out to obtain an effective theory of the remaining light mode (Goldstone scalar ϕ). Or, from a different perspective, we saw an explicit example of how an effective theory of a light mode (Goldstone scalar ϕ) could be partially UV-completed by a coupling to heavy mode (scalar H).

The generic scalar EFT (2.1) is parametrised by a set of unknown Wilson coefficients $\{c_{mn}\}$. We argued that it is possible to constrain the values of these coefficients by making some reasonable assumptions about the physical properties of the UV-theory. Specifically, we can rule out parts of the $\{c_{mn}\}$ parameter space which would lead to a violation of causality. We define causality as the condition

$$\Delta T \gtrsim -\omega^{-1}, \tag{2.51}$$

where ΔT is the asymptotic scattering time delay for a wave of frequency ω.

We considered two examples of scalar EFTs: the Goldstone scalar,

$$S_{\rm GS} = \int \mathrm{d}^D x \left[-\frac{1}{2}\left(\partial\phi\right)^2 + \frac{c_{\rm GS}}{\Lambda^D}\left(\partial\phi\right)^4\right], \tag{2.52}$$

and the quartic Galileon,

$$S_{\rm QG} = \int \mathrm{d}^D x \left[-\frac{1}{2}\left(\partial\phi\right)^2 + \frac{c_{\rm QG}}{\Lambda^{D+2}}\left(\partial\phi\right)^2\left([K^2]-[K]^2\right)\right]. \tag{2.53}$$

We showed that each theory could exhibit locally superluminal wave speeds for a particular sign choice of their Wilson coefficients ($c_{\mathrm{GS}} < 0$ and $c_{\mathrm{QG}} > 0$, respectively). We saw how scattered waves experience a time advance $\Delta T < 0$ (as opposed to a time delay $\Delta T > 0$) for those sign choices. However, in order to conclude that this behaviour truly indicated a violation of causality, we needed to check whether it was resolvable within the EFT's regime of validity.

The regime of validity reflects the energy scales for which the EFT expansion is under control. For the scalar EFTs, it amounts to the following set of constraints on the wave frequency ω, field strength α and impact parameter b,

$$b \gg \Lambda^{-1}, \tag{2.54a}$$

$$\omega \ll \Lambda^2 b, \tag{2.54b}$$

$$\frac{\alpha}{b^{D-2}} \ll \Lambda^{D/2} \text{ (Goldstone)} \qquad \text{or} \qquad \frac{\alpha}{b^{D-1}} \ll \Lambda^{(D+2)/2} \text{ (quartic Galileon)}\,, \tag{2.54c}$$

$$\omega^2 \ll \frac{\Lambda^{(D+6)/2} b^{D-1}}{\alpha}. \tag{2.54d}$$

By imposing the above conditions on the time advances, the best bound we can achieve (in both theories) is $\omega|\Delta T_{\mathrm{x}}| \ll |c_{\mathrm{x}}|(b\Lambda)^2$, which is no bound at all because $b\Lambda$ can be made arbitrarily large. In other words, remaining within the EFT's regime of validity does not prevent us from generating a resolvably large time advance when $c_{\mathrm{GS}} < 0$ or $c_{\mathrm{QG}} > 0$, respectively.

Up to some subtleties, we will apply the same logic to the EFT of gravity over the coming two chapters. We will find that, unlike the above scalar operators, we cannot generate a resolvable time advance within the Einstein–Gauss–Bonnet effective theory and thus there is no causality constraint on its Wilson coefficient.

Chapter 3

The EFT of gravity

> "All models are wrong, but some are useful"
>
> — George E. P. Box

Much like LEO in his scalar universe, we seem to lack a fundamental understanding of the microscopic degrees of freedom in our gravitational universe. At a macroscopic level, gravity is remarkably well-described by Einstein's theory of General Relativity (GR) [4]. Predictions of GR (and the associated equivalence principle) agree closely with experiment (see e.g. [71] for a review) and, starting in 2015, observations of gravitational waves [5]. However, the theory itself speaks to its own demise at singularities in spacetime — at the centre of black holes or the Big Bang at the beginning of the universe, for example — where presumably quantum effects become crucial to the proper description of physics. Moreover, it provides no microscopic origin for the "dark energy" which is currently driving the accelerated expansion of the universe.

GR may be treated as a field theory of the spin-2 particle known as a graviton. This theory is already non-renormalisable, however, so extending it to the full EFT of gravity is not unnatural. The EFT of gravity follows the same principles as the EFT of a scalar field. Its action consists of all (local) scalars built from the fundamental field of a gravitational theory, the metric, and its derivatives. Schematically, in D-spacetime dimensions, the action for the EFT of gravity is

$$\begin{aligned} S_{\text{EFT}} = &\int \mathrm{d}^D x \sqrt{-g}\, M_{\text{Pl}}^{D-2} \left(\frac{1}{2} R + \Lambda^2 \sum_{m\geq 0, n\geq 2} c_{mn} \left(\frac{\nabla}{\Lambda} \right)^m \left(\frac{\text{Riemann}}{\Lambda^2} \right)^n \right) \\ &+ \int \mathrm{d}^D x \sqrt{-g}\, \tilde{\Lambda}^D \sum_{m\geq 0, n\geq 2} \tilde{c}_{mn} \left(\frac{\nabla}{\tilde{\Lambda}} \right)^m \left(\frac{\text{Riemann}}{\tilde{\Lambda}^2} \right)^n \end{aligned} \tag{3.1}$$

where $M_{\rm Pl}$ is the Planck mass. The leading-order term in this action is the familiar Einstein–Hilbert action of GR. Beyond that, the sums represent all possible contractions of any number of Riemann tensors and its derivatives. Both Λ and $\tilde{\Lambda}$ are cut-off scales and $\{c_{mn}, \tilde{c}_{mn}\}$ are sets of Wilson coefficients. Although there appears to be a redundancy in this description, the two scales have been introduced to draw a distinction between two types of processes which contribute to the low-energy EFT when massive particles have been integrated out [72, 73]. Terms from the top line would arise as an effective description of tree-level exchange of higher-spin ($s \geq 2$) particles of mass Λ. These higher-spin effects are typical of weakly coupled string theories. Terms from the second line would arise as an effective description of loop-corrections from particles of any spin (including $s < 2$) and of mass $\tilde{\Lambda}$. This could include, for example, loops of Standard Model particles. For $\Lambda \sim \tilde{\Lambda}$, second-line terms are suppressed by $(\Lambda/M_{\rm Pl})^{D-2}$ relative to their top-line partners. From a low-energy perspective, ignorant of the UV-theory, it is impossible to know whether a particular curvature operator arose from tree-level or loop effects in the UV and so both must be generally allowed for with their respective parametrisation. In this thesis, without loss of too much generality, we will only focus on terms from the top line.

In this chapter, we establish some basic results about gravitational wave propagation in the EFT of gravity at leading order on some particularly interesting spacetimes.

3.1 Einstein–Gauss–Bonnet gravity

The first terms in the sum of (3.1) (that is, $m = 0, n = 2$) are the dimension-4 operators

$$\mathcal{L}_{\rm D4} = c_1 R^2 + c_2 R_{\alpha\beta} R^{\alpha\beta} + c_3 R_{\alpha\beta\gamma\delta} R^{\alpha\beta\gamma\delta}. \tag{3.2}$$

We will consider only vacuum solutions of GR for which $R = R_{\alpha\beta} = 0$ to zeroth-order in the EFT. Consequently, only the last of the three terms in (3.2) survives at leading order. It can be recast in terms of the Gauss–Bonnet (GB) operator

$$R^2_{\rm GB} = R_{\alpha\beta\gamma\delta} R^{\alpha\beta\gamma\delta} - 4 R_{\alpha\beta} R^{\alpha\beta} + R^2, \tag{3.3}$$

so that the leading-order effective action in vacuum coincides with Einstein–Gauss–Bonnet (EGB) theory

$$S_{\rm EGB} = \int \mathrm{d}^D x \sqrt{-g}\, M_{\rm Pl}^{D-2} \left(\frac{1}{2} R + \frac{c_{\rm GB}}{\Lambda^2} R^2_{\rm GB} + \dots \right). \tag{3.4}$$

The Wilson coefficient $c_{\rm GB}$ is unknown *a-priori* without access to the precise UV-theory of quantum gravity. In [31], it is argued that the GB term violates causality irrespective of the sign of $c_{\rm GB}$ except in the presence of an infinite tower of massive higher-spin particles, thus effectively fixing $c_{\rm GB}$ to a value arising from string theory. Contrary to this result, we will argue in this thesis (as in [1, 2]) that the GB term does not violate causality as long as its coefficient is (at most) any order-one number, $|c_{\rm GB}| \lesssim \mathcal{O}(1)$. This is the subject of chapter 4. The motivation for revisiting the result of [31] is that, from a low-energy perspective, the UV-origin of an effective operator is unknown and unknowable. As such, the physical properties we associate to a particular operator (the causality of the GB operator, in this case), should not be tied to any one particular completion (like string theory). Instead, they should be determined within a low-energy framework. In chapter 4, we provide a prescription for determining whether an EFT operator is causal or not based solely on the calculation of a low-energy observable — namely, the time delay.

Note that in $D = 4$-dimensions, where the GB term is topological, the leading-order terms in the EFT would start at dimension-6 [74]. For this reason, we focus only on $D \geq 5$-dimensions.

The fact that (3.4) is a Lovelock theory — its equations of motion are second order — is a coincidence. The EFT does not distinguish between second- and higher-order equations of motion since higher derivatives can be removed perturbatively by substituting in the lower-order equations of motion. Outside of vacuum solutions, all three terms in $\mathcal{L}_{\rm D4}$ would be generically expected to contribute in the low-energy EFT. Unless some symmetry dictates, their coefficients need not be fixed to the values in (3.3).

The vacuum EGB equations are

$$\mathcal{E}_{\alpha\beta} \coloneqq G_{\alpha\beta} + \frac{2c_{\rm GB}}{\Lambda^2} B_{\alpha\beta} = 0, \tag{3.5}$$

where

$$B_{\alpha\beta} = 4R_{\sigma\alpha\beta\rho}R^{\sigma\rho} + 2R_{\alpha}{}^{\sigma\rho\kappa}R_{\beta\sigma\rho\kappa} - 4R_{\alpha\sigma}R_{\beta}{}^{\sigma} + 2RR_{\alpha\beta} - \frac{1}{2}R^2_{\rm GB}\, g_{\alpha\beta}. \tag{3.6}$$

Throughout this thesis, we will consider two solutions to (3.5) and study the causal properties of propagating metric perturbations on those backgrounds. The first is a static, spherically symmetric, black hole solution which reduces to the Schwarzschild solution in GR ($c_{\rm GB} = 0$). The second solution is the pp-wave metric, which is an exact solution to all orders in the EFT of gravity. This latter example represents a broad class of spacetimes, given its universality as the

Penrose limit of any spacetime [75].

Unlike the flat-space scalar field theories studied in chapter 2, in these dynamical gravitational theories there is both a time delay associated to the geometry of the curved spacetime (famously known as the Shapiro time delay) as well as a time delay associated to the EFT operator. In chapter 4, we will argue that only the latter has a bearing on causality. In both cases, we will arrive at the same conclusion: there is no violation of causality on these spacetimes for any $|c_{\rm GB}| \lesssim \mathcal{O}(1)$, regardless of the UV-origin of the operator. For lack of a counter-example, the GB term is thus considered a causal contribution in the EFT of gravity.

3.1.1 Black hole solution

While the exact background solution and master equations for static black holes in EGB theory are known [76–78] — in fact, they are known for any Lovelock theory in any dimension [79–82] — we will only be interested in their leading-order behaviour in the EFT of gravity. The perspective we take in this thesis is that the GB term is just the first in an infinite series of higher-dimensional operators in the EFT of gravity. Its subleading behaviour would be degenerate with other higher-order terms that could enter into the EFT (e.g. $R^3, (\nabla R)^2, R^4$ etc.). In this context, the expansion parameter is roughly the ratio of the spacetime curvature to the cut-off energy. For ease of notation, in the context of the black hole background, we denote this small dimensionless parameter by $\mu = (r_g \Lambda)^{-2}$ where r_g is the Schwarzschild radius of the BH in GR. Unless otherwise stated, throughout all sections pertaining to the black hole solution, we will work up to linear order in μ, thus implicitly assuming that higher-dimension curvature operators can be neglected compared to the GB term. We will check this assumption in section 3.3 and use it to define the EFT's regime of validity.

With this, the leading-order Schwarzschild-like (static, spherically symmetric and asymptotically flat) solution to (3.5) is the metric

$$g_{\alpha\beta}\mathrm{d}x^\alpha \mathrm{d}x^\beta = -f(r)\mathrm{d}t^2 + \frac{1}{f(r)}\mathrm{d}r^2 + r^2 \mathrm{d}\Omega_{D-2}^2 \tag{3.7}$$

where $\mathrm{d}\Omega_{D-2}^2 = \gamma_{ab}\mathrm{d}\theta^a \mathrm{d}\theta^b$ is the line element on the $(D-2)$-sphere S^{D-2} and the metric function is

$$f(r) = 1 - \left(\frac{r_g}{r}\right)^{D-3} + 2(D-3)(D-4)c_{\rm GB}\mu \left(\frac{r_g}{r}\right)^{2D-4} + \mathcal{O}\left(\mu^2\right) \tag{3.8}$$

See appendix B.1 for a derivation. The location of the horizon r_H of this black hole, set by

$f(r_H) = 0$, is shifted relative to its GR value $r_H = r_g(1 - 2(D-4)c_{\rm GB}\mu + \mathcal{O}(\mu^2))$. The Riemann components of this metric are

$$R_{ABCD} = -\frac{f''(r)}{2}\left(g_{AC}g_{BD} - g_{AD}g_{BC}\right), \tag{3.9a}$$

$$R_{AaBb} = -\frac{f'(r)}{2r}g_{AB}g_{ab}, \tag{3.9b}$$

$$R_{abcd} = \frac{1 - f(r)}{r^2}\left(g_{ac}g_{bd} - g_{ad}g_{bc}\right), \tag{3.9c}$$

where prime denotes a derivative with respect to r, upper-case letters $\{A, B, C, \dots\}$ denote indices on the 2-dimensional orbit space (i.e. (t, r)-coordinates) and lower-case letters $\{a, b, c, \dots\}$ denote indices on the $(D-2)$-sphere. In particular, we have this relation between metric components: $g_{ab} = r^2\gamma_{ab}$.

3.1.2 pp-wave solution

The second solution we will consider is the stationary, asymptotically flat pp-wave metric, given in Brinkmann coordinates:

$$g_{\alpha\beta}\mathrm{d}x^\alpha \mathrm{d}x^\beta = 2\mathrm{d}u\mathrm{d}v + H(u, \mathbf{x})\mathrm{d}u^2 + \delta_{ij}\mathrm{d}x^i\mathrm{d}x^j, \tag{3.10}$$

where $u = x_1 - t$ and $v = x_1 + t$ are the lightcone variables, and $\mathbf{x}$ are the remaining coordinates on the $d = (D-2)$-dimensional Euclidean "transverse" subspace. Every metric, with a choice of null geodesic, can be associated to a pp-wave metric via the Penrose limit process [75]. The upshot is that they can be used as analogues to study the physics of systems where the exact metric is unknown. For example, a pp-wave metric (3.10) with appropriately localised singularities in $H(u, \mathbf{x})$ is analogous to a mutli-black hole spacetime via an Aichelburg-Sexl boost [83]. By this association, the (a)causality of an EFT operator on the pp-wave metric should be reflective of its (a)causality on a much broader class of metrics.

The only non-zero component of the Riemann tensor (up to symmetry) of the pp-wave metric is

$$R_{uiuj} = -\frac{1}{2}\partial_i\partial_j H(u, \mathbf{x}). \tag{3.11}$$

The only non-zero component of the Ricci tensor is $R_{uu} = -\frac{1}{2}\nabla_d^2 H(u, \mathbf{x})$ and the Ricci scalar automatically vanishes because the inverse metric component g^{uu} is zero. The metric (3.10) is thus a solution to the vacuum EGB equations (3.5) if H is harmonic in transverse space

$\nabla_d^2 H(u,\mathbf{x}) = 0$. Actually, we will be interested in spacetimes sourced by point particles (analogue black holes) for which the Laplacian of H is non-zero at a discrete set of points $\{\mathbf{b}_i\}$:

$$-\nabla_d^2 H(u,\mathbf{x}) = \frac{2\pi^{\frac{d}{2}}}{\Gamma\left(\frac{d}{2}\right)} \sum_i j_i(u)\delta^{(d)}(\mathbf{x}-\mathbf{b}_i). \tag{3.12}$$

The functions of the u-coordinate $j_i(u)$ must be positive for such a source to satisfy the null energy condition but are otherwise unspecified at this time. The asymptotically flat solution to (3.12),

$$H(u,\mathbf{x}) = \sum_i \frac{j_i(u)}{|\mathbf{x}-\mathbf{b}_i|^{d-2}}, \tag{3.13}$$

is singular at each $\mathbf{b}_i$.

Throughout this thesis, we will consider two simple cases:

1. a point source located at the origin with spherical symmetry in the transverse directions,

$$H_{\text{pt}}(u,r) = \frac{j(u)}{r^{d-2}}, \tag{3.14}$$

   and

2. two equal strength sources located at $\pm\mathbf{b}$, which we shall refer to as the "balancing" case for reasons which will become clear in section 4.4.1,

$$H_{\text{bal}}(u,\mathbf{x}) = j(u)\left(\frac{1}{|\mathbf{x}-\mathbf{b}|^{d-2}} + \frac{1}{|\mathbf{x}+\mathbf{b}|^{d-2}}\right). \tag{3.15}$$

For the most part, the arguments in this thesis apply for arbitrary $j(u)$ but there are some specific examples we will refer to for illustrative purposes. Firstly, the "shockwave",

$$j_{\text{sw}}(u) = \frac{4\Gamma\left(\frac{d-2}{2}\right)}{\pi^{\frac{d-2}{2}}} G P_u \delta(u), \tag{3.16}$$

corresponds to a point particle moving very fast in the v-direction with momentum P_u, and features prominently in the discussion on causality in [31]. Second, the "sequence of shockwaves",

$$j_{\text{ssw}}(u) = \sum_{i=1}^{N} j_{\text{sw}}(u-u_i), \tag{3.17}$$

corresponds to series of shockwaves which occur one after another in the u-direction. Lastly, we consider a constant $j(u) = j$, which can be seen as the limit of j_{ssw} as the number of shocks

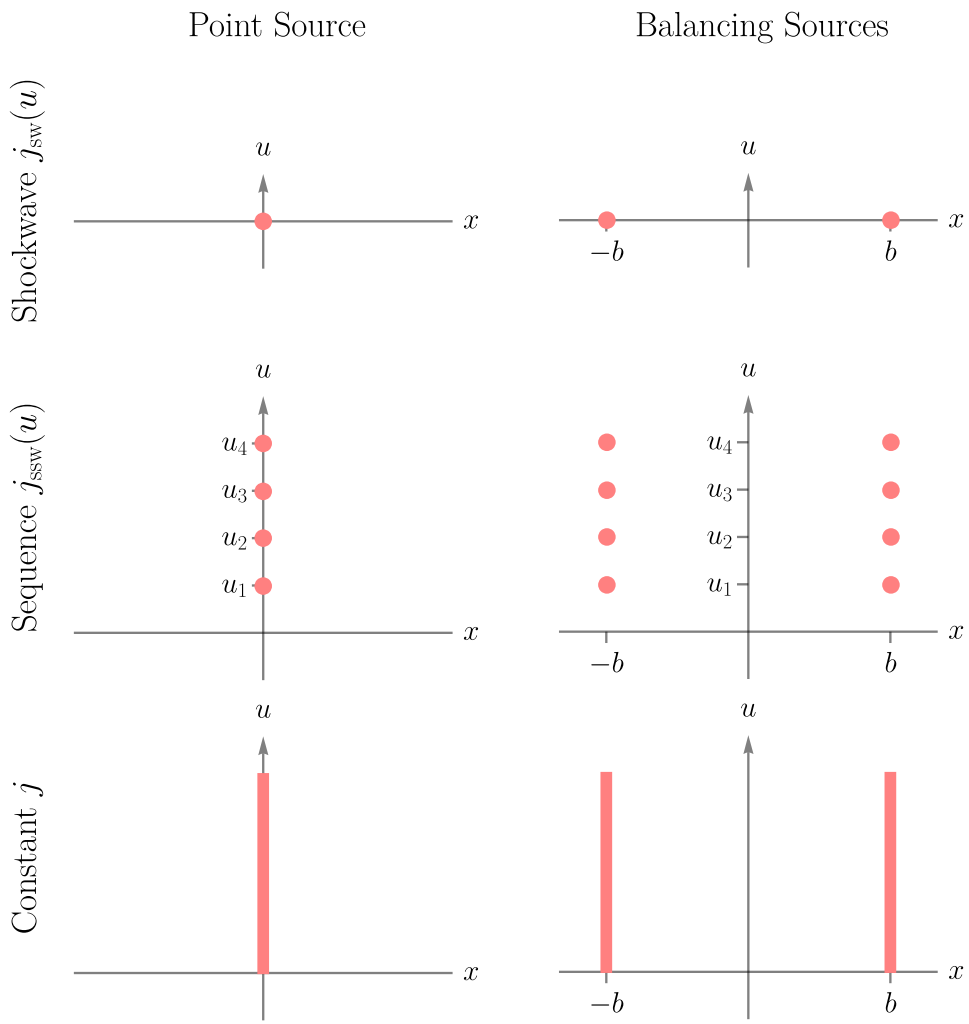

Figure 3.1: An illustration of the pp-wave sources referred to in the text. Each dot represents a Dirac delta function in the u-direction.

grows very large $N \to \infty$ while the u-distance between them goes to zero $u_i - u_{i+1} \to 0$. All of the possible configurations are illustrated in figure 3.1.

It can be shown that there are no non-vanishing curvature invariants on a pp-wave background. In brief: On one hand, any components of the Riemann tensor with a covariant v-index or a contravariant u-index are zero. On the other hand, any non-zero component of the Riemann tensor contains either a covariant u-index or a contravariant v-index. Hence, there are no non-zero scalars involving contractions of Riemann tensors only. Allowing for covariant derivatives, a covariant u-index (say) on a Riemann component could only be contracted with ∇_v. However, $\partial_v H = 0$ and the Christoffel symbols with a lower v-index must also vanish because of the above restrictions on the Riemann components.

The consequence is that the pp-wave metric (3.10) is an exact (background) solution, not only

to GR or EGB theory, but to any EFT of pure gravity, for any choice of metric function $j(u)$. In particular, it is often studied as an example of an exact solution to string theory. This should be contrasted with the BH solution (3.7), which (generally) has to be solved for order-by-order in the EFT expansion. It is clear that the BH solution as given in (3.8) is only good until the next-order term at $\mathcal{O}(\mu^2)$ become important. Naïvely, there seems to be no such restriction on the pp-wave solution. Having a well-defined regime of validity will play an important role in establishing the causality of the GB operator (see e.g. section 4.3.2). Without it, one might be tempted to think that a real violation of causality is possible on the pp-wave spacetime. Fortunately for GB, the presence of metric perturbations $g_{\alpha\beta} \to g_{\alpha\beta} + h_{\alpha\beta}$ on a pp-wave means the total metric is no longer an exact solution to the EFT of gravity. As we will see in section 3.2.2, their equations of motion are corrected at each order in the EFT, thus introducing a non-trivial regime of validity for pp-wave spacetimes. In other words, probing the spacetime in any way ruins the "exactness" which makes it special.

3.2 Gravitational waves in the EFT

We will now introduce metric perturbations $h_{\alpha\beta}$ on top of the background metrics described above. It is their dynamics which will determine the causal properties of the GB operator. Their field equations are given by

$$\delta\mathcal{E}_{\alpha\beta} = 0. \tag{3.18}$$

In D-spacetime dimensions, there are $D(D-3)/2$ propagating gravitational degrees of freedom parameterised by so-called "master variables". In this section, we will use the symmetries of the black hole and pp-wave spacetimes to identify their master variables from the $D(D+1)/2$ components of the symmetric $h_{\alpha\beta}$-tensor, and derive their governing master equations. Since EGB gravity is a Lovelock theory, the linear perturbation equations will be naturally second-order in derivatives.

3.2.1 On black hole background

The master equations of a 4-dimensional Schwarzschild black hole in GR were first derived for the so-called "axial" mode by Regge and Wheeler [84] and later for the "polar" mode by Zerilli [85]. This formalism was extended to higher-dimension, maximally symmetric black holes by Kodama, Ishibashi and Seto in [86–88]. It has also been extended for EGB gravity by Dotti

and Gleiser [77, 78] and, more recently, for Lovelock gravity by Takahashi and Soda [80–82].

In this section we will specialise the results of Dotti and Gleiser [77, 78] to the spherically symmetric case (constant sectional curvature of 1) and treat the GB parts as a perturbation to GR. More detail is provided in appendix B. Due to the spherical symmetry of the background, the components of $h_{\alpha\beta}$ are naturally decomposed according to their transformation properties under the symmetry group $SO(D-1)$. Accordingly, perturbations are split into three types: scalar (S), vector (V) or tensor (T). The form of the master equation is the same for all three types and is given below in (3.28)

The scalar-type perturbations can be expanded in terms of scalar spherical harmonics $\mathbb{S}$ as

$$h_{AB} = f_{AB}\mathbb{S}, \quad h_{Aa} = r f_A \mathbb{S}_a, \quad h_{ab} = 2r^2 \left(H_L \gamma_{ab}\mathbb{S} + H_T \mathbb{S}_{ab}\right), \tag{3.19}$$

where

$$\left(\hat{\Delta}_{D-2} + \kappa_S^2\right)\mathbb{S} = 0, \tag{3.20a}$$

$$\mathbb{S}_a = -\frac{1}{\kappa_S}\hat{D}_a\mathbb{S}, \tag{3.20b}$$

$$\mathbb{S}_{ab} = \frac{1}{\kappa_S^2}\hat{D}_a\hat{D}_b\mathbb{S} + \frac{1}{D-2}\gamma_{ab}\mathbb{S}. \tag{3.20c}$$

As suggested by (3.20a), the scalar spherical harmonics are eigenmodes of the Laplace–Beltrami operator on the $(D-2)$-sphere $\hat{\Delta}_{D-2} = \gamma^{ab}\hat{D}_a\hat{D}_b$ with eigenvalue $-\kappa_S^2$, where

$$\kappa_S^2 = l(l+D-3), \quad l = 0, 1, 2, \ldots . \tag{3.21}$$

Expressions for the scalar (and vector and tensor) spherical harmonics on the N-sphere can be found in [89], but their exact form is not important for what follows. There is a mapping between this parametrisation $\{f_{AB}, f_A, H_L, H_T\}$ and the scalar master variable Φ_S, which is the higher-dimensional analogue of the 4-dimensional polar mode. However, the mapping is rather complicated. It is discussed in appendix B.4.

The vector-type perturbations can be expanded in terms of transverse vector spherical harmonics $\mathbb{V}_a$ as

$$h_{AB} = 0, \quad h_{Aa} = r f_A \mathbb{V}_a, \quad h_{ab} = 2r^2 H_T \mathbb{V}_{ab}, \tag{3.22}$$

where

$$\left(\hat{\Delta}_{D-2} + \kappa_V^2\right) \mathbb{V}_a = 0, \tag{3.23a}$$

$$\mathbb{V}_{ab} = -\frac{1}{2\kappa_V}\left(\hat{D}_a \mathbb{V}_b + \hat{D}_b \mathbb{V}_a\right). \tag{3.23b}$$

The vector spherical harmonics are eigenmodes of the Laplace–Beltrami operator with eigenvalue $-\kappa_V^2$ where

$$\kappa_V^2 = \ell(\ell + D - 3) - 1, \quad \ell = 1, 2, \ldots. \tag{3.24}$$

The mapping between this parameterisation $\{f_A, H_T\}$ and the vector master variable Φ_V, which is the higher-dimensional analogue of the 4-dimensional axial mode, is discussed in appendix B.3.

Lastly, the tensor modes are expanded in terms of transverse-traceless tensor spherical harmonics $\mathbb{T}_{ab}$ as

$$h_{AB} = 0, \quad h_{Aa} = 0, \quad h_{ab} = 2r^2 H_T \mathbb{T}_{ab}, \tag{3.25}$$

where

$$\left(\hat{\Delta}_{D-2} + \kappa_T^2\right) \mathbb{T}_{ab} = 0. \tag{3.26}$$

The tensor spherical harmonics are eigenmodes of the Laplace–Beltrami operator with eigenvalue $-\kappa_T^2$ where

$$\kappa_T^2 = \ell(\ell + D - 3) - 2, \quad \ell = 1, 2, \ldots. \tag{3.27}$$

The tensor modes do not have an analogue in 4-dimensions with transverse-traceless tensor spherical harmonics $\mathbb{T}_{ab}$ only existing in higher dimensions. The mapping between H_T and the tensor master variable Φ_T is straightforward, and is discussed in appendix B.2. The tensor modes come first in the appendices simply because they are easiest to understand, followed by vectors, followed by scalars.

The resulting master equations for each mode $M \in \{S, V, T\}$ can be cast in the form of a Schrödinger-like wave equation with potential V_M sourced by the background curvature, and depending on the perturbation type,

$$-\frac{\partial^2}{\partial t^2}\Phi_M + f\frac{\partial}{\partial r}\left(f\frac{\partial}{\partial r}\Phi_M\right) - V_M \Phi_M = 0. \tag{3.28}$$

Each partial wave (with usual label l omitted here) for each perturbation type M evolves

independently according to the above. We may also write this equation as

$$\Box_2 \Phi_M - \frac{V_M}{f}\Phi_M = 0, \tag{3.29}$$

where $\Box_2$ is the d'Alembertian operator in the 2-dimensional orbit space — that is,

$$\Box_2 \Phi_M \equiv -\frac{1}{f}\frac{\partial^2}{\partial t^2}\Phi_M + \frac{\partial}{\partial r}\left(f\frac{\partial}{\partial r}\Phi_M\right). \tag{3.30}$$

All three potentials V_M are given explicitly to leading order in μ in appendix B — see (B.20) for V_T, (B.33) for V_V and (B.50) for V_S. Here, they are presented with a further truncation to leading order in large-l:

$$\frac{V_M}{f} = \frac{\omega^2 b^2}{r^2}\left(1 + A_M c_{\rm GB}\mu\left(\frac{r_g}{r}\right)^{D-1}\right) + \mathcal{O}\left(\frac{l^0}{r^2}\right), \tag{3.31}$$

where

$$A_T = 8(D-1), \tag{3.32a}$$

$$A_V = -4(D-1)(D-4), \tag{3.32b}$$

$$A_S = -8(D-1)(D-4). \tag{3.32c}$$

As usual, ω is the frequency of the perturbation and b is classical impact parameter, related to l by the convention

$$b = \frac{1}{\omega}\left(l + \frac{D-3}{2}\right), \tag{3.33}$$

the same as in chapter 2. In section 4.3.1, in order to make contact with causality, we will consider the scattering problem of a propagating GW against a BH in the eikonal (large-l) limit. In this sense, $V_M(r)$ is the central potential of the black hole source as felt by a wave of type M.

In the limit of vanishing Schwarzschild radius $r_g \to 0$, the apparent potential is independent of mode-type, being only an artefact of the spherical-coordinate choice,

$$V_M(r) = \frac{\omega^2 b^2}{r^2} - \frac{1}{4r^2}. \tag{3.34}$$

There is no large-l or small-μ truncation in this expression. In the context of the scattering

problem, the impact parameter b would be (almost[1]) the point of closest approach to the origin on the Minkowski geodesic ($r_g = 0$). In the presence of the BH, the actual point of closest approach will be referred to as the "turning point". The turning point r_t coincides with the impact parameter when $r_g = 0$, but the curvature corrections will depend on whether we are considering scalar-, vector- or tensor-type perturbations. As explained by the derivation in appendix A, it is not strictly necessary to calculate the turning point for our purposes.

3.2.2 On pp-wave background

On the pp-wave background, we work in lightcone gauge, as in [90]:

$$h_{v\alpha} = 0 \quad \forall\, \alpha. \tag{3.35}$$

The full set of perturbation equations is given in appendix C. The $\delta\mathcal{E}_{v\alpha}$ equations reduce to two constraint equations

$$h_{ii} = 0, \tag{3.36}$$

$$\partial_v h_{iu} + \partial_j h_{ij} = 0. \tag{3.37}$$

Taking the trace of the $\delta\mathcal{E}_{ij}$ equation, and applying the above two constraints, produces a third constraint,

$$\partial_v h_{uu} + \partial_i h_{iu} = -4\frac{d-2}{d}\frac{c_{\rm GB}}{\Lambda^2}\partial_i\partial_j H \partial_v h_{ij}, \tag{3.38}$$

so that the h_{uu} and h_{ui} components are all specified in terms of the h_{ij} components, as long as $\partial_v h_{\alpha\beta} \neq 0$. This leaves only the $D(D-3)/2$ components of the traceless h_{ij} as the dynamical

[1] In this thesis, all analysis on the BH spacetime is performed in the standard radial coordinate r. As first mentioned in section 2.1.2, we would see that b is the exact point of closest approach for the Langer field if we had chosen to work in the corresponding Langer coordinates.

degrees of freedom. Their equations of motion[2] are given by

$$\begin{aligned}&\tilde{\Box}h_{ij} - 8\frac{c_{\rm GB}}{\Lambda^2}\partial_v^2 X_{ij} = 0,\\ &X_{ij} = \frac{1}{2}\left(h_{ik}\partial_j\partial_k H + h_{jk}\partial_i\partial_k H\right) - \frac{1}{d}\delta_{ij}h_{kl}\partial_k\partial_l H,\end{aligned} \tag{3.39}$$

where

$$\tilde{\Box}h_{ij} = 2\partial_u\partial_v h_{ij} - H\partial_v^2 h_{ij} + \partial_k\partial_k h_{ij}. \tag{3.40}$$

Unlike the pp-wave background solution, the equation for the perturbations is modified by the GB operator in the action. In fact, it would generically receive corrections from any effective gravitational operator. Demanding that these corrections are under control will define the regime of validity of the EFT in the next section.

The decoupled master variables are some linear combination of the h_{ij}, depending on the form of $H(u, \mathbf{x})$. In the case of the point source (3.14), the spherical symmetry means the equations (3.39) are all but immediately decoupled when expressed in spherical coordinates. The single caveat is that not all of the diagonal components of h_{ij} are independent because of the traceless condition (3.36). Choosing h_{DD} as the dependent component, the master variables are

$$\Phi \in \{h_{rr}, h_{ra}, h_{ab} \text{ for } a \neq b, h_{aa} - h_{DD} \text{ (no sum)}\}, \tag{3.41}$$

where $\{a, b, \dots\}$ label the angular directions. Their master equations are

$$\tilde{\Box}\Phi + A\frac{c_{\rm GB}}{\Lambda^2}\frac{\partial_r H}{r}\partial_v^2\Phi = 0, \tag{3.42}$$

where A is a number depending on the master variable in consideration,

$$A \in \{8(d-2), 4(d-2), -8, -8\} \tag{3.43}$$

respectively, and we have used the fact that H is harmonic (away from the origin) to replace $\partial_r^2 H = -(D-3)\partial_r H/r$. In the balancing source case (3.15), it is less straightforward to identify

[2]Interestingly, unlike the black hole master equations given in (3.28), the pp-wave master equations (3.39) are not derived perturbatively in Λ^{-1}. That is, the pp-wave master equations in EGB theory are simply linear in $c_{\rm GB}$ and do not need to be expanded to make them EFT-compatible. This is just a quirk of the GB operator. By ways of contrast, the extended EFT considered at the end of section 3.3.2 has master equation (3.66) which is only perturbative in Λ^{-1}.

the master variables. Some details are given in appendix C but are not crucial in what follows. Suffice to say, the master equations will take a similar form to (3.42).

3.3 Regime of validity of gravitational EFT

As discussed in section 2.1.3, a feature of all EFTs is that they cease to be a good description of physics above a certain energy, related to the cut-off scale. The reason for this is that in artificially truncating an infinite series of possible higher-dimensional operators at some finite order, it is implicitly assumed that the first few terms dominate. In the present context, the EGB action (3.4) is understood to be only the leading-order terms from an infinite series of curvature operators (3.1), corresponding to truncation at dimension-4 (R^2-operators). However, the low-energy expansion of a real UV-theory would generically contain all possible dimension-6, -8, -10,... operators unless some symmetry prohibits them. The requirement that these operators are "under control", and so don't contribute significantly to physics at low energies, defines the regime of validity [1, 36]. Physically, this translates into a number of bounds on the various parameters of the theory (i.e. the length scales in the metric or the frequency of gravitational waves), which we investigate in this section.

While there is a general consensus in the literature that EFTs are only valid below a certain energy scale, careful consideration is not always given to defining this scale. It is sometimes wrongly assumed that validity amounts to bounding the frequency of wave perturbations by the cut-off energy "$\omega \ll \Lambda$". However, this is not a Lorentz-invariant statement since energy itself is not a scalar quantity. Therefore, its meaning is ill-defined, being frame-dependent. Below, we endeavour to extract the EFT regime of validity by bounding only scalar quantities built from the metric tensor and its derivatives. In fact, we will find in the case of the BH spacetime that we are allowed to consider frequencies a certain amount beyond the cut-off scale while still remaining within the EFT regime of validity.

Schematically, the regime of validity for a gravitational EFT corresponds to

$$\left(\frac{\nabla}{\Lambda}\right)^m \left(\frac{\text{Riemann}}{\Lambda^2}\right)^n \ll 1 \tag{3.44}$$

where the left-hand-side represents all possible scalar contractions built out of m covariant derivatives and n powers of the Riemann tensor. For a spacetime with perturbations, the "Riemann" tensor in (3.44) refers to sum of the background Riemann tensor (henceforth $\bar{R}$) and

its perturbation δR. On highly symmetric backgrounds, the perturbed Riemann tensor generally has a much richer structure than its background counterpart and thus provides important information about the EFT's validity. This observation will be especially crucial to defining the regime of validity of pp-waves in section 3.3.2 where all curvature invariants vanish on the background.

Throughout this discussion, we use the GR values of the (background and perturbed) Riemann tensor components on the left-hand-side of (3.44), instead of the full EFT values, as a matter of consistency. In the regime where the expansion is well-controlled, the GB corrections to the GR components are additionally suppressed by factors of Λ^{-1} and would lead to weaker bounds.

3.3.1 Black hole validity

In this section, we specialise the generic statement about EFT validity (3.44) to the black hole spacetime introduced in 3.1.1. First we deal with constraints on the background geometry, and then with constraints on the energy of gravitational wave perturbations. At the level of the action of a tensor theory, the idea of "control" over EFT operators may seem a bit abstract. To address this, in the final part of this section we will track the effects of an explicit example of a higher-dimension operator on the potential of GWs and show how requiring its sub-dominance (to the GB terms) leads to a constraint on the GW frequency.

Constraints on background

To obtain a complete picture of the EFT's validity, we should consider all possible scalar contractions of the Riemann tensor and its covariant derivatives. However, the Schwarzschild background is Ricci-flat at leading order which means any contractions involving a Ricci tensor/scalar will lead to weaker bounds. Thus, all indices on a Riemann tensor components should be contracted elsewhere, as in e.g.

$$\nabla_\alpha \nabla^\alpha R_{\beta\sigma\rho\kappa} R^{\beta\sigma\rho\kappa} \ll \Lambda^6. \tag{3.45}$$

Components of the Riemann tensor scale like $\sim r_g^{D-3}/r^{D-1}$, so the strongest bounds are of the form

$$\nabla^m \bar{R}^n \sim \frac{r_g^{(D-3)n}}{r^{(D-1)n+m}} \ll \Lambda^{m+2n}. \tag{3.46}$$

In particular, the $n \to \infty$ limit gives

$$\frac{r_g^{D-3}}{r^{D-1}} \ll \Lambda^2 \tag{3.47}$$

and the $m \to \infty$ limit gives

$$r \gg \Lambda^{-1}. \tag{3.48}$$

These bounds on the distance scales are a reflection of the fact that we cannot look too closely at the geometry of the spacetime while remaining within the regime of validity of the EFT. At short distances (high energies) the low-energy effective description breaks down and microscopic degrees of freedom should be described in their own right.

Evaluating the above at the impact parameter b of a scattering GW, we obtain two constraints for the EFT regime of validity:

$$\frac{r_g^{D-3}}{b^{D-1}} \ll \Lambda^2 \tag{3.49}$$

$$b \gg \Lambda^{-1} \tag{3.50}$$

The first of these (3.49) is the requirement that the BH radius of curvature is small relative to the distance of the probing GW, or that the GW doesn't pass too close to the BH. The second (3.50) is the requirement that the probing distance scale b is not smaller than the inverse cut-off.

Constraints on perturbations

So far, we have constrained the curvature of the background spacetime. To test causality with propagating GWs, we should ensure that their own energy does not cause large distortions and ruin our control over the EFT. Consider GWs of momentum $(k^\alpha) = (\omega, \mathbf{k})$ so that the perturbed Riemann components, which depend on second derivatives of the metric perturbations, may be replaced with powers of the momentum tensor $\delta R_{\alpha\sigma\beta\rho} \sim \nabla_\alpha \nabla_\beta h_{\sigma\rho} \sim k_\alpha k_\beta h_{\sigma\rho}$. As such, the regime of validity for perturbations is determined by scalar bounds of the form

$$\left(\frac{\nabla}{\Lambda}\right)^m \left(\frac{\bar{R}}{\Lambda^2}\right)^n \left(\frac{k}{\Lambda}\right)^p \ll 1. \tag{3.51}$$

Once again, there are a number of possible contractions which would simply lead to weaker bounds. As before, indices on a given background Riemann tensor should not be contracted with each other. Additionally, the divergence of the Riemann tensor $\nabla^\alpha R_{\alpha\beta\sigma\rho}$ vanishes to leading order in the GR vacuum (a consequence of the contracted second Bianchi identity). Then, by its symmetries, the Riemann tensor may only enter via contractions with at most two k's, at most two ∇'s and at most two other Riemann tensors. We should also note that the GR equation of

motion for the metric perturbations is $\nabla_\alpha \nabla^\alpha h_{\sigma\rho} = 0 + \ldots$, so to leading order $k^2 = k_\alpha k^\alpha \approx 0$. The upshot of all this is that the strongest EFT validity bounds come from contractions of the form

$$(k \cdot \nabla)^m (k \cdot \bar{R} \cdot k)^{2n} \ll \Lambda^{2m+8n}, \tag{3.52a}$$

$$(\nabla \cdot \nabla)^m (k \cdot \bar{R} \cdot k)^{2n} \ll \Lambda^{2m+8n}. \tag{3.52b}$$

A non-trivial $m = 1, n = 1$ example of (3.52a) written in terms of components is

$$k_\alpha \nabla^\alpha (k^\beta R_{\beta\gamma\delta\sigma} k^\delta k_\kappa R^{\kappa\gamma\rho\sigma} k_\rho) \ll \Lambda^{10}.$$

Similarly, k_α may be replaced with ∇_α for an example of (3.52b).

Taking the $n \to \infty$ limit of (3.52), replacing $k \sim \omega$ and evaluating at $r \sim b$ gives

$$\omega^2 \ll \frac{\Lambda^4 b^{D-1}}{r_g^{D-3}}. \tag{3.53}$$

Taking the $m \to \infty$ limit of (3.52a) with the same replacements gives

$$\omega \ll \Lambda^2 b. \tag{3.54}$$

Lastly, the $m \to \infty$ limit of (3.52b) reproduces (3.50).

Both (3.53) and (3.54) put upper bounds on the energy of GWs which are allowed to safely propagate within the EFT. In particular, GWs used to probe the causal properties of the GB operator on this spacetime, by the scattering process described in section 4.3, must obey these constraints. In fact, as long as the scattered wave passes far from the Schwarzschild radius $b \gg r_g$, the constraint in (3.54) is always stronger than the constraint in (3.53). For all practical purposes, the maximum wave frequency for which the EFT may be trusted is $\omega \sim \Lambda^2 b$.

Explicit example

The above arguments to establish a regime of validity rely only on generic assumptions about the EFT series expansion, but were largely schematic. In this section, we will consider an explicit example of a higher-order truncated EFT expansion. Demanding that the higher-dimension operators in the expansion are subdominant to the GB operator will concretely reproduce the

black hole EFT validity bound (3.53).

Consider the following effective action, which contains (3.4) as its leading-order part and then a further higher-dimension operator:

$$S_{\rm EFT} = \int \mathrm{d}^D x\sqrt{-g}\, M_{\rm Pl}^{D-2}\left(\frac{1}{2}R + \frac{c_{\rm GB}}{\Lambda^2}R^2_{\rm GB} + \frac{c_{\rm R4}}{\Lambda^6}R_{\alpha\beta\gamma\delta}R^{\gamma\delta\sigma\rho}R_{\sigma\rho\kappa\lambda}R^{\kappa\lambda\alpha\beta} + \dots\right), \tag{3.55}$$

where $c_{\rm R4} \sim \mathcal{O}(1)$ is a new Wilson coefficient. The presence of the R^4-operator will modify the equation of motion of GWs by introducing higher-derivative, $\mathcal{O}(\mu^3)$-corrections. In the context of effective field theory, the appearance of higher derivatives does not mean the appearance of ghostly degrees of freedom. Rather, they should be replaced perturbatively using the lower-order, lower-derivative equations until we return to a second-order linear differential equations for the master variables. Ultimately, the net effect is a correction to the effective potential V_M in the master equation. At large-l, the dominant contribution from this process can be obtained by tracking only the highest- (four-) derivative terms, which is done explicitly for the tensor modes in appendix B.5. The resulting new contribution to the potential is

$$V_T^{\rm R4} = -16(D-1)^2 c_{\rm R4}\mu^3\left(\frac{r_g}{r}\right)^{2D}\frac{\kappa_T^4}{r^2} + \dots \tag{3.56}$$

where $\dots$ represents terms lower-order in κ_T^2, the tensor-eigenvalue of the angular-derivatives. Comparing this term to the leading-in-κ_T GB term in (B.20),

$$V_T^{\rm GB} = 8c_{\rm GB}\mu(D-1)\left(\frac{r_g}{r}\right)^{D-1}\frac{\kappa_T^2}{r^2} + \dots, \tag{3.57}$$

and replacing $\kappa_T^2 \sim l^2 \sim (b\omega)^2$, we see that $V_T^{\rm R4} \ll V_T^{\rm GB}$ when the EFT validity condition (3.53) is satisfied, assuming the Wilson coefficients $(c_{\rm GB}, c_{\rm R4})$ are themselves $\mathcal{O}(1)$ numbers.

There is nothing special about this particular choice of dimension-8 operator. It would generically be expected to enter the low-energy expansion of any UV-theory with some non-zero Wilson coefficient $c_{\rm R4}$. However, if chance or symmetry had it vanish, other higher-derivative operators could play the same role. Without extreme fine-tuning of all their Wilson coefficients, the conclusion that the effective EGB theory is only valid in a certain regime is unavoidable. That being said, it happens for the highly-symmetric Schwarzschild spacetime that dimension-4 and -6 operators would not have produced the necessary higher-derivative terms in the tensor potential which bound the frequency. This was our motive for extending the EFT with a dimension-8

operator, as explained in appendix B.5.

3.3.2 pp-wave validity

The arguments which establish the pp-wave regime of validity follow very much along the same lines as those for the black hole spacetime. One major difference is that there are no non-vanishing scalar invariants built purely from background quantities on the pp-wave metric, meaning there are no bounds of the form (3.46). Naïvely, without the experience gained from the BH example, one might (wrongly) assume that the pp-wave regime of validity is trivial, that there are no constraints on its parameters, since the background metric as given in (3.10) is an exact solution to all orders in the EFT of gravity. However, as we have seen already from their equation of motion (3.39), metric perturbations spoil this exactness. We must still demand that their energy is under control, thus leading to a highly non-trivial EFT regime of validity for the pp-wave spacetime as soon as GWs are allowed to propagate.

Constraints on perturbations

In Brinkmann coordinates, the GW wavevector is $(k_\alpha) = (k_u, k_v, \mathbf{k})$. On the pp-wave spacetime, the v-momentum k_v is conjugate to the Killing vector ∂_v and is therefore analogous to the frequency ω on the BH spacetime, which is conjugate to its Killing vector ∂_t. Bounds on wave energy will take the form of bounds on k_v.

Aside from this difference, the strongest EFT validity requirements still arise from (3.52). Taking the $n \to \infty$ limit of (3.52) gives us our first EFT regime of validity bound:

$$(k_v \partial_i \partial_j H k_v)^2 \ll \Lambda^8$$

or

$$\partial_i \partial_j H \ll \frac{\Lambda^4}{k_v^2} \tag{3.58}$$

where this bound is understood to apply for any i, j. In particular, for the spherically symmetric point source, it can be written as

$$\partial_r^2 H \sim \frac{\partial_r H}{r} \ll \frac{\Lambda^4}{k_v^2}. \tag{3.59}$$

This represents a bound on the strength of the source at any given distance from its singularity

in transverse space.

Taking the $m \to \infty$ limit of (3.52a) gives

$$k^\alpha \nabla_\alpha \ll \Lambda^2, \tag{3.60}$$

where ∇ is understood to be acting on a scalar (i.e. the metric function $H(u, \mathbf{x})$). In particular, for a non-zero momentum in the v-direction k_v, we obtain a bound on the u-derivative of H:

$$\frac{\partial_u H}{H} \ll \frac{\Lambda^2}{k_v}. \tag{3.61}$$

Lastly, taking the $m \to \infty$ of (3.52b) gives

$$\tilde{\Box} \ll \Lambda^2, \tag{3.62}$$

where $\tilde{\Box}$ is understood to be acting on a scalar (e.g. H^2). Isolating the transverse Laplacian results in a distance-resolution scale (say, again, for the spherically symmetric source),

$$r \gg \Lambda^{-1}. \tag{3.63}$$

Below we gather the three EFT regime of validity bounds. On the left hand side, they are written in their generic form as they would apply without specifying a metric function explicitly. In the middle, they are specialised to the point-source metric (3.14). On the right hand side, they are further specified at a particular impact parameter $\mathbf{x} = \mathbf{b} = b\hat{\mathbf{b}}$, which (in an analogous fashion to the BH set-up) corresponds to the transverse distance at which a test GW passes by the pp-wave source as it probes the spacetime.

$$\tilde{\Box} \ll \Lambda^2 \qquad r \gg \Lambda^{-1} \qquad b \gg \Lambda^{-1} \tag{3.64a}$$

$$\partial_i \partial_j H \ll \frac{\Lambda^4}{k_v^2} \qquad \frac{\partial_r H}{r} \ll \frac{\Lambda^4}{k_v^2} \qquad \frac{j(u)}{b^d} \ll \frac{\Lambda^4}{k_v^2} \tag{3.64b}$$

$$k^\alpha \nabla_\alpha \ll \Lambda^2 \qquad \frac{\partial_u H}{H} \ll \frac{\Lambda^2}{k_v} \qquad \frac{j'(u)}{j(u)} \ll \frac{\Lambda^2}{k_v} \tag{3.64c}$$

The top line (3.64a) represents the familiar limit on the distance scales we may probe within the regime of the validity of the EFT. The middle line (3.64b), as mentioned previously, represents a bound on the strength of the pp-wave source at a given distance from the source. The last

line (3.64c) represents a bound on how quickly $j(u)$ many vary in u-time. The latter two depend not only on the EFT cut-off Λ, but also on the energy k_v of the gravitational wave probing the spacetime. This underlines the role that metric perturbations (or any other probe) play in establishing an EFT regime of validity on a pp-wave spacetime.

Explicit example

Once again, the above arguments to establish a regime of validity rely only on generic assumptions about the EFT series expansion, but were largely schematic. In this section, we will consider an explicit example of a truncated EFT expansion. As with the BH example, demanding that the higher-dimension operators in the expansion are subdominant to the GB operator will concretely reproduce the pp-wave regime of validity given in (3.64).

Consider the following effective action, which contains (3.4) as its leading-order part and then two further higher-dimension operators (including the same R^4-operator as in the BH example):

$$S_{\rm EFT} = \int \mathrm{d}^D x\sqrt{-g}\, M_{\rm Pl}^{D-2}\left(\frac{1}{2}R + \frac{c_{\rm GB}}{\Lambda^2}R^2_{\rm GB} + \frac{c_{\rm R3}}{\Lambda^4}R_{\alpha\beta\gamma\delta}R^{\gamma\delta\sigma\rho}R_{\sigma\rho}{}^{\alpha\beta} + \frac{c_{\rm R4}}{\Lambda^6}R_{\alpha\beta\gamma\delta}R^{\gamma\delta\sigma\rho}R_{\sigma\rho\kappa\lambda}R^{\kappa\lambda\alpha\beta} + \dots\right). \tag{3.65}$$

The full field equations for the background and perturbations are provided in appendix C. The pp-wave metric (3.10) of course remains an exact (background) solution to (3.65). Choosing lightcone gauge as before, the traceless components of the metric perturbations in the transverse directions h_{ij} remain the dynamical degrees of freedom. With the addition of the new operators, it is less straightforward to decouple the equations of motion and identify the master variables. In the case of the spherically symmetric point source, one can perform an scalar-vector-tensor decomposition on the transverse space with the result that the tensor modes Φ_T are immediately decoupled. For our purposes, it is enough just to consider their master equation, up to corrections of $\mathcal{O}(\Lambda^{-8})$:

$$0 = \tilde{\Box}\Phi_T - \frac{\kappa_T^2+2}{r^2}\Phi_T - 8\frac{c_{\rm GB}}{\Lambda^2}\frac{\partial_r H}{r}\partial_v^2\Phi_T + 24\frac{c_{\rm R3}}{\Lambda^4}\partial_v^2\left[d\frac{\partial_r H}{r^2}\left(\partial_r\Phi_T + \frac{\Phi_T}{r}\right) - \frac{\partial_u\partial_r H}{r}\partial_v\Phi_T\right] + 16\frac{c_{\rm R4}-12c_{\rm GB}c_{\rm R3}}{\Lambda^6}\left(\frac{\partial_r H}{r}\right)^2\partial_v^4\Phi_T, \tag{3.66}$$

where κ_T^2 is here the eigenvalue of the tensor spherical harmonic on the $(d-1)$-sphere. This equation can be expressed in v-momentum space by replacing $\partial_v \to -ik_v$. For the GB operator

to truly be the leading-order term in the EFT expansion, the contributions of the higher-order operators to this equation of motion ($\propto c_{\rm R3}, c_{\rm R4}$), specifically to the potential, should be subdominant to the contribution from the GB operator itself ($\propto c_{\rm GB}$). Assuming that the Wilson coefficients ($c_{\rm GB}, c_{\rm R3}, c_{\rm R4}$) are themselves $\mathcal{O}(1)$ numbers, then control of the EFT amounts to:

$$24d\frac{c_{\rm R3}}{\Lambda^4}\frac{\partial_r H}{r^3}\partial_v^2\Phi_T \ll 8\frac{c_{\rm GB}}{\Lambda^2}\frac{\partial_r H}{r}\partial_v^2\Phi_T \qquad \Longrightarrow \qquad r \ll \Lambda^{-1} \tag{3.67}$$

$$16\frac{c_{\rm R4}}{\Lambda^6}\left(\frac{\partial_r H}{r}\right)^2\partial_v^4\Phi_T \ll 8\frac{c_{\rm GB}}{\Lambda^2}\frac{\partial_r H}{r}\partial_v^2\Phi_T \qquad \Longrightarrow \qquad \frac{\partial_r H}{r} \ll \frac{\Lambda^4}{k_v^2} \tag{3.68}$$

$$24\frac{c_{\rm R3}}{\Lambda^4}\frac{\partial_u\partial_r H}{r}\partial_v^3\Phi_T \ll 8\frac{c_{\rm GB}}{\Lambda^2}\frac{\partial_r H}{r}\partial_v^2\Phi_T \qquad \Longrightarrow \qquad \frac{\partial_u H}{H} \ll \frac{\Lambda^2}{k_v} \tag{3.69}$$

which is exactly the regime of validity of the EFT obtained in the previous section (3.64). Note, it was not strictly necessary to include the dimension-8 operator $\sim$ Riemann^4 since the subleading correction from the dimension-6 operator produced the same term. Its inclusion illustrates that there is nothing particular about our choice of higher-dimension operators in reproducing the regime of validity. There are many possible higher-dimension operators whose presence in the EFT of gravity would constrain the parameters of the spacetime in the same way.

Regulating the shockwave (and friends) in the EFT of gravity

In light of the bounds (3.64) obtained above, the pp-wave solutions provided in section 3.1.2 need to be revisited. In particular, the singular shockwave solution $j_{\rm sw}(u)$ (3.16) is clearly against the spirit of the bound (3.64c) on $j'(u)/j(u)$. The shockwave may be regulated to bring it within the remit of the EFT by expressing it as a Gaussian,

$$j_{\rm sw}^{\rm reg}(u) = \alpha\frac{1}{\sqrt{2\pi L^2}}\exp\left[-\frac{u^2}{2L^2}\right]. \tag{3.70}$$

where α is a dimensionful constant. The singular shockwave is recovered in the limit of vanishing width, $\lim_{L\to 0} j_{\rm sw}^{\rm reg}(u) = j_{\rm sw}(u)$. Plugging the regulated expression into the left hand side of the bound (3.64c)

$$\left|\frac{\partial}{\partial u}\log j_{\rm sw}^{\rm reg}(u)\right| = \left|\frac{u}{L^2}\right| \quad \xrightarrow{L\to 0} \quad \infty \tag{3.71}$$

shows how the singular limit clearly violates the bound for any finite EFT cut-off Λ. It also provides a lower bound on the width of the regulated solution by evaluating at $u \sim L$,

$$L \gg \frac{k_v}{\Lambda^2}. \tag{3.72}$$

This means that the more highly-peaked the source (the smaller L), the slower the GW needs to be (the smaller k_v) in order to probe the spacetime within the regime of the validity of the EFT.

The sequence of shockwaves may be regulated in an analogous way: $j^{\rm reg}_{\rm ssw} = \sum j^{\rm reg}_{\rm sw}(u-u_i)$. Since each regulated shock now has a finite spread $\sim L$ and height $\sim \alpha L^{-1}$, if the distance between them shrinks, they become indistinguishable and approach a constant source $j(u) = j \sim \alpha L^{-1}$. Conversely, if they are to remain distinguishable, there must be a minimum u-separation between them $\Delta u \sim u_{i+1} - u_i > L$.

3.4 Chapter summary

In this chapter, we introduced the EFT of gravity as an expansion in higher-dimension curvature operators (3.1) before specialising to the leading-order action on a vacuum background in dimensions $D \geq 5$,

$$S_{\rm EGB} = \int \mathrm{d}^D x \sqrt{-g}\, M_{\rm Pl}^{D-2} \left(\frac{1}{2} R + \frac{c_{\rm GB}}{\Lambda^2} R^2_{\rm GB} + \dots \right). \tag{3.73}$$

We consider the following two vacuum solutions: first, the Schwarzschild-like BH,

$$\begin{aligned} &g_{\alpha\beta}\mathrm{d}x^\alpha \mathrm{d}x^\beta = -f(r)\mathrm{d}t^2 + \frac{1}{f(r)}\mathrm{d}r^2 + r^2 \mathrm{d}\Omega^2_{D-2}, \\ &f(r) = 1 - \left(\frac{r_g}{r}\right)^{D-3} + 2(D-3)(D-4) c_{\rm GB} \mu \left(\frac{r_g}{r}\right)^{2D-4} + \mathcal{O}\left(\mu^2\right), \end{aligned} \tag{3.74}$$

where $\mu = 1/(r_g \Lambda)^2$, and second the pp-wave with singular point sources,

$$\begin{aligned} &g_{\alpha\beta}\mathrm{d}x^\alpha \mathrm{d}x^\beta = 2\mathrm{d}u\mathrm{d}v + H(u,\mathbf{x})\mathrm{d}u^2 + \delta_{ij}\mathrm{d}x^i \mathrm{d}x^j, \\ &H(u,\mathbf{x}) = \sum_i \frac{j_i(u)}{|\mathbf{x} - \mathbf{b}_i|^{d-2}}. \end{aligned} \tag{3.75}$$

GW propagation on these backgrounds is governed by the following master equations. On

the BH background we have

$$-\partial_t^2\Phi_M + f\partial_r\left(f\partial_r\Phi_M\right) - V_M\Phi_M = 0, \tag{3.76}$$

where the potential $V_M = V_M(r)$ for the three types of perturbations $M \in \{S, V, T\}$ are given approximately in (3.31). On the point-like pp-wave background we have

$$2\partial_u\partial_v\Phi - H\partial_v^2\Phi + \nabla_d^2\Phi + A\frac{c_{\rm GB}}{\Lambda^2}\frac{\partial_r H}{r}\partial_v^2\Phi = 0, \tag{3.77}$$

where A is a real number given in (3.43) for the corresponding master variables in (3.41).

In the next chapter, we will ask whether GW propagation in this EFT, and on these backgrounds, is causal. To answer this question, it will prove crucial to understand the EFT's regime of validity. The regime of validity corresponds to the range of parameters (describing the background spacetime and GW energy) for which the EFT is under control, i.e. the regime in which (3.73) is truly the leading-order action. This will feed into the question of whether an apparent causality violation is resolvable within the EFT. On the BH background, the regime of validity is defined by the following four constraints:

$$\frac{r_g^{D-3}}{b^{D-1}} \ll \Lambda^2, \tag{3.78a}$$

$$b \gg \Lambda^{-1}, \tag{3.78b}$$

$$\omega^2 \ll \frac{\Lambda^4 b^{D-1}}{r_g^{D-3}}, \tag{3.78c}$$

$$\omega \ll \Lambda^2 b, \tag{3.78d}$$

where ω is the GW energy and b is the classical impact parameter. On the pp-wave background, the regime of validity is defined by the following three constraints:

$$b \gg \Lambda^{-1}, \tag{3.79a}$$

$$\frac{j(u)}{b^d} \ll \frac{\Lambda^4}{k_v^2}, \tag{3.79b}$$

$$\frac{j'(u)}{j(u)} \ll \frac{\Lambda^2}{k_v}, \tag{3.79c}$$

where k_v is the GW momentum in the v-direction.

Chapter 4

Causality

In this chapter, we explain how the question of causality arises in the EFT of gravity, provide a definition for causality in this context and show how it can be used to constrain (or not) the Wilson coefficients in the EFT expansion.

In GR, the speed of all massless particles minimally coupled to the background metric, including photons and gravitational waves, is the same constant $v_{m=0} = v_\gamma = v_{\rm GW} = 1$. In the EFT of gravity, the higher-order curvature operators modify the coupling of metric perturbations to the background metric and thus change their local speed of propagation in a background-dependent sense [35]. For example, consider the potential for tensor modes propagating on the BH background (B.20), reproduced here for convenience:

$$\begin{aligned}\frac{V_T}{f} = \frac{1}{r^2}\Bigg[&\kappa_T^2\left(1+8(D-1)c_{\rm GB}\mu\left(\frac{r_g}{r}\right)^{D-1}\right)\\ &+\frac{D(D-6)+16}{4}\left(1-\frac{32(D-1)(D-6)}{D(D-6)+16}c_{\rm GB}\mu\left(\frac{r_g}{r}\right)^{D-1}\right)\\ &+\frac{(D-2)^2}{4}\left(\frac{r_g}{r}\right)^{D-3}\left(1-\frac{6(D-4)(D^2-7D+4)}{D-2}c_{\rm GB}\mu\left(\frac{r_g}{r}\right)^{D-1}\right)\Bigg].\end{aligned} \tag{4.1}$$

From here, we can identify the angular speed $v_{\Omega T}$ of the tensor modes as the coefficient of κ_T^2/r^2,

$$v_{\Omega T}^2 = 1+8(D-1)c_{\rm GB}\mu\left(\frac{r_g}{r}\right)^{D-1}, \tag{4.2}$$

which deviates from 1 at leading-order in the EFT expansion ($\propto c_{\rm GB}\mu$) by an amount depending on the curvature of the background. (As a side note, we see from the Schrödinger equation (3.28) that the GB term does not modify the radial speed of GWs.) In theories with a positive Wilson coefficient $c_{\rm GB} > 0$, the tensor modes would be locally superluminal ($v_{\Omega T} > 1$). That is, they

could propagate slightly outside the lightcone set up by the background metric. To avoid such a fate, one might be tempted to conclude that causal UV theories must lead to only $c_{\rm GB} \leq 0$ when their heavy modes are integrated out. However, examination of the vector potential (B.33) reveals that their angular speed

$$v_{\Omega V}^2 = 1 - 4(D-1)(D-4)c_{\rm GB}\mu \left(\frac{r_g}{r}\right)^{D-1} \tag{4.3}$$

would be superluminal for $c_{\rm GB} < 0$. Thus, with this logic, it seems we should be forced to conclude that $c_{\rm GB} = 0$ is the only viable option and that the GB term is not a good, causal operator. This would be a rather unfortunate, since it is known that integrating out loops of heavy (e.g. Standard Model) fields leads to a non-zero $c_{\rm GB}$.

The implications for causality of the apparently enlarged lightcone have been considered in the literature [91–98]. However, an implicit assumption in such works (and the flawed argument above) is that EGB (or Lovelock, respectively) theory is a complete theory in and of itself. In [1, 2], we view EGB theory as just an effective theory of gravity, the leading orders in an infinite series. Within this context, it is important to ask whether any apparent violation of causality is *resolvable within the EFT's regime of validity*. As discussed in chapter 2, there is an optical resolution scale proportional to the wavelength of the propagating modes, as a consequence of Heisenberg's uncertainty principle. But without knowledge of the EFT regime of validity, there would be no reason to suspect that the magnitude of apparent causality violation could be limited (in a way made precise below) and thereby pushed into unresolvable territory. Said another way, without a proper understanding of the regime of validity, the superluminality of the vector/tensor modes could be made very large indeed.

Another reason that the above argument is flawed is that local superluminality alone is not necessarily problematic unless it can lead to closed time-like curves [35]. Depending on the spacetime, it may be possible for local superluminality to be compensated by subluminality later down the trajectory such that a closed time-like curve may never be achieved. To capture this cumulative effect, we instead calculate the time delay of a gravitational wave travelling between asymptotic infinities and scattering off a potential set up by the curvature of the spacetime in the interim.

On asymptotically flat spacetimes, one can define a generalised Eisenbud–Wigner time delay [59–62] from the energy-derivative of the phase shift, which are eigenvalues of the S-matrix.

The bulk of this chapter is dedicated to various classical, semi-classical and quantum methods for calculating the phase shift of a gravitational wave scattering off a BH or pp-wave spacetime. After that, it is simply a matter of differentiating with respect to ω, in the case of the BH, or k_v, in the case of the pp-wave, to obtain a time delay. Physically, this time delay represents the difference in journey time of a GW traversing the curved spacetime in question as compared to the same journey in flat (Minkowski) space. This is analogous to the scalar field examples of chapter 2 where the time delay was the difference in wave propagation between a non-trivial background field configuration and a zero-background field. However, unlike those toy examples, the time delay on a curved spacetime is non-vanishing even when the Wilson coefficient of the EFT operator is vanishing $\Delta T(c_{\rm GB} = 0) \neq 0$. The time delay may be split into two contributions:

$$\Delta T_{\rm net} = \Delta T_{\rm GR} + \Delta T_{\rm EFT} \tag{4.4}$$

where

$$\Delta T_{\rm GR} = \lim_{\Lambda\to\infty} \Delta T_{\rm net} \tag{4.5}$$

is known as the Shapiro time delay and represents the time delay due to the geometry of the spacetime in GR. The remaining contribution $\Delta T_{\rm EFT}$ captures terms from the expansion in the inverse cut-off scale, including explicitly terms from the GB operator ($\propto c_{\rm GB}$). It encodes the effect of interactions of the scattering particle with high-energy modes, inlcuding e.g. heavy Standard Model particles or higher-spin string states. While the GR time delay is in general positive on reasonable spacetimes, the EFT term may be positive or negative depending on the mode under consideration and the sign of $c_{\rm GB}$. This will become clear after some explicit calculations coming up in sections 4.3 and 4.4.

4.1 Infrared vs asymptotic causality

The definition of causality presented in [99] and used in the arguments of [31] is that the total time delay should be positive, i.e. there should be no net time advance,

$$\Delta T_{\rm net} > 0. \tag{4.6}$$

This is known as "asymptotic causality" because it corresponds to the condition that waves cannot travel faster than they would have on the asymptotic (in this case, Minkowski) spacetime.

Actually, as eluded to already in this chapter, and discussed previously in chapter 2, a small time advance is not a problem as long as it is not resolvable. The resolvability scale is set by the uncertainty principle for the scattering waves — a time delay for a wave of energy E is only resolvable if $E|\Delta T| \gtrsim 1$. As a consequence, asymptotic causality is really the weak positivity condition

$$\Delta T_{\text{net}} \gtrsim -E^{-1}, \tag{4.7}$$

where $E = \omega$ in the case of the BH spacetime and $E = k_v$ in the case of the pp-wave spacetime.

In this thesis, we take the different perspective that causality should be defined accounting for the local background geometry, and not just the asymptotic geometry. Our definition of "infrared causality" (so-named because it is solely determined from low-energy behaviour) is that EFT contribution to the time delay should be weakly positive,

$$\Delta T_{\text{EFT}} \gtrsim -E^{-1}. \tag{4.8}$$

In general, if this condition for infrared (IR) causality is satisfied, then the condition for asymptotic causality will be satisfied (since $\Delta T_{\text{GR}} \geq 0$), although the converse is not true. That is, asymptotic causality is a weaker condition than IR causality.

This stronger condition for causality is analogous to the field theory criteria that causality is determined by the front velocity (and not phase nor group velocities) of propagating waves. As stated in chapter 2, the front velocity is the same as the phase velocity of high-frequency (beyond the EFT regime of validity) modes. We consider the GR metric (the standard Schwarzschild metric in the BH case, and the same pp-wave metric) to represent the fundamental geometry that those high-frequency GWs are coupled to. Thus they, and all other massless particles minimally coupled to the metric, experience the GR time delay ΔT_{GR}. It is the universal time delay experienced by particles sticking always to the local lightcone of the background geometry. In this sense, having a net time delay of that value $\Delta T_{\text{net}} = \Delta T_{\text{GR}}$ corresponds to "having speed $v = 1$". The EFT time delay contribution ΔT_{EFT} is uniquely felt by low-frequency GWs due to their interactions with heavy states as captured in the EFT. A negative value of ΔT_{EFT} corresponds to travelling faster than speed $v = 1$ in aggregate which must be a result of violating relativistic causality locally via interactions with heavy states.

We will use this IR definition of causality in both sections 4.3 and 4.4 of this chapter. As we will see on both the BH and pp-wave spacetimes, there is no choice of Wilson coefficient

$c_{\rm GB}$ which will guarantee $\Delta T_{\rm EFT} > 0$ for all propagating GWs. This precisely corresponds to the different signs in the speeds of vector (4.3) and tensor (4.2) modes on the BH background discussed above. Therefore, the only possible recourse for the causality of the GB operator is to show that the *magnitude* of the EFT time delay is unresolvable for all propagating modes on both spacetimes, that is

$$|\Delta T_{\rm EFT}| \ll E^{-1}. \tag{4.9}$$

Recall, when checking this condition, we need only concern ourselves with the time delays of scattered GWs which are within the EFT regime of validity. Otherwise, there is no reason to trust that the EFT was a good description of physics to begin with. The bounds on the spacetime and wave parameters which define this regime were found in section 3.3. By applying these bounds, we will in fact find in all scenarios that the EFT time delay obeys

$$E|\Delta T_{\rm EFT}| \ll |c_{\rm GB}|. \tag{4.10}$$

Thus, we conclude that the GB operator, as it enters the EFT action in (3.4), is perfectly causal if and only if its Wilson coefficient is at most an order-one number,

$$\text{GB causal} \quad \Longleftrightarrow \quad |c_{\rm GB}| \lesssim \mathcal{O}(1). \tag{4.11}$$

Said another way, if we absorb $c_{\rm GB}$ into the scale Λ to define the "strong coupling scale" $\Lambda_{\rm sc} \sim \Lambda/c_{\rm GB}$, then there is no indication that the GB operator violates causality as long as the cut-off scale is not far above the strong coupling scale, $\Lambda \lesssim \Lambda_{\rm sc}$. An EFT has its limits and should not be abused beyond those limits. This is the main result of this chapter.

4.2 Toy example: Goldstone scalar

Before we turn to pure gravitational theories, we will first reconsider the Goldstone scalar field, this time minimally coupled to gravity. This toy example will serve as evidence for IR causality as the correct definition of causality. Consider, once again, the massless scalar with shift symmetry $\phi \to \phi + \text{constant}$ on a curved spacetime:

$$S_{\rm GS} = \int \mathrm{d}^D x \sqrt{-g} \left[-\frac{1}{2}(\nabla\phi)^2 + \frac{c_{\rm GS}}{\Lambda^D}(\nabla\phi)^4 + \dots \right]. \tag{4.12}$$

In this action, $(\nabla\phi)^4$ is considered the effective operator with Wilson coefficient $c_{\rm GS}$ and cut-off scale Λ. As we have seen in chapter 2, in the absence of gravity, there are known positivity bounds on the coefficient $c_{\rm GS}$ which demand that it is strictly positive $c_{\rm GS} > 0$ [13,16,17]. More recently, there have been efforts to establish analogous positivity bounds in the presence of gravity [100–103] with the conclusion that, for this type of operator,

$$c_{\rm GS} \gtrsim -\left(\frac{\Lambda}{M_{\rm Pl}}\right)^{D-2}, \tag{4.13}$$

up to numerical coefficients. In this section we will show how the condition of IR causality (4.8) correctly reproduces both the standard and the gravitational positivity bounds, while asymptotic causality (4.7) produces much weaker statements.

Consider the scalar on a general spherically symmetric background spacetime

$$\mathrm{d}s^2 = -B(r)^2\mathrm{d}t^2 + A(r)^2\mathrm{d}r^2 + r^2\mathrm{d}\Omega_{D-2}^2. \tag{4.14}$$

On a curved vacuum spacetime, such as a black hole, the metric coefficients would take values $B(r)^2 = A(r)^{-2} = f(r) = 1 - (r_g/r)^{D-3}$. And, if the Goldstone boson itself has a backreaction on the spacetime, the metric would be $B(r)^2 \sim A(r)^2 \sim 1 + h$. For the time being, we keep the metric quite general but we will return to these two cases.

The corresponding spherically symmetric background field configuration $\bar{\phi}(r)$ for the Goldstone boson is determined by

$$\bar{\phi}'(r) = \frac{\alpha}{r^{D-2}C(r)} \tag{4.15}$$

at leading order, where prime denote a derivative with respect to r, α is a constant and $C(r) = B(r)/A(r)$. Fluctuations around this background $\phi = \bar{\phi} + \delta\phi$ have the following equation of motion to leading order in the EFT, for each partial wave,

$$\begin{aligned}\frac{\partial^2\delta\phi_l}{\partial r^2} + \frac{\partial}{\partial r}\left[\ln(r^{D-2}C) - \frac{12c_{\rm GS}}{\Lambda^D}\left(\frac{\alpha}{r^{D-2}AC}\right)^2\right]\frac{\partial\delta\phi_l}{\partial r} \\ + \left(\frac{\omega^2}{C^2} - \frac{A^2\kappa_S^2}{r^2}\right)\left(1 + \frac{8c_{\rm GS}}{\Lambda^D}\left(\frac{\alpha}{r^{D-2}AC}\right)^2\right)\delta\phi_l = 0\end{aligned} \tag{4.16}$$

where

$$\delta\phi(t, r, \Omega_{D-2}) = e^{-i\omega t}\sum_{l=0}^{\infty}\delta\phi_l(r)Y_l(\Omega_{D-2}) \tag{4.17}$$

as usual. Defining

$$\chi_l = r^{\frac{D-2}{2}}\sqrt{C}\left[1 - \frac{6c_{\rm GS}}{\Lambda^D}\left(\frac{\alpha}{r^{D-2}AC}\right)^2\right]\delta\phi_l \tag{4.18}$$

we obtain an equation of the form

$$\frac{\mathrm{d}^2\chi_l}{\mathrm{d}r^2} + W_{\rm GS}(r)\chi_l(r) = 0 \tag{4.19}$$

where

$$W_{\rm GS}(r) = \omega^2\left(\frac{1}{C^2} - A^2\frac{b^2}{r^2}\right)\left(1 + \frac{8c_{\rm GS}}{\Lambda^D}\left(\frac{\alpha}{r^{D-2}AC}\right)^2\right) + \dots \tag{4.20}$$

to leading order in large-l and leading order in Λ^{-1}.

4.2.1 Asymptotic time delays

The equation of motion for the χ-field (4.19) is now in a form appropriate for a WKB analysis. Such an analysis is performed in appendix A with the main result that the phase shift due to a source $W_{\rm source}$ is

$$\delta = \frac{1}{2\omega}\int_b^\infty \mathrm{d}r \frac{W_{\rm source}(r)}{\sqrt{1 - b^2/r^2}}. \tag{4.21}$$

The time delay is calculated from the phase shift as

$$\Delta T = 2\left.\frac{\partial\delta}{\partial\omega}\right|_l. \tag{4.22}$$

There are three "sources" of a phase shift/time delay for the Goldstone scalar coupled to gravity. They are: the curvature of the background spacetime, the dimension-$(2D)$ effective operator in the action, and the gravitational backreaction of the scalar field on the spacetime. We will deal with each in turn.

On a BH background, in the weak field limit $r_g/r \ll 1$, we have

$$W_{\rm GS} = \underbrace{\omega^2\left(1 - \frac{b^2}{r^2}\right)}_{W_{\rm coord}} + \underbrace{\omega^2\left(\frac{r_g}{r}\right)^{D-3}\left(2 - \frac{b^2}{r^2}\right)}_{W_{\rm BH}} + \underbrace{\frac{8c_{\rm GS}\alpha^2\omega^2}{\Lambda^D r^{2D-4}}\left(1 - \frac{b^2}{r^2}\right)}_{W_{\rm EFT}} + \dots. \tag{4.23}$$

For the remainder of this section we will work with order-of-magnitude estimates, as it will be enough to establish the differences between asymptotic and IR causality. With this in mind, the time delay due to the BH background source (which is calculated by replacing $W_{\rm source}$ with $W_{\rm BH}$

in (4.21) explicitly in appendix A.4) is

$$\Delta T_{\rm BH} \sim \left(\frac{r_g}{b}\right)^{D-3} b \tag{4.24}$$

and the time delay due to the effective operator in the action (replace $W_{\rm source}$ with $W_{\rm EFT}$ in (4.21)) is

$$\Delta T_{\rm EFT} \sim \frac{c_{\rm GS}\alpha^2}{\Lambda^D b^{2D-5}}. \tag{4.25}$$

It remains to estimate the backreaction of the scalar field on the spacetime. In harmonic gauge, the linearised metric perturbations satisfy

$$\Box\left(h_{\alpha\beta} - \frac{1}{2}g_{\alpha\beta}h\right) = -\frac{2}{M_{\rm Pl}^{D-2}}T_{\alpha\beta}. \tag{4.26}$$

For the spherically symmetric scalar source (4.15) the stress-energy tensor has magnitude $T \sim \alpha^2/r^{2(D-2)}$ and thus the scale of metric perturbations is

$$h \sim \frac{\alpha^2}{M_{\rm Pl}^{D-2} r^{2(D-3)}}. \tag{4.27}$$

For the purposes of estimating the effect of the backreaction on the time delay, we take $A^2 \sim B^2 \sim 1 + h$ in the expression for $W_{\rm GS}$ (4.20) and find

$$W_{\rm br} \sim \frac{\omega^2 b^2 \alpha^2}{M_{\rm Pl}^{D-2} r^{2(D-2)}}, \tag{4.28}$$

with corresponding time delay,

$$\Delta T_{\rm br} \sim \frac{\alpha^2}{M_{\rm Pl}^{D-2} b^{2D-7}}. \tag{4.29}$$

The net time delay is the sum of the above three contributions (to leading order in each of the appropriate expansions):

$$\Delta T_{\rm net} \sim \frac{r_g^{D-3}}{b^{D-4}} + \frac{\alpha^2}{\Lambda^D b^{2D-5}}\left(c_{\rm GS} + \frac{b^2\Lambda^D}{M_{\rm Pl}^{D-2}}\right). \tag{4.30}$$

Recall, asymptotic causality is the condition that $\Delta T_{\rm net} \gtrsim -\omega^{-1}$, while IR causality is the condition that $\Delta T_{\rm EFT} \gtrsim -\omega^{-1}$. Both of these conditions would put a bound on the Wilson coefficient $c_{\rm GS}$. Clearly, if $c_{\rm GS}$ is positive then there is no violation of either causality condition because both $\Delta T_{\rm net}$ and $\Delta T_{\rm EFT}$ would be positive. If $c_{\rm GS}$ is negative, it may be possible to

generate a time advance. However, the magnitude, and thus resolvability, of that time advance depends on the allowed range for the other parameters in the theory. Just as in sections 2.1.3 and 3.3, we should determine the regime of validity of this EFT.

4.2.2 Regime of validity

A number of constraints carry over directly from the non-gravitational version of the Goldstone theory. As before, there is a distance resolution scale coming from the requirement that $\Box \cdot \text{scalar} \ll \Lambda^2 \cdot \text{scalar}$ meaning that the impact parameter is bounded from below: $b \gg \Lambda^{-1}$. In addition, the requirement that the background field is under control puts a bound on its magnitude:

$$\left(\nabla\bar{\phi}\right)^2 \ll \Lambda^D \quad \Longrightarrow \quad \frac{\alpha^2}{b^{2(D-2)}} \ll \Lambda^D. \tag{4.31}$$

Lastly from an EFT perspective, the energy of the scalar fluctuations cannot be too large, i.e. the Lorentz-invariant bound $k \cdot \nabla \ll \Lambda^2$ gives the bound on frequency $\omega \ll \Lambda^2 b$.

On top of the EFT requirements above, we must also demand that the backreaction of the scalar field on the gravitational field is under control, as that has been implicit in our calculations so far. This condition $h \ll 1$ gives us the following bound

$$\frac{\alpha^2}{M_{\rm Pl}^{D-2} b^{2(D-3)}} \ll 1, \tag{4.32}$$

which, as we will see, plays a crucial role in determining the correct gravitational bound on the Wilson coefficient $c_{\rm GS}$.

4.2.3 Asymptotic causality

Asymptotic causality is the condition that $\Delta T_{\rm net} \gtrsim -\omega^{-1}$, or

$$c_{\rm GS} \gtrsim -\frac{r_g^{D-3} b^{D-1} \Lambda^D}{\alpha^2} - \frac{b^{2D-5}\Lambda^D}{\omega\alpha^2} - \frac{b^2\Lambda^D}{M_{\rm Pl}^{D-2}}. \tag{4.33}$$

To find the tightest possible bound on $c_{\rm GS}$, we would want to make the RHS of the above as large as possible. Since the RHS is strictly negative, this corresponds to making its magnitude as small as possible. To this end, we choose $r_g \to 0$ so that the Schwarzschild contribution is negligible and we push the frequency to its maximum $\omega \sim \Lambda^2 b$ within the regime of validity. This

leaves us with

$$c_{\rm GS} \gtrsim -\frac{b^{2D-6}\Lambda^{D-2}}{\alpha^2} - \frac{b^2\Lambda^D}{M_{\rm Pl}^{D-2}}. \tag{4.34}$$

Now, we have a choice of bounds, the "background bound" (4.31) or the "backreaction bound" (4.32), to fix the maximum possible α. Since neither condition is obviously stronger, we try each in turn. Starting with the background bound (4.31), we have

$$c_{\rm GS} \gtrsim -\frac{1}{b^2\Lambda^2} - \frac{b^2\Lambda^D}{M_{\rm Pl}^{D-2}}. \tag{4.35}$$

The RHS of this inequality is extremised with respect to the impact parameter at $b^2 \sim M_{\rm Pl}^{(D-2)/2}/\Lambda^{(D+2)/2}$, which is well within the regime of validity $b \gg \Lambda^{-1}$ since Λ is generally well below the Planck mass. It can also be checked that the backreaction is under control at this impact parameter and choice of α, $h \sim (\Lambda/M_{\rm Pl})^{(D-2)/2} \ll 1$. At this value of b, both elements on the RHS of (4.35) contribute equally and we obtain the following bound on $c_{\rm GS}$,

$$c_{\rm GS} \gtrsim -\left(\frac{\Lambda}{M_{\rm Pl}}\right)^{\frac{D-2}{2}}. \tag{4.36}$$

Note that this is a weaker bound than the gravitational positivity bound (4.13) coming from [100–103].

If, instead, we use the backreaction bound (4.32) to set $\alpha^2 \sim b^{2D-6}M_{\rm Pl}^{D-2}$, we find

$$c_{\rm GS} \gtrsim -\left(\frac{\Lambda}{M_{\rm Pl}}\right)^{D-2} - b^2\Lambda^2\left(\frac{\Lambda}{M_{\rm Pl}}\right)^{D-2}. \tag{4.37}$$

This time, the minimum value of b is obtained from the background bound (4.31) with α already fixed, as above, to give $b \sim M_{\rm Pl}^{(D-2)/2}/\Lambda^{D/2}$. This leads to the even weaker bound on $c_{\rm GS}$,

$$c_{\rm GS} \gtrsim -1. \tag{4.38}$$

Therefore, the bound in (4.36) is the strongest bound on c to be had from asymptotic causality.

4.2.4 Infrared causality

Having seen how asymptotic causality produces weak bounds on the Wilsonian coefficient $c_{\rm GS}$, we will now show how IR causality exactly reproduces the known positivity bounds. IR causality is the condition that $\Delta T_{\rm EFT} \gtrsim -\omega^{-1}$. In this case, $\Delta T_{\rm EFT}$ is given by (4.25), so IR causality

means

$$c_{\rm GS} \gtrsim -\frac{b^{2D-5}\Lambda^D}{\omega\alpha^2} \tag{4.39}$$

Once again, maximising the RHS means setting the frequency to its maximum $\omega \sim \Lambda^2 b$,

$$c_{\rm GS} \gtrsim -\frac{b^{2D-6}\Lambda^{D-2}}{\alpha^2}, \tag{4.40}$$

and choosing a maximum for α. Mirroring the above discussion for asymptotic causality, we first choose $\alpha^2 \sim b^{2D-4}\Lambda^D$ from the background bound (4.31),

$$c \gtrsim -\frac{1}{(b\Lambda)^2}. \tag{4.41}$$

Now, since $b\Lambda$ can be made arbitrarily large with the appropriate choice of b, we effectively have $c_{\rm GS} > 0$, which is consistent with the standard positivity bound in Minkowski spacetime [13,16,17]. Really, we have just reproduced the result of section 2.1.3 by ignoring all gravitational input to the theory.

If, instead, we use the gravitational backreaction bound (4.32) to set $\alpha^2 \sim b^{2D-6}M_{\rm Pl}^{D-2}$, we find

$$c_{\rm GS} \gtrsim -\left(\frac{\Lambda}{M_{\rm Pl}}\right)^{D-2} \tag{4.42}$$

which is precisely the recent gravitational positivity bound (up to numerical coefficients) [100–103].

The lesson of this toy example is that IR causality correctly reproduces known positivity bounds where asymptotic causality fails, suggesting that IR causality is the correct definition of causality in theories with dynamical gravity.

4.3 Black hole spacetime

Having convinced ourselves that IR causality is a good definition, we will now apply it to GWs scattering in a BH background to show that the GB operator does not violate causality on this background. In complete analogy to the scalar field scattering problems of the previous section and of chapter 2, GW scattering in the central BH potential may be treated by a WKB approximation. Our approach is first to bring the Schrödinger-like master equation to a form appropriate for WKB analysis, then use the results of appendix A to calculate the asymptotic time delay.

4.3.1 Scattering phase shift and time delays

The master equations for GWs on a Schwarzschild BH background are given by (3.28) for each mode $M \in \{S, V, T\}$ where the scalar/vector/tensor potentials are given by (B.50), (B.33) and (B.20) respectively, or to leading order in large-l by (3.31). Performing a field redefinition to remove the single derivative term from the equation, and making a wave-ansatz for the time dependence of the solution,

$$\Phi_M(t, r) = \frac{e^{-i\omega t}}{\sqrt{f}} \chi_M(r), \tag{4.43}$$

the master equation becomes

$$\frac{\mathrm{d}^2 \chi_M}{\mathrm{d}r^2} + W_M(r) \chi_M = 0, \tag{4.44}$$

where

$$W_M(r) = \frac{\omega^2 - V_M}{f^2} - \frac{f''}{2f} + \left(\frac{f'}{2f}\right)^2. \tag{4.45}$$

The master equation is now in an appropriate form for the WKB analysis described in appendix A. We focus on the high-energy regime $l \sim b\omega \gg 1$ where issues of causality could potentially arise, and assume $b \gg r_g$ to avoid quantum complications at the horizon. In these eikonal $l \gg 1$ and weak-field $r \gg r_g$ limits, the leading-order terms in the functions W_M are

$$W_M \approx \underbrace{\omega^2 \left(1 - \frac{b^2}{r^2}\right)}_{W_{\text{coord}}} + \underbrace{\omega^2 \left(\frac{r_g}{r}\right)^{D-3} \left(2 - \frac{b^2}{r^2}\right)}_{W_{\text{GR}}} + \underbrace{A_M c_{\text{GB}} \mu \omega^2 \left(\frac{r_g}{r}\right)^{D-1} \frac{b^2}{r^2}}_{W_{\text{EFT}}} \tag{4.46}$$

where, as a reminder, the numbers A_M are

$$A_T = 8(D-1), \quad A_V = -4(D-1)(D-4), \quad A_S = -8(D-1)(D-4). \tag{4.47}$$

From here, it is clear that the asymptotic time delay of the GWs will have the two contributions claimed in the introduction to this chapter (4.4). The first is the "GR" Shapiro time delay. It is the exact same as the "BH" effect felt by the Goldstone boson in the previous section, and is calculated explicitly in appendix A.4. The second is due to the EFT coupling of the GWs with the curved background spacetime. The asymptotic phase shift due to this term may be calculated by (see appendix A for derivation)

$$\delta_{\text{EFT}} = \frac{1}{2\omega} \int_b^\infty \mathrm{d}r \frac{W_{\text{EFT}}(r)}{\sqrt{1 - b^2/r^2}}. \tag{4.48}$$

with the result that the net time delays (at fixed-l) for the three types of perturbations are

$$\Delta T^{T}_{\rm net} = \Delta T_{\rm GR}\left(1 - \frac{8(D-1)(D-4)}{D-3} c_{\rm GB}\mu \left(\frac{r_g}{b}\right)^2\right), \tag{4.49a}$$

$$\Delta T^{V}_{\rm net} = \Delta T_{\rm GR}\left(1 + \frac{4(D-1)(D-4)^2}{D-3} c_{\rm GB}\mu \left(\frac{r_g}{b}\right)^2\right), \tag{4.49b}$$

$$\Delta T^{S}_{\rm net} = \Delta T_{\rm GR}\left(1 + \frac{8(D-1)(D-4)^2}{D-3} c_{\rm GB}\mu \left(\frac{r_g}{b}\right)^2\right), \tag{4.49c}$$

where

$$\Delta T_{\rm GR} = \frac{(D-2)\sqrt{\pi}}{2}\frac{\Gamma\left(\frac{D-4}{2}\right)}{\Gamma\left(\frac{D-3}{2}\right)}\left(\frac{r_g}{b}\right)^{D-3} b. \tag{4.50}$$

Note that the time delays vanish in the Minkowski limit $r_g \to 0$, as they should by definition. Also, all three time delays agree in the GR limit $c_{\rm GB} \to 0$, which is another reflection of the universal speed of massless perturbations in GR.

When the GB term is included, the time delay experienced by GWs depends on their polarisation. If, for example, $c_{\rm GB}$ is positive then the tensor modes gain a time advance as compared to the GR time delay, while the vectors and scalars receive an additional delay. This is consistent with the expectation that tensor modes would travel superluminally, while vectors and scalars would travel subluminally for $c_{\rm GB} > 0$. As claimed previously, there is no choice of $c_{\rm GB}$ for which $\Delta T^{M}_{\rm EFT} > 0$ for all three $M \in \{S, V, T\}$. Thus, we are faced with an apparent violation of IR causality. It may also seem possible to violate asymptotic causality by choosing $b^2 \sim c_{\rm GB}\mu r_g^2 = c_{\rm GB}\Lambda^{-2}$ so that $\Delta T^{M}_{\rm EFT}$ could rival $\Delta T_{\rm GR}$ in magnitude. Then, since at least one $\Delta T^{M}_{\rm EFT}$ must be negative, it would be possible to have a negative net time delay (i.e. time advance). This is analogous to the shockwave situation in reference [31] where, in their notation, $b^2 \sim |\lambda_{GB}|$ (e.g. below their equation (2.19)).

4.3.2 Unresolvability of EFT time delay

Despite appearances, our central claim in [1] is that *there is no violation of either causality condition when the EFT regime of validity is properly accounted for.* The regime of validity is defined on the BH background in section 3.3.1. It amounts to four constraints (3.49), (3.50), (3.53) and (3.54) which bound the curvature of the background spacetime and the energy of the propagating GWs. We show below that to violate either causality condition (4.7) or (4.8) would require going to energies beyond this regime and thus does not represent a true violation

of causality at all.

As said at the end of the last subsection, to stand a chance of generating an asymptotic acausality, one would need to push the impact parameter down to $b^2 \sim c_{\rm GB}\Lambda^{-2}$. Assuming $c_{\rm GB} \sim \mathcal{O}(1)$, as we have throughout, this represents a simple and immediate violation of (3.50). So there is certainly no violation of asymptotic causality in the regime in which the EFT can be trusted as a good description of physics.

As for the stronger IR causality condition, consider the magnitude of the GB contribution to the time delay relative to the GW frequency:

$$\omega\left|\Delta T^M_{\rm EFT}\right| \sim |c_{\rm GB}|\mu\omega b\left(\frac{r_g}{b}\right)^{D-1} \sim |c_{\rm GB}|\frac{\omega}{b\Lambda^2}\left(\frac{r_g}{b}\right)^{D-3}, \tag{4.51}$$

where we have used $\mu = (r_g\Lambda)^{-2}$. Using either bound on frequency (3.53) or (3.54) provides effectively the same result. Firstly, applying (3.53):

$$\omega\left|\Delta T^M_{\rm EFT}\right| \ll |c_{\rm GB}|\left(\frac{r_g}{b}\right)^{\frac{D-3}{2}} \ll |c_{\rm GB}|, \tag{4.52}$$

assuming $b \gg r_g$. Or, applying (3.54) gives the slightly stronger

$$\omega\left|\Delta T^M_{\rm EFT}\right| \ll |c_{\rm GB}|\left(\frac{r_g}{b}\right)^{D-3} \ll |c_{\rm GB}|. \tag{4.53}$$

Either way, we arrive at the same conclusion: the GB time delay is unresolvable $\left|\Delta T^M_{\rm EFT}\right| \ll \omega^{-1}$ for $|c_{\rm GB}| \lesssim \mathcal{O}(1)$. Thus, in this context, the EFT described by the action (3.4) is causal. This conclusion holds regardless of the magnitude of the other parameters in the theory. It does not matter how heavy the black hole is, or how big the scale Λ is, as long as they are within the regime of validity of the EFT then GW propagation is causal. The same result is obtained for cosmological solutions in [36].

Having found that one BH could not generate a resolvable causality violation, a natural question is whether many BHs could? Could enough small (unresolvable) time advances be accumulated, one after another, to generate one large (resolvable) time advance? We claim the answer is no. To study this scenario, we turn to the analog pp-wave system. We will find that, effectively, the scattering problem cannot be sustained for long enough in a multi-shock (analog multi-BH), EFT-valid spacetime to generate a resolvable time advance. So once again, there will be no violation of causality.

4.4 pp-wave spacetime

The set-up for the scattering problem in the pp-wave spacetime is somewhat different from the BH spacetime. The conserved quantity is now momentum k_v in the v-direction, rather than energy ω, of the scattering particle. As we will see below, the other null coordinate u plays the roll of time in this Schrödinger-like problem. At any instance in time u_0, the potential $V(u_0, \mathbf{x})$ extends in the v-direction with a constant strength determined by $j(u_0)$ and decays in the transverse direction as $1/r^{d-2}$. If the source $j(u)$ is "switched on" for long enough (i.e. doesn't decay to zero with growing u), the ultimate fate of any particle at finite transverse distance from the source is to collide with the source. Thus, to maintain a well-defined scattering problem, the pp-wave source needs to be "switched off" before scattering in the transverse direction becomes too significant. The aim of this section is to estimate the maximum allowable scattering time, according to the given initial impact parameter b and v-momentum k_v, and from there estimate the phase shift/time delay of the scattered particle. A fully quantum definition and calculation of the time delay is postponed until section 4.4.3. First, we discuss some more intuitive (semi-)classical derivations and arguments that bound the magnitude of the time delay.

4.4.1 Classical time delay

For now, we will consider the behaviour of a point-like test particle scattering on a point-like pp-wave background (see figure 3.1 for possible background spacetime configurations). This captures the main physics at play, except for the possibility of an equilibrium point in the potential, which will be addressed later at the end of this subsection. The test particle's phase shift can only be calculated in the limit where scattering is minimal. Within this limit, the EFT contribution to the time delay is here shown to be unresolvable when the EFT-validity bounds of section 3.3.2 are applied. Outside this limit, scattering is significant enough that the test particle would soon collide with the singular source and the concept of "asymptotic phase shift" loses meaning.

Scattering due to point source

After performing a Fourier transform in the v-coordinate $\partial_v \to ik_v$, the EGB master equation for the point-source (3.42) can be recast as a Schrödinger equation

$$i\frac{\partial}{\partial u}\Phi(u,\mathbf{x}) = -\frac{1}{2k_v}\nabla_d^2\,\Phi(u,\mathbf{x}) + V(u,\mathbf{x})\Phi(u,\mathbf{x}) \tag{4.54}$$

where the u-coordinate plays the role of time, $\nabla_d^2 = \partial_i\partial^i$ is the Laplacian on the d-dimensional transverse Euclidean space and the potential term arises from the curvature of the spacetime. With this language, we can treat the metric perturbations as a particle of mass k_v being scattered off a potential V sourced by the pp-wave metric. At present, we leave the u-dependence of the source arbitrary. The point source potential is

$$V(u,r) = -\frac{k_v}{2}H(u,r) + Ak_v\frac{c_{\rm GB}}{\Lambda^2}\frac{\partial_r H(u,r)}{r}, \tag{4.55}$$

where A is some number depending on the particular master variable mode.

Recall, our criteria for acausality is being able to generate a resolvably large EFT time advance within the regime of validity defined by (3.64). We will return to make a precise quantum calculation of the time delay in section 4.4.3, but for now we will follow the approximations taken in [31] and neglect scattering in the transverse directions. This amounts to ignoring the Laplacian-term in (4.54) so that the particle deviates from its initial configuration only by a phase. Setting up our initial conditions $\Phi = \Phi_0$ at time $u = 0$ with initial particle displacement $\mathbf{x} = \mathbf{b} = b\hat{\mathbf{b}}$, then the approximate solution at a later time is

$$\Phi(u,\mathbf{b}) = \Phi_0 \exp\left[i\delta(u,\mathbf{b})\right], \tag{4.56}$$

$$\delta(u,\mathbf{x}) = -\int_0^u \mathrm{d}u' V(u',\mathbf{x}). \tag{4.57}$$

The corresponding time delay accumulated up until time u is thus

$$\begin{aligned}\Delta T_{\rm net}(u) &= \left.\frac{\partial\delta(u,\mathbf{x})}{\partial k_v}\right|_{\mathbf{x}=\mathbf{b}} \\ &= -\frac{1}{k_v}\int_0^u \mathrm{d}u' V(u',\mathbf{x})\Big|_{\mathbf{x}=\mathbf{b}} \\ &= \left(\frac{1}{2}\int_0^u \mathrm{d}u' H(u',r) - A\frac{c_{\rm GB}}{\Lambda^2}\int_0^u \mathrm{d}u'\frac{\partial_r H(u',r)}{r}\right)\Big|_{r=b}.\end{aligned} \tag{4.58}$$

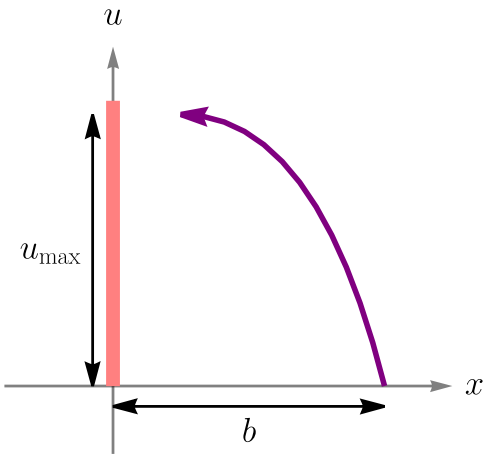

Figure 4.1: The probe particle (purple) scatters in the transverse directions on the pp-wave spacetime. It begins a distance b from the source (pink) and approaches the source after a finite time $u_{\max}$.

(Note, the time delay defined in the first line above differs from the definition in the BH spacetime by a factor of 2. The reason for this difference is simply because we have "switched on" the interaction at finite time ($u = 0$) and distance ($\mathbf{x} = \mathbf{b}$), without allowing the test-particle to approach from asymptotic infinity. The factor of 2 in the BH case reflected the symmetry of that scattering problem.) As anticipated, there are two contributions to this expression. The first $\Delta T_{\rm GR}(u)$ is from the non-trivial spacetime curvature (represented by the metric function H) and would be present in any theory of gravity, including GR. The second term $\propto c_{\rm GB}$ is due to the presence of the GB operator in the action. The criteria for IR causality [1] is that the GB contribution is not resolvably negative $\Delta T_{\rm EFT}(u) \gtrsim -k_v^{-1}$. Since the theory contains propagating modes for which the constant A can be either positive or negative (3.43), neither sign choice for $c_{\rm GB}$ can guarantee causality on this spacetime either. As such, the magnitude of the EFT time delay $|\Delta T_{\rm EFT}(u)|$ must be bounded from above to preserve causality.

On the pp-wave spacetime, it turns out that the GB contribution to the time delay cannot be meaningfully bounded from above by EFT validity constraints (3.64) alone. However, the key is that the approximations used to obtain (4.58) do not hold for all time. As such, we need only concern ourselves with the magnitude of the time delay accumulated by some time $u_{\max}$ when our approximations break down. Physically, this is the time at which the particle has scattered significantly in the transverse directions so as to make the ∂_i-derivatives non-negligible, see figure 4.1.

A Newtonian perspective

An estimate for this time can be obtained by considering the classical trajectory a particle of mass k_v experiencing a force due to the potential $V(u, \mathbf{x})$ would follow:

$$k_v \frac{d^2\mathbf{x}}{du^2} = -\boldsymbol{\nabla} V(u, \mathbf{x}). \tag{4.59}$$

Since the main contribution to the potential is from the GR term, we will neglect the GB term for the sake of estimating $u_{\max}$. The amount scattered in the transverse direction is thus approximately

$$\Delta r(u) \sim -\frac{1}{k_v} \int_0^u \mathrm{d}u' \int_0^{u'} \mathrm{d}u'' \partial_r V(u, r)\Big|_{r=b} \sim -\int_0^u \mathrm{d}u' \int_0^{u'} \mathrm{d}u'' \partial_r H(u, r)\Big|_{r=b}, \tag{4.60}$$

and $u_{\max}$ is defined by the condition

$$\Delta r(u_{\max}) \sim b \quad \Longrightarrow \quad \int_0^{u_{\max}} \mathrm{d}u \int_0^u \mathrm{d}u' \frac{j(u')}{b^d} \sim 1. \tag{4.61}$$

This could be understood in two ways. First, if the parameters of the spacetime background (i.e. $j(u)$) are fixed, (4.61) tells us the timescale on which the test particle is expected to encounter the source singularity. In other words, the source must be switched off by time $u_{\max}$ to avoid significant corrections to (4.58). The second option is to view the time $u_{\max}$ as arbitrary, and (4.61) as a condition on the strength of the source in order to avoid collision by that time (just).

Returning to consider the maximum EFT time delay generated by time $u_{\max}$,

$$|\Delta T_{\mathrm{EFT}}(u_{\max})| \sim \frac{|c_{\mathrm{GB}}|}{\Lambda^2} \int_0^{u_{\max}} \mathrm{d}u \frac{j(u)}{b^d}, \tag{4.62}$$

and making the judicious choice to express $j(u)$ as the integral of its derivative,

$$|\Delta T_{\mathrm{EFT}}(u_{\max})| \sim \frac{|c_{\mathrm{GB}}|}{\Lambda^2} \int_0^{u_{\max}} \mathrm{d}u \int_0^u \mathrm{d}u' \frac{j'(u')}{b^d}, \tag{4.63}$$

and finally applying the EFT-validity bound (3.64c) $j'(u)/j(u) \ll \Lambda^2/k_v$, we obtain the desired result with the application of (4.61):

$$|\Delta T_{\mathrm{EFT}}(u_{\max})| \ll \frac{|c_{\mathrm{GB}}|}{k_v} \int_0^{u_{\max}} \mathrm{d}u \int_0^u \mathrm{d}u' \frac{j(u')}{b^d} \sim \frac{|c_{\mathrm{GB}}|}{k_v}. \tag{4.64}$$

That is, $k_v|\Delta T_{\rm EFT}(u_{\rm max})| \ll c_{\rm GB}$, or the EFT time delay is unresolvable for any $|c_{\rm GB}| \lesssim \mathcal{O}(1)$.

A WKB perspective

For a more sophisticated argument, rather than just ignoring the spatial derivatives, we will treat them perturbatively via a WKB-type approximation. Now treating

$$\Phi(u,\mathbf{x}) = \Phi_0 \exp\left[i\delta(u,\mathbf{x})\right] \tag{4.65}$$

as an ansatz for the full solution, the phase must obey

$$-\frac{\partial\delta\left(u,\mathbf{x}\right)}{\partial u} = \frac{1}{2k_v}\left(\boldsymbol{\nabla}\delta\left(u,\mathbf{x}\right)\right)^2 - \frac{i}{2k_v}\nabla_d^2\delta\left(u,\mathbf{x}\right) + V\left(u,\mathbf{x}\right). \tag{4.66}$$

The leading-order solution $\delta^{(0)}\left(u,\mathbf{x}\right)$ in the WKB expansion is already given by (4.57). The first correction $\delta^{(1)}\left(u,\mathbf{x}\right)$ is obtained by substituting the leading term back into (4.66),

$$-\frac{\partial\delta^{(1)}\left(u,\mathbf{x}\right)}{\partial u} = \frac{1}{2k_v}\left(\boldsymbol{\nabla}\delta^{(0)}\left(u,\mathbf{x}\right)\right)^2 - \frac{i}{2k_v}\nabla_d^2\delta^{(0)}\left(u,\mathbf{x}\right). \tag{4.67}$$

Given that V is harmonic, the solution is simply

$$\delta^{(1)}\left(u,\mathbf{x}\right) = -\frac{1}{2k_v}\int_0^u \mathrm{d}u'\left(\int_0^{u'}\mathrm{d}u''\boldsymbol{\nabla}V\left(u'',\mathbf{x}\right)\right)^2. \tag{4.68}$$

Using the magnitude of this correction term as a proxy for the effects of scattering, we say $u_{\rm max}$ is the time at which it becomes comparable to $\delta^{(0)}(u,\mathbf{x})$. At the level of the phase equation (4.66), we ask when their partial-u derivatives become comparable, i.e.

$$\frac{1}{2k_v}\left(\int_0^{u_{\rm max}}\mathrm{d}u\boldsymbol{\nabla}V\left(u,\mathbf{x}\right)\right)^2 \sim V\left(u_{\rm max},\mathbf{x}\right). \tag{4.69}$$

Evaluating at the initial impact parameter b, the condition for $u_{\rm max}$ is (c.f. (4.61))

$$\int_0^{u_{\rm max}}\mathrm{d}u\frac{j(u)}{b^d} \sim \sqrt{\frac{j(u_{\rm max})}{b^d}}. \tag{4.70}$$

The left hand side of (4.70) can be directly replaced by the right in the expression for the

EFT time delay (4.62) to give

$$|\Delta T_{\rm EFT}(u_{\rm max})| \sim \frac{|c_{\rm GB}|}{\Lambda^2}\sqrt{\frac{j(u_{\rm max})}{b^d}}. \tag{4.71}$$

We can now deploy a second EFT validity bound (3.64b), in the form $\sqrt{j(u)/b^d} \ll \Lambda^2/k_v$, to arrive again at the expected result: $k_v|\Delta T_{\rm EFT}(u_{\rm max})| \ll |c_{\rm GB}|$.

Neither of the above arguments required a specific choice for the time-dependence of the background spacetime, $j(u)$. The conclusion — that the EFT contribution to the time delay is unresolvable for $|c_{\rm GB}| \lesssim \mathcal{O}(1)$ — holds for any choice of spherically symmetric pp-wave. Regardless of whether there is one shockwave or many shockwaves, as long as they are contained within time $u_{\rm max}$ and respect the EFT regime of validity, there is no violation of causality.

Scattering due to balancing source

Aside from the EFT validity bounds, it should now be clear that the obstruction to generating an observably large EFT time advance is scattering in the transverse directions. This scattering is the result of an attractive gravitational potential pulling waves propagating in the v-direction towards the source. The source must be "switched off" before the wave encounters the singularity (before time $u_{\rm max}$), or else the question of its time delay loses all meaning.

Naïvely, it may seem like this fate could be avoided by engineering an equilibrium point in the potential at which the v-moving-waves could sit without deviation. To this end, we now consider the balanced metric function (3.15), which sets up a symmetric potential sourced by two pp-waves located at $\mathbf{x} = \pm\mathbf{b}$. The GR term in the potential is

$$V(u,\mathbf{x}) = -\frac{k_v j(u)}{2}\left(\frac{1}{|\mathbf{x}-\mathbf{b}|^{d-2}} + \frac{1}{|\mathbf{x}+\mathbf{b}|^{d-2}}\right). \tag{4.72}$$

We refer to this scenario as "balancing" pp-waves because there is an unstable equilibrium at $\mathbf{x} = \mathbf{0}$ at which the forces are perfectly balanced, $\boldsymbol{\nabla} V = 0$. An ideal point particle perfectly localised at the origin in transverse space could move in the v-direction without fear of scattering into a gravitational well. In terms of the previous arguments, it is clear that both strategies for obtaining a $u_{\rm max}$ (4.59) and (4.69), which rely on a non-zero gradient of the potential, are now scuppered.

However, with the potential being unstable along the $\mathbf{b}$-direction, any small perturbation will lead to an instability on a timescale associated to the second derivative of the potential in

that direction. If the sources were not time-dependent and, for example, aligned along the z-axis $\mathbf{b} = b\,\hat{\mathbf{z}}$, this would simply be

$$u_{\text{inst}} \sim \frac{1}{|\omega|}, \tag{4.73}$$

$$\omega^2 = \frac{1}{k_v}\frac{\partial^2 V(\mathbf{x})}{\partial z^2}\bigg|_{\mathbf{x}=\mathbf{0}}, \tag{4.74}$$

where ω is the imaginary instability frequency of the unstable direction. Quantum in nature, our test particle's position will be inherently uncertain and thus experience fluctuations which will trigger this instability. It is therefore impossible to truly "balance" a quantum particle in such an attractive potential.

In the case of a time-dependent problem $\omega = \omega(u)$, it is useful to consider again the classical equation of motion in the z-direction near the origin,

$$k_v \frac{d^2 z}{du^2} = -\frac{\partial V(u,z)}{\partial z} \approx -k_v \omega^2(u) z. \tag{4.75}$$

Assuming that the potential is slowly varying in space, we may once more use a WKB approximate solution

$$z(u) \propto \frac{1}{\omega(u)^{1/2}} \exp\left[\pm i \int_0^u \mathrm{d}u' \omega(u')\right] \tag{4.76}$$

to see that the instability emerges around

$$\left|\int_0^{u_{\text{inst}}} \mathrm{d}u\, \omega(u)\right| \sim \int_0^{u_{\text{inst}}} \mathrm{d}u \sqrt{\frac{j(u)}{b^d}} \sim 1. \tag{4.77}$$

Treating u_{inst} as our u_{max} (c.f. (4.61) and (4.70)) we can again bound the maximum achievable EFT time delay. The master equations in the balancing potential are very similar to the point source potential and can be found in appendix C.2. The parameter dependence of the EFT-induced time delay is still given by (4.62). This time, first applying the (square-rooted) EFT validity bound (3.64b) $\sqrt{j(u)/b^d} \ll \Lambda^2/k_v$ and then using the expression for the instability timescale (4.77) we arrive at the (by this point, usual) conclusion:

$$|\Delta T_{\text{EFT}}(u_{\text{max}})| \sim \frac{|c_{\text{GB}}|}{\Lambda^2}\int_0^{u_{\text{max}}} \mathrm{d}u \frac{j(u)}{b^d} \ll \frac{|c_{\text{GB}}|}{k_v}\int_0^{u_{\text{max}}} \mathrm{d}u \sqrt{\frac{j(u)}{b^d}} \sim \frac{|c_{\text{GB}}|}{k_v}, \tag{4.78}$$

i.e. the EFT time delay is unresolvable for $|c_{\text{GB}}| \lesssim \mathcal{O}(1)$.

4.4.2 Becoming quantum

A crucial fact which has been brushed over in the above discussion is that a generic initial scalar field configuration Φ_0 will typically have support beyond a single point. Viewed as a wavefunction for a quantum particle, it must at least obey the uncertainty principle $\Delta\mathbf{x} \cdot \Delta\mathbf{k} \gtrsim 1$ and thus have some spread in transverse space. Viewed as a field in a low energy EFT, its spatial extent $\sigma \sim |\Delta\mathbf{x}|$ is additionally bounded below by the EFT cut-off as $\sigma \gg \Lambda^{-1}$ (see appendix D.1 for a precise argument). In the balancing case above, this means that a realistic state cannot be perfectly localised at the equilibrium point and will always feel the effects of the potential's gradient away from that point. In fact, there are two effects which drive a localised quantum state away from the equilibrium:

1. free-field diffusion and

2. scattering due to the attractive gravitational potential.

To see these effects in action, consider an initial spherically symmetric Gaussian profile,

$$\Phi_0(\mathbf{x}) = \frac{1}{(2\pi\sigma^2)^{d/4}} \exp\left[-\frac{\mathbf{x}^2}{4\sigma^2}\right], \tag{4.79}$$

centred on the origin with width σ much smaller than the distance to the source(s) $\sigma \ll b$. After time u under free evolution, the wavepacket for a particle of mass k_v will diffuse to an effective width of $\sigma^2_{\text{eff}}(u) = \sigma^2 + (u/2k_v\sigma)^2$. Relative to the pp-wave background, we say diffusion of the wavepacket is "complete" when its effective width is comparable to its distance from the source(s),

$$\sigma_{\text{eff}}(u_{\text{diff}}) = b \quad \Longrightarrow \quad u_{\text{diff}} = 2k_v\sigma\sqrt{b^2 - \sigma^2}. \tag{4.80}$$

Thus the wavefunction $\Phi(u, \mathbf{x})$ can no longer be considered localised after a finite time u_{diff} and its time delay is not well captured by (4.58). Moreover, on top of diffusion, the wavefunction is now subject to scattering by the source(s) because at most one point of measure-zero can be at equilibrium. The remainder of the wavepacket is probing points with non-zero potential gradient and feels the tug of the pp-waves.

To correctly account for both of these effects, and to see the limitation they impose on the time delay, it is necessary to perform a fully quantum calculation as in the next section. Nonetheless, the result of the last section will remain unchanged: bounds imposed due to scattering in the transverse space render the GB time delay unresolvable within the EFT regime of validity.

4.4.3 Quantum time delay

As eluded to earlier, the scattering process described by the Schrödinger equation (4.54) has a well-defined S-matrix $\hat{S}$ if the source is only switched on for a finite amount of time so that the scattered particle may escape to asymptotic infinity. The eigenvalues of $\hat{S}$ are then exactly the asymptotic phase shifts $e^{i\delta}$ of its eigenstates. An Hermitian time delay operator, known as the Wigner–Smith operator [61, 62], can thus be defined in terms of the S-matrix as

$$\widehat{\Delta T} = -i\hat{S}^\dagger \frac{d\hat{S}}{dk_v}. \tag{4.81}$$

Connection can be made with the semi-classical definition in (4.58) by acting with $\widehat{\Delta T}$ on an eigenstate of $\hat{S}$. Denoting the eigenstates by $|\delta\rangle$, then we see

$$\widehat{\Delta T}\,|\delta\rangle = -ie^{-i\delta}\frac{d(e^{i\delta})}{dk_v}\,|\delta\rangle = \frac{d\delta}{dk_v}\,|\delta\rangle\,, \tag{4.82}$$

i.e. eigenstates of the S-matrix are eigenstates of the time delay operator with eigenvalues precisely equal to the semi-classical expression. In this formalism, causality is equivalent to an unresolvable (and/or strictly positive) EFT contribution to the expectation value of $\widehat{\Delta T}$ for any physical state $|\Phi\rangle$,

$$\langle\widehat{\Delta T}\rangle^{\Phi}_{\rm EFT} \equiv \langle\Phi|\,\widehat{\Delta T}\,|\Phi\rangle_{\rm EFT} \gtrsim -k_v^{-1}. \tag{4.83}$$

Below we will use tools from perturbation theory in the interacting picture to calculate $\langle\widehat{\Delta T}\rangle^{\Phi}$ order-by-order for both the point source and balancing potentials. Actually, we will explicitly calculate only the GR terms $\langle\widehat{\Delta T}\rangle^{\Phi}_{\rm GR}$ in this expansion with the understanding that the corresponding EFT terms differ typically only by an $\mathcal{O}(1)$ number and a suppression factor of $1/(b\Lambda)^2$. Demanding that this perturbative expansion is under control will define the scattering time, or $u_{\rm max}$, in a fashion analogous to the WKB approach of the previous section. However, since the eigenbasis for physical states in this system is not known analytically, we will satisfy ourselves with performing this calculation and checking (4.83) for a typical in-state of the form

$$|\Phi_0\rangle = \int \mathrm{d}^d x \Phi_0(\mathbf{x})\,|\mathbf{x}\rangle\,, \tag{4.84}$$

where $|\mathbf{x}\rangle$ is a position eigenstate and the wavefunction $\Phi_0(\mathbf{x})$ is the Gaussian wavepacket in (4.79). In the interaction picture's in-in formalism, the system's time-evolution is captured in

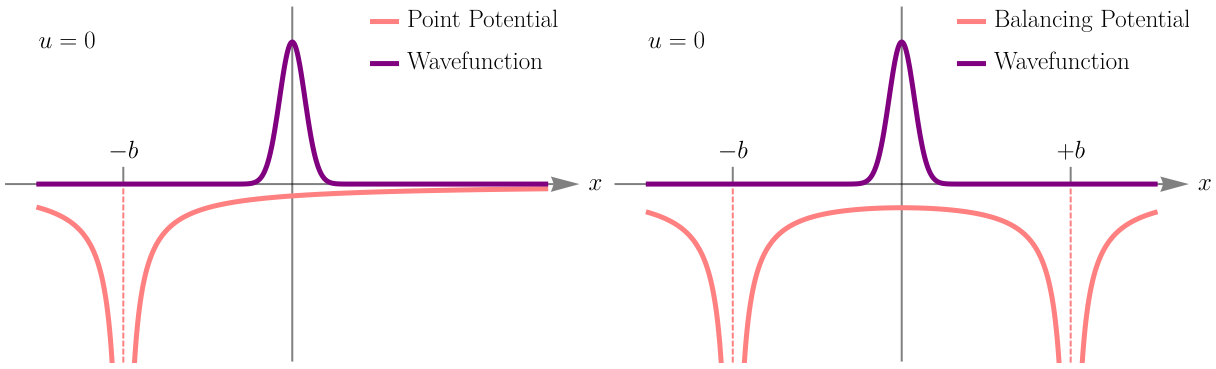

Figure 4.2: Snapshot at time $u = 0$ of the point-source and balancing potentials and the wavefunction which probes the spacetime.

the operator's time-dependence, which is coming up next. Expectation values are computed over this fixed in-state, chosen to represent the initial state of our test particle at time $u = 0$. In other words, the time delay we compute below is the expected asymptotic time delay for a given initial state, automatically averaged over all possible final states. The physical scenario for the two types of potential we have in mind is illustrated in figure 4.2.

The S-matrix is defined by

$$\hat{S} = \mathcal{T}\left\{\exp\left[-i\int_{-\infty}^{+\infty} \mathrm{d}u\, \hat{V}_I(u)\right]\right\} \tag{4.85}$$

where $\mathcal{T}$ is the (u-)time-ordering operator and $\hat{V}_I$ is the interaction picture potential. The interaction picture potential $\hat{V}_I(u)$ is related to the Schrödinger potential,

$$\hat{V}(u) \equiv V(u, \hat{\mathbf{x}}) \equiv \int \mathrm{d}^d x V(u, \mathbf{x}) \left|\mathbf{x}\right\rangle \left\langle\mathbf{x}\right|, \tag{4.86}$$

via conjugation with the free Hamiltonian $\mathcal{H}_0$:

$$\hat{V}_I(u) = e^{i\hat{\mathcal{H}}_0 u} \hat{V}(u) e^{-i\hat{\mathcal{H}}_0 u}. \tag{4.87}$$

For a particle with mass k_v, the free Hamiltonian may be written as

$$\hat{\mathcal{H}}_0 = \frac{\hat{\mathbf{k}}^2}{2k_v} = -\frac{1}{2k_v}\int \mathrm{d}^d x \nabla_d^2 \left|\mathbf{x}\right\rangle \left\langle\mathbf{x}\right|. \tag{4.88}$$

where $\mathbf{k}$ is the particle's momentum in transverse space. The interaction potential can thus be

expressed as the Schrödinger potential with a translated space coordinate,

$$\hat{V}_I(u) = V\left(u, \hat{\mathbf{x}} + \frac{u}{k_v}\hat{\mathbf{k}}\right). \tag{4.89}$$

Already the appearance of $\mathbf{k}$ is an indication that the quantum formalism will account for motion in transverse space where the semi-classical formalism failed.

Away from any singularities, the potential $\hat{V}_I$ may be treated as a perturbation. By definition, the time-ordered exponential in (4.85) may be expanded as

$$\hat{S} = 1 + \underbrace{(-i)\int_{-\infty}^{+\infty} \mathrm{d}u\, \hat{V}_I(u)}_{\hat{S}^{(1)}} + \underbrace{(-i)^2 \int_{-\infty}^{+\infty} \mathrm{d}u \int_{-\infty}^{u} \mathrm{d}u'\, \hat{V}_I(u)\hat{V}_I(u')}_{\hat{S}^{(2)}} + \ldots, \tag{4.90}$$

and the time delay can be identified order-by-order in powers of $\hat{V}_I$. The first three terms in the series expansion for the time delay are

$$\widehat{\Delta T}^{(1)} = -i\frac{\partial \hat{S}^{(1)}}{\partial k_v}, \tag{4.91}$$

$$\widehat{\Delta T}^{(2)} = -i\left(\frac{\partial \hat{S}^{(2)}}{\partial k_v} + \hat{S}^{(1)\dagger}\frac{\partial \hat{S}^{(1)}}{\partial k_v}\right), \tag{4.92}$$

$$\widehat{\Delta T}^{(3)} = -i\left(\frac{\partial \hat{S}^{(3)}}{\partial k_v} + \hat{S}^{(1)\dagger}\frac{\partial \hat{S}^{(2)}}{\partial k_v} + \hat{S}^{(2)\dagger}\frac{\partial \hat{S}^{(1)}}{\partial k_v}\right). \tag{4.93}$$

Since we will only ever consider the one type of in-state (4.84), without ambiguity we denote the corresponding n-th order term in the expectation value simply by

$$\Delta T^{(n)} = \langle \Phi_0 | \widehat{\Delta T}^{(n)} | \Phi_0 \rangle . \tag{4.94}$$

The first three orders in the expectation value of ΔT_{GR} are calculated in appendix D.2, with the results below. As noted at the top, the S-matrix is only well-defined when interactions are turned on for a finite amount of time. We have already chosen to start the clock at $u = 0$ by defining our in-state at that time. In other words, it should be understood that $j(u < 0) = 0$. The source must also be switched off at some finite time which we continue to call $u_{\max}$, i.e. $j(u > u_{\max}) = 0$. The expressions below correspond to the time delay accumulated up until some interim time $0 < u < u_{\max}$. The infinite limits on the integrals in the expressions for $\hat{S}^{(n)}$ have been replaced accordingly. For a potential generated by either a single point source located

at $\mathbf{x} = -\mathbf{b}$ or balancing sources at $\pm\mathbf{b}$ the first three orders in the GR time delay are

$$\Delta T^{(1)}_{\rm GR}(u) = \int_0^u \mathrm{d}u_1\, j(u_1) \left(1 - u_1 \frac{\partial}{\partial u_1}\right) K^{(1)}(u_1), \tag{4.95a}$$

$$\begin{aligned}\Delta T^{(2)}_{\rm GR}(u) = k_v \left(\prod_{i=1}^{2} \int_0^u \mathrm{d}u_i\, j(u_i)\right) \times \\ \left[\theta(u_1 - u_2)\left(1 - u_1 \frac{\partial}{\partial u_1}\right) - \theta(u_2 - u_1)\left(1 - u_2 \frac{\partial}{\partial u_2}\right)\right] K^{(2)}(u_1, u_2),\end{aligned} \tag{4.95b}$$

$$\begin{aligned}\Delta T^{(3)}_{\rm GR}(u) = k_v^2 \left(\prod_{i=1}^{3} \int_0^u \mathrm{d}u_i\, j(u_i)\right) \times \\ \left[\theta(u_1 - u_2)\theta(u_2 - u_3)\left(3 - u_1 \frac{\partial}{\partial u_1} - u_2 \frac{\partial}{\partial u_2} - u_3 \frac{\partial}{\partial u_3}\right)\right. \\ \left. - \theta(u_2 - u_3)\left(2 - u_2 \frac{\partial}{\partial u_2} - u_3 \frac{\partial}{\partial u_3}\right) + \theta(u_2 - u_1)\left(1 - u_3 \frac{\partial}{\partial u_3}\right)\right] K^{(3)}(u_1, u_2, u_3),\end{aligned} \tag{4.95c}$$

where $\theta(u)$ is the Heaviside step function and

$$\begin{aligned}K^{(n)}(u_1, \ldots, u_n) =& (-i)^{n+1} \left(-\frac{2\pi^{\frac{d}{2}}}{\Gamma\left(\frac{d-2}{2}\right)}\right)^n \left(\prod_{i=1}^{n} \int \frac{\mathrm{d}^d q_i}{(2\pi)^d} \frac{e^{i\mathbf{q}_i\cdot\mathbf{b}} + \Theta_{\rm bal} e^{-i\mathbf{q}_i\cdot\mathbf{b}}}{\mathbf{q}_i^2}\right) \\ & \exp\left[-\frac{\sigma^2}{2}\left(\left(\sum_{i=1}^{n} \mathbf{q}_i\right)^2 + \left(\frac{1}{2k_v\sigma^2}\sum_{i=1}^{n} u_i \mathbf{q}_i\right)^2\right) + \frac{i}{2k_v}\sum_{i<j=1}^{n} (u_i - u_j)\mathbf{q}_i \cdot \mathbf{q}_j\right],\end{aligned} \tag{4.96}$$

and we have introduced the notation

$$\Theta_{\rm bal} = \begin{cases} 0, & \text{point source} \\ 1, & \text{balancing sources} \end{cases}$$

in order to deal with both cases simultaneously.

The classical limit — identifying diffusion and scattering

The effect of diffusion is captured at every order in ΔT by the first (bracketed) term in the exponential on the second line of (4.96), which is proportional to the initial spread of the wavepacket σ^2. The classical limit of this quantum calculation indeed corresponds to vanishing

wavefunction width $\sigma \to 0$. In this limit, the first-order term becomes

$$\lim_{\sigma\to 0} \Delta T^{(1)}_{\rm GR}(u) = -\frac{1}{k_v}\int_0^u \mathrm{d}u_1 V(u_1, \mathbf{b})(1+\Theta_{\rm bal}), \tag{4.97}$$

which is exactly the semi-classical expression of (4.58). In this section, we use the classical limit to argue that the higher-order terms in the time delay expansion are the manifestation of scattering effects. In particular: the higher-order terms will be shown to vanish in the classical limit of the balancing source case but not in the classical limit of the point source case. This is attributed to the fact there is no classical scattering in the balancing case (because a point-like particle may rest at the equilibrium), unlike the point source. Crucially, however, the higher-order terms $\Delta T^{(n>1)}$ in the balancing case do not vanish outside the classical limit. That is, there is some "diffusion-induced" scattering effects which leads to corrections to the classical expression (4.97). In the next section, we use the growth of those corrections to bound how big $\Delta T^{(1)}(u)$ may become before it ceases to be a good approximation to the full time delay.

After some manipulation, the classical limit $\sigma \to 0$ of the second- and third-order terms in the time delay expansion can be written as

$$\begin{aligned}\lim_{\sigma\to 0} \Delta T^{(2)}_{\rm GR}(u) = &-\left(-\frac{2\pi^{\frac{d}{2}}}{\Gamma\left(\frac{d-2}{2}\right)}\right)^2 k_v \int_0^u \mathrm{d}u_1 j(u_1)\int_0^{u_1}\mathrm{d}u_2 j(u_2)\int \frac{\mathrm{d}^d q_1}{(2\pi)^2}\frac{\mathrm{d}^d q_2}{(2\pi)^2}\\ &\frac{e^{i\mathbf{q}_1\cdot\mathbf{b}}+\Theta_{\rm bal}e^{-i\mathbf{q}_1\cdot\mathbf{b}}}{\mathbf{q}_1^2}\frac{e^{i\mathbf{q}_2\cdot\mathbf{b}}+\Theta_{\rm bal}e^{-i\mathbf{q}_2\cdot\mathbf{b}}}{\mathbf{q}_2^2}\\ &\left(\sin\left[\frac{1}{2k_v}(u_1-u_2)\mathbf{q}_1\cdot\mathbf{q}_2\right]-\frac{u_1}{2k_v}\mathbf{q}_1\cdot\mathbf{q}_2\cos\left[\frac{1}{2k_v}(u_1-u_2)\mathbf{q}_1\cdot\mathbf{q}_2\right]\right),\end{aligned} \tag{4.98}$$

and

$$\begin{aligned}\lim_{\sigma\to 0} \Delta T^{(3)}_{\rm GR}(u) = &\left(-\frac{2\pi^{\frac{d}{2}}}{\Gamma\left(\frac{d-2}{2}\right)}\right)^3 k_v^2 \int_0^u \mathrm{d}u_1 j(u_1)\int_0^{u}\mathrm{d}u_2 j(u_2)\int_0^{u}\mathrm{d}u_3 j(u_3)\int \frac{\mathrm{d}^d q_1}{(2\pi)^2}\frac{\mathrm{d}^d q_2}{(2\pi)^2}\frac{\mathrm{d}^d q_3}{(2\pi)^2}\\ &\frac{e^{i\mathbf{q}_1\cdot\mathbf{b}}+\Theta_{\rm bal}e^{-i\mathbf{q}_1\cdot\mathbf{b}}}{\mathbf{q}_1^2}\frac{e^{i\mathbf{q}_2\cdot\mathbf{b}}+\Theta_{\rm bal}e^{-i\mathbf{q}_2\cdot\mathbf{b}}}{\mathbf{q}_2^2}\frac{e^{i\mathbf{q}_3\cdot\mathbf{b}}+\Theta_{\rm bal}e^{-i\mathbf{q}_3\cdot\mathbf{b}}}{\mathbf{q}_3^2}\\ &\left[\theta(u_1-u_2)\theta(u_2-u_3)\left(1-u_1\frac{\partial}{\partial u_1}\right)\right.\\ &-\theta(u_2-u_1)\theta(u_2-u_3)\left(1-u_2\frac{\partial}{\partial u_2}\right)\\ &\left.+\theta(u_2-u_1)\theta(u_3-u_2)\left(1-u_3\frac{\partial}{\partial u_3}\right)\right]\\ &\exp\left[\frac{i}{2k_v}\left((u_1-u_2)\mathbf{q}_1\cdot\mathbf{q}_2+(u_1-u_3)\mathbf{q}_1\cdot\mathbf{q}_3+(u_2-u_3)\mathbf{q}_2\cdot\mathbf{q}_3\right)\right].\end{aligned} \tag{4.99}$$

For the second order term, in the balancing case $\Theta_{\text{bal}} = 1$, it is easy to see that the integrand of (4.98) is odd under $\mathbf{q}_1 \to -\mathbf{q}_1$ (or $\mathbf{q}_2 \to -\mathbf{q}_2$) and thus the integral vanishes. In the point source case, there is no such anti-symmetry so the integral does not vanish.

The vanishing of the third order term in the balancing case is less straightforward. The trusting reader may be happy to believe that it does indeed vanish and skip to the next paragraph. Otherwise, first note that as the eigenvalue of an Hermitian operator the expression in (4.99) should be real. We can verify that it is real by simultaneously exchanging

$$u_1 \longleftrightarrow u_3 \quad \text{and} \quad \mathbf{q}_1 \longleftrightarrow \mathbf{q}_3, \tag{4.100}$$

in the integrand to retrieve its complex conjugate. Thus, the exponential factor at the bottom of (4.99) may be replaced by its real part, a cosine. Then, in the balancing case only, we have the following situation

$$\begin{aligned}\lim_{\sigma\to 0} \Delta T^{(3)}_{\text{GR}}(u) = \int_0^u \mathrm{d}u_1 \mathrm{d}u_2 \mathrm{d}u_3 j(u_1) j(u_2) j(u_3) \Big[&\theta(u_1-u_2)\theta(u_2-u_3)\left(1 - u_1 \frac{\partial}{\partial u_1}\right) \\ &-\theta(u_2-u_1)\theta(u_2-u_3)\left(1 - u_2 \frac{\partial}{\partial u_2}\right) \\ &+\theta(u_2-u_1)\theta(u_3-u_2)\left(1 - u_3 \frac{\partial}{\partial u_3}\right)\Big] G(u_1,u_2,u_3)\end{aligned} \tag{4.101}$$

where $G(u_1, u_2, u_3)$ is a function that is invariant under any permutation of the u_i's. (For example, the exchange $u_1 \leftrightarrow u_2$ in G may be offset by the exchange of the integration variables $\mathbf{q}_1 \leftrightarrow \mathbf{q}_2$ and the change of variables $\mathbf{q}_3 \to -\mathbf{q}_3$ to leave it invariant.) With this in mind, the first and third terms in the square brackets give the same contribution overall (by exchange of $u_1 \leftrightarrow u_3$). Merging these terms and additionally exchanging $u_1 \leftrightarrow u_2$ in the second term, we obtain:

$$\begin{aligned}\lim_{\sigma\to 0} \Delta T^{(3)}_{\text{GR}}(u) = \int_0^u \mathrm{d}u_1 j(u_1) \int_0^{u_1} \mathrm{d}u_2 j(u_2) \left(2\int_0^{u_2} \mathrm{d}u_3 - \int_0^{u_1} \mathrm{d}u_3\right) j(u_3) \\ \left(1 - u_1 \frac{\partial}{\partial u_1}\right) G(u_1,u_2,u_3).\end{aligned} \tag{4.102}$$

Now, note that

$$\begin{aligned}\int_0^{u_1} \mathrm{d}u_2 \left(2\int_0^{u_2} \mathrm{d}u_3 - \int_0^{u_1} \mathrm{d}u_3\right) &= \int_0^{u_1} \mathrm{d}u_2 \left(\int_0^{u_2} \mathrm{d}u_3 - \int_{u_2}^{u_1} \mathrm{d}u_3\right) \\ &= \int_0^{u_1} \mathrm{d}u_2 \int_0^{u_2} \mathrm{d}u_3 - \int_0^{u_1} \mathrm{d}u_3 \int_0^{u_3} \mathrm{d}u_2\end{aligned} \tag{4.103}$$

and since the integrand is invariant under the exchange of $u_2 \leftrightarrow u_3$, the whole integral in (4.102) is zero.

It is expected that all higher-order corrections to the leading term (4.97) in the balancing-source time delay vanish in the classical limit. Again, let it be stressed that this is a reflection of the fact that there is classically no scattering from the unstable equilibrium point in the balancing potential. Thus, outside the classical limit, the higher-order terms $\Delta T^{(n>1)}$ may be regarded as the result of diffusion-induced scattering in the quantum problem.

Scattering bounds

Just as in section 4.4.1, the requirement that the higher-order scattering-induced terms $\Delta T^{(n>1)}_{\text{GR}}(u)$ are under control compared to the leading-order GR term $\Delta T^{(1)}_{\text{GR}}(u)$ imposes a time cut-off u_{max} beyond which we may no longer trust perturbation theory. With the help of the EFT validity bounds (3.64), we will again find that u_{max} is such that $\Delta T^{(1)}_{\text{EFT}}(u_{\text{max}})$ is unresolvable. Below, we will determine the parameter "ϵ" which controls the series expansion of $\Delta T_{\text{GR}}(u)$. As we will see, this parameter will grow with time u itself — at early times, the series expansion is under better control and $\Delta T^{(1)}_{\text{GR}}(u)$ represents a good approximation for $\Delta T_{\text{GR}}(u)$, but at late times that approximation begins to fail. The scattering timescale u_{scatt} will be defined as the time at which it becomes large, $\epsilon(u_{\text{scatt}}) \sim 1$.

As a concession to simplicity, consider the case of a constant $j(u) = j$, i.e. a potential with no time dependence. In fact, not only will this make the expressions in (4.95) less unwieldy, it's also the physical scenario with the best chance of violating causality, for two reasons. First, one of the three EFT validity bounds (3.64c) is automatically satisfied because $\partial_u H = 0$. Secondly, the metric function $H(u, \mathbf{x})$ is constantly (in time) at its maximum allowed by the third EFT bound (3.64b) meaning the growth of $\Delta T^{(1)}_{\text{EFT}}(u)$ never slows down due to dips in H. From the perspective of trying to generate acausality, there is no benefit to varying $H(u, \mathbf{x})$ in time (e.g. with a sequence of N time-separated shockwaves). While you may gain a longer run without significant scattering (a bigger u_{max}), you lose out in the magnitude of the integrand of $\Delta T^{(1)}_{\text{EFT}}(u)$.

With this simplification, the u-derivative-terms in expressions (4.95) may be integrated by

parts so that for $u < u_{\max}$ we get, explicitly,

$$\begin{aligned}\Delta T^{(1)}_{\mathrm{GR}}(u) = &-2\left(-\frac{2\pi^{\frac{d}{2}}}{\Gamma\left(\frac{d-2}{2}\right)}\right) j \int_0^u \mathrm{d}u_1 \int \frac{\mathrm{d}^d q_1}{(2\pi)^d} \\ &\frac{e^{i\mathbf{q}_1\cdot\mathbf{b}} + \Theta_{\mathrm{bal}} e^{-i\mathbf{q}_1\cdot\mathbf{b}}}{\mathbf{q}_1^2} \exp\left[-\frac{\sigma^2\mathbf{q}_1^2}{2} - \frac{u_1^2\mathbf{q}_1^2}{8k_v^2\sigma^2}\right],\end{aligned} \tag{4.104a}$$

$$\begin{aligned}\Delta T^{(2)}_{\mathrm{GR}}(u) = &-2\left(-\frac{2\pi^{\frac{d}{2}}}{\Gamma\left(\frac{d-2}{2}\right)}\right)^2 k_v j^2 \int_0^u \mathrm{d}u_1\mathrm{d}u_2 \int \frac{\mathrm{d}^d q_1}{(2\pi)^d}\frac{\mathrm{d}^d q_2}{(2\pi)^d} \\ &\frac{e^{i\mathbf{q}_1\cdot\mathbf{b}} + \Theta_{\mathrm{bal}} e^{-i\mathbf{q}_1\cdot\mathbf{b}}}{\mathbf{q}_1^2}\frac{e^{i\mathbf{q}_2\cdot\mathbf{b}} + \Theta_{\mathrm{bal}} e^{-i\mathbf{q}_2\cdot\mathbf{b}}}{\mathbf{q}_2^2} \\ &\exp\left[-\frac{\sigma^2}{2}\left(\mathbf{q}_1+\mathbf{q}_2\right)^2 - \frac{1}{8k_v^2\sigma^2}\left(u_1\mathbf{q}_1 + u_2\mathbf{q}_2\right)^2\right] \\ &\sin\left[\frac{1}{2k_v}(u_1-u_2)\mathbf{q}_1\cdot\mathbf{q}_2\right],\end{aligned} \tag{4.104b}$$

$$\begin{aligned}\Delta T^{(3)}_{\mathrm{GR}}(u) = &\,2\left(-\frac{2\pi^{\frac{d}{2}}}{\Gamma\left(\frac{d-2}{2}\right)}\right)^3 k_v^2 j^3 \int_0^u \mathrm{d}u_1\mathrm{d}u_2\mathrm{d}u_3 \int \frac{\mathrm{d}^d q_1}{(2\pi)^d}\frac{\mathrm{d}^d q_2}{(2\pi)^d}\frac{\mathrm{d}^d q_3}{(2\pi)^d} \\ &\frac{e^{i\mathbf{q}_1\cdot\mathbf{b}} + \Theta_{\mathrm{bal}} e^{-i\mathbf{q}_1\cdot\mathbf{b}}}{\mathbf{q}_1^2}\frac{e^{i\mathbf{q}_2\cdot\mathbf{b}} + \Theta_{\mathrm{bal}} e^{-i\mathbf{q}_2\cdot\mathbf{b}}}{\mathbf{q}_2^2}\frac{e^{i\mathbf{q}_3\cdot\mathbf{b}} + \Theta_{\mathrm{bal}} e^{-i\mathbf{q}_3\cdot\mathbf{b}}}{\mathbf{q}_3^2} \\ &\exp\left[-\frac{\sigma^2}{2}\left(\mathbf{q}_1+\mathbf{q}_2+\mathbf{q_3}\right)^2 - \frac{1}{8k_v^2\sigma^2}\left(u_1\mathbf{q}_1 + u_2\mathbf{q}_2 + u_3\mathbf{q}_3\right)^2\right] \\ &\cos\left[\frac{1}{2k_v}\left((u_1-u_2)\mathbf{q}_1\cdot\mathbf{q}_2 + (u_1-u_3)\mathbf{q}_1\cdot\mathbf{q}_3 + (u_2-u_3)\mathbf{q}_2\cdot\mathbf{q}_3\right)\right] \\ &\left(2\Theta(u_1-u_2)\Theta(u_2-u_3) - \Theta(u_2-u_1)\Theta(u_2-u_3)\right),\end{aligned} \tag{4.104c}$$

While the cross-terms in the integrands mean these expressions are not readily integrated, we can estimate the parameter dependence of each $\Delta T^{(n)}_{\mathrm{GR}}(u)$ as long as we make the following assumptions:

$$\sigma \ll b, \tag{4.105}$$

$$u \ll k_v \sigma b. \tag{4.106}$$

Physically, the first assumption (4.105) corresponds to the (very natural) requirement that the width of the initial Gaussian wavepacket σ is much smaller than the distance to the source b, or that the initial configuration is well localised compared to the background profile. The second assumption (4.106) is that the timescale under consideration u is earlier than the diffusion time $u_{\mathrm{diff}} \sim k_v \sigma b$ (see (4.80) with the first assumption $\sigma \ll b$). This one may not seem like a given —

why should all the action happen before diffusion has taken hold? — but, as we will check later, this is the main regime of interest. If it were the case that the scattering timescale came after the diffusion timescale $u_{\rm scatt} > u_{\rm diff}$, we would have to find ourselves in a potential so weak that even the GR time delay is unresolvable (see later).

Scattering before diffusion

By switching to dimensionless integration variables $w_i = u_i/u$ and $\mathbf{p}_i = b\mathbf{q}_i$, the parameter dependence of $\Delta T^{(n)}_{\rm GR}(u)$ can be extracted to leading order in σ/b and $u/k_v\sigma b$:

$$\Delta T^{(1)}_{\rm GR}(u) \sim \frac{ju}{b^{d-2}}, \tag{4.107a}$$

$$\Delta T^{(2)}_{\rm GR}(u) \sim \frac{j^2u^3}{b^{2d-2}}\left[1+\Theta_{\rm bal}\left(-1+a^{(2)}\frac{\sigma^2}{b^2}+\tilde{a}^{(2)}\frac{u^2}{k_v^2b^2\sigma^2}\right)\right], \tag{4.107b}$$

$$\Delta T^{(3)}_{\rm GR}(u) \sim \frac{k_v^2j^3u^3}{b^{3d-6}}\left[1+\Theta_{\rm bal}\left(-1+a^{(3)}\frac{\sigma^2}{b^2}+\tilde{a}^{(3)}\frac{u^2}{k_v^2b^2\sigma^2}\right)\right], \tag{4.107c}$$

where $a^{(n)}$ and $\tilde{a}^{(n)}$ are numbers expressed in terms of $n(d+1)$ dimensionless integrals (given in appendix D.3).

There are two notable features of (4.107). Firstly, all higher-order time delays $\Delta T^{(n\geq 2)}_{\rm GR}(u)$ in the balancing case are further suppressed compared to the point-source case. This is a reflection of the fact that all higher-order terms vanish in the particle limit $\sigma \to 0$ as discussed in the previous section. Outside this limit, even a very small initial spread σ will drive growth in the higher-order corrections due to the diffusion term growing like $(u/k_vb\sigma)^2$.

The second thing to note is that the ratio of one term $\Delta T^{(n)}_{\rm GR}(u)$ to the next $\Delta T^{(n+1)}_{\rm GR}(u)$ is not the same for all n. The even terms $\Delta T^{(2n)}_{\rm GR}(u)$ are artificially suppressed by the presence of an odd sine in their integrands compared to the even cosine in odd terms $\Delta T^{(2n+1)}_{\rm GR}(u)$. In other words, the third-order term $\Delta T^{(3)}_{\rm GR}(u)$ is not necessarily subdominant to the second-order term $\Delta T^{(2)}_{\rm GR}(u)$, and so on. This means that the ratio which truly controls the expansion is not the ratio of one term to the next $\Delta T^{(n+1)}_{\rm GR}(u)/\Delta T^{(n)}_{\rm GR}(u)$ but instead it is the ratio of even terms $\Delta T^{(2n+2)}_{\rm GR}(u)/\Delta T^{(2n)}_{\rm GR}(u)$ (or equivalently, the ratio of odd terms $\Delta T^{(2n+1)}_{\rm GR}(u)/\Delta T^{(2n+3)}_{\rm GR}(u)$).

Although the explicit parameter dependence of the generic n-th term is not given here, it is apparent from the general expression (4.96) and the examples (4.107) that the series expansion

of the time delay is controlled by

$$\epsilon(u) \sim \frac{\Delta T_{\rm GR}^{(2n)}(u)}{\Delta T_{\rm GR}^{(2n+2)}(u)} \sim \left(\frac{k_v j u}{b^{d-2}}\right)^2 . \tag{4.108}$$

The S-matrix expansion is under control when $\epsilon(u) \ll 1$. The expansion is no longer valid when $\epsilon(u) \sim 1$. Since the higher-order terms represent the effect of scattering, we identify this time with the scattering timescale and say

$$\epsilon(u_{\rm scatt}) \sim 1 \quad \Longrightarrow \quad u_{\rm scatt} \sim \frac{1}{k_v}\frac{b^{d-2}}{j}. \tag{4.109}$$

To compare with the classical estimates, see (4.61), (4.70) and (4.77).

How does this scattering timescale compare to the diffusion timescale? In fact, using the expressions for the two timescales, (4.80) and (4.109), and the approximation for the leading order time delay (4.107a), we find

$$u_{\rm scatt} \ll u_{\rm diff} \quad \Longleftrightarrow \quad k_v \left|\Delta T_{\rm GR}^{(1)}(u_{\rm diff})\right| \gg 1. \tag{4.110}$$

In other words, the assumption that scattering takes effect before diffusion is consistent as long as the GR time delay generated by $u_{\rm diff}$ is resolvable. As the time delay is a monotonically increasing function of time u, the condition that $\Delta T_{\rm GR}^{(1)}(u_{\rm diff})$ is resolvable is even weaker than the condition that $\Delta T_{\rm GR}^{(1)}(u_{\rm scatt})$ is resolvable. Simply using (4.107a) to evaluate $\Delta T_{\rm GR}^{(1)}(u_{\rm scatt}) \sim 1/k_v$ suggests that the GR time delay is on the edge of resolvability by the time the test wave has scattered.

While we haven't explicitly calculated the EFT contribution to the time delay in this formalism, its leading order can generally be estimated as

$$\Delta T_{\rm EFT}^{(1)}(u) \sim \frac{c_{\rm GB}}{b^2\Lambda^2}\Delta T_{\rm GR}^{(1)}(u) \sim c_{\rm GB}\frac{ju}{b^d\Lambda^2} \tag{4.111}$$

since the GB Lagrangian is suppressed by $\bar{R}/\Lambda^2$ compared to the Einstein–Hilbert Lagrangian. Treating $u_{\rm scatt}$ as the time $u_{\rm max}$ at which we switch off our source, the total EFT time delay

$$\Delta T_{\rm EFT}^{(1)}(u_{\rm scatt}) \sim \frac{c_{\rm GB}}{b^2\Lambda^2}\frac{1}{k_v} \tag{4.112}$$

is evidently unresolvable for $|c_{\rm GB}| \lesssim \mathcal{O}(1)$ due to the EFT-validity bound $b\Lambda \gg 1$.

Diffusion before scattering

We have already seen that the assumption $u_{\rm scatt} < u_{\rm diff}$ is self-consistent, and we will now show that it is actually the only regime of interest. Assuming that we can trust the expressions for $\Delta T^{(n)}_{\rm GR}(u)$ given in (4.107) all the way up until $u \sim u_{\rm diff}$, we can write

$$\Delta T^{(3)}_{\rm GR}(u_{\rm diff}) \sim k_v^2 \left(\Delta T^{(1)}_{\rm GR}(u_{\rm diff})\right)^3 \left[1 + \Theta_{\rm bal}\left(-1 + a^{(3)}\frac{\sigma^2}{b^2} + \tilde{a}^{(3)}\right)\right]. \tag{4.113}$$

Of the parts that are exclusive to the balancing case, $\tilde{a}^{(3)}$ will dominate over $a^{(3)}\,(\sigma/b)^2$, so we can write-off the totality of the square brackets as an $\mathcal{O}(1)$ number plus suppressed corrections. If the scattering time comes after the diffusion time then, by our definition of scattering, the first-order term $\Delta T^{(1)}_{\rm GR}(u)$ should still dominate the series expansion by $u = u_{\rm diff}$. However, asking for the third-order term to be sub-dominant, $\left|\Delta T^{(3)}_{\rm GR}(u_{\rm diff})\right| < \left|\Delta T^{(1)}_{\rm GR}(u_{\rm diff})\right|$ leads to the conclusion

$$\left|k_v^2 \left(\Delta T^{(1)}_{\rm GR}(u_{\rm diff})\right)^3\right| < \left|\Delta T^{(1)}_{\rm GR}(u_{\rm diff})\right| \quad \Longrightarrow \quad k_v\left|\Delta T^{(1)}_{\rm GR}(u_{\rm diff})\right| < 1, \tag{4.114}$$

the first-order GR time delay is unresolvable. As hinted at previously, we see that if we try to slow down the effects of scattering for long enough that diffusion takes hold first, then the price to pay is a potential so weak (i.e. j so small) that even the leading-order GR time delay cannot be resolved. Since the EFT contribution is further suppressed by $1/b^2\Lambda^2 \ll 1$ compared to the GR contribution, it will certainly not be resolvable.

To summarise the logic of this section: defining the quantum scattering timescale $u_{\rm scatt}$ as the time at which the series expansion of the time delay $\Delta T(u) = \Delta T^{(1)}(u) + \Delta T^{(2)}(u) + \dots$ stops being under control $\epsilon(u_{\rm scatt}) \sim 1$, the EFT time delay accumulated up until $u_{\rm scatt}$ is unresolvable $k_v\left|\Delta T^{(1)}_{\rm EFT}(u_{\rm scatt})\right| \ll |c_{\rm GB}|$ as long as the EFT validity bounds (3.64) are satisfied.

4.5 Chapter summary

In this chapter, we introduced two notions of causality on a curved spacetime based on the asymptotic time delay experienced by propagating waves. The first, known as asymptotic causality, is the condition that the net time delay (GR + EFT) is weakly positive,

$$\Delta T_{\rm net} \gtrsim -E^{-1}. \tag{4.115}$$

The second, dubbed infrared or IR causality, is the condition that the EFT time delay is weakly positive,

$$\Delta T_{\rm EFT} \gtrsim -E^{-1}. \tag{4.116}$$

We argued for the latter as the correct definition of causality based on the fact that it is the front (and not phase/group) velocity which determines the causality of waves. In addition, we supported this argument by showing that IR causality correctly reproduces previously known positivity bounds for the Goldstone boson.

We then applied IR causality to GW propagation on BH and pp-wave spacetimes in the leading-order EFT of gravity. With various appropriate approximations, we calculated the time delays experienced by each of the GW polarisations on both spacetimes. There is no choice of GB Wilson coefficient $c_{\rm GB}$ which ensures $\Delta T_{\rm EFT} > 0$ for all polarisations, thus we instead ask whether $|\Delta T_{\rm EFT}|$ is resolvable. Such a question may only be asked within the EFT's regime of validity, which was found in section 3.3, otherwise the whole problem loses meaning. In the case of the BH, showing that $|\Delta T_{\rm EFT}|$ is indeed unresolvable was a direct application of the constraints defining the BH regime of validity. In the case of the pp-wave, we additionally need to cut-off the interaction time of the GW with the background in order to control the scattering problem. In both cases, we arrived at the same conclusion: the GB operator is causal on these spacetimes as long as its Wilson coefficient is an order-1 number, $|c_{\rm GB}| \lesssim \mathcal{O}(1)$. This is the main result of this portion of the thesis. The methods used to obtain it — the definition of IR causality, determining the EFT time delay, applying the EFT regime of validity — may be applied to any effective operator on a curved spacetime.

Chapter 5

Phase decoherence of gravitational wave backgrounds

Over the course of the last three chapters, we saw how the phase shift of a scattered gravitational wave can determine the causality of effective operators in the EFT of gravity. A negative phase shift/time delay corresponded to faster-than-light signalling and indicated a possible causality violation. However, if the phase shift were too small to be resolved $|\delta| \ll 1$ (or $|\Delta T| \ll \omega^{-1}$ in the language of the preceding chapters), then there was no true violation of causality.

For the last section of this thesis, we will find ourselves in the entirely opposite regime: dealing with very large phase shifts indeed, and taking causality as a given. Our focus remains on scattered gravitational waves, but we return to the concrete case of $D = 4$ dimensions, gravity described strictly by Einstein's GR, and a perturbatively inhomogeneous cosmological spacetime. Moreover, we're upping our game from one gravitational wave to a whole multitude of them singing in chorus (rather discordantly, as we will see...) from the dawn of time. In this chapter, we will show how inhomogeneities in the metric of our universe cause the phase decoherence of the so-called Stochastic Gravitational Wave Background (SGWB).

There are a number of sources of gravitational waves in our universe. Famously, there have already been a number of direct detections of gravitational waves generated by compact binary mergers by the LIGO–Virgo–KAGRA collaboration [104–106], starting with GW150914 [5]. However, only very few GW-producing events, relative to their expected occurrence, are loud enough to be resolved above the background noise in our detectors. The remainder fall below some effective confusion limit, which is particular to each detector, and form a stochastic background signal [107]. These overlapping signals from many individual sources form the astrophysical

component of the SGWB. They are likely to include signals from black hole/neutron star binaries in their early phases of coalescence, white dwarf binaries, pulsar systems and supernovae [108–114]. This SGWB should act as a tracer for Large Scale Structure [115, 116] and sophisticated mapping techniques are being developed for data from future generations of detectors, [117–119] for example.

The other component of the SGWB is primordial in origin. These backgrounds were seeded in the early universe, during inflation or reheating, by (e.g.) phase transitions (electroweak or otherwise) or topological defects [120, 121]. These cosmological SGWBs are the signals we will be interested in, though the exact mechanism which generated them is not important for our purposes.

One major difference between the astrophysical SGWB and the cosmological SGWB is that the latter is expected to be "phase-coherent" at origin, whereas the former is not. The phase of a GW from some binary merger, for example, is entirely random and there is no reason to expect any two individual events to share a phase [122, 123]. Indeed, causality should ensure that there is no correlation over large angular scales for signals generated by subhorizon mechanisms (i.e. astrophysical sources). On the other hand, different patches of the sky *were* in causal contact with each other during inflation, meaning signals arriving from different directions could very well share the same cosmological origin and thus oscillate in-phase. For this reason, an inflationary SGWB would form a standing wave [124], a feature which would distinguish it from other types of backgrounds [125].

In principle, this feature of the cosmological SGWB could be tested by coherent GW detectors such as LIGO and the upcoming LISA [126–128], which measure both the amplitude and phase of the metric strain h for passing waves. Phase-coherent methods to solve for the underlying signal using this full wealth of data have already been developed [129–131]. For transient astrophysical point sources, access to the phase of a GW signal can help determine the direction of the source on the sky, especially with a network of multiple detectors [132]. And from the above discussion about the stochastic background, it may seem like phase-coherence in a particular frequency band could be the smoking gun for a cosmological origin.

Unfortunately, in [3] (and this thesis chapter) we argue that any SGWB would quickly lose its phase coherence. Before arriving at our detectors, GWs emitted in the early universe are repeatedly scattered off perturbations in the background metric. As we have seen in previous chapters, these scattering processes generate a phase shift. The process is analogous

to the integrated Sachs-Wolfe [133] (or Rees-Sciama [134]) effect for the photons in the Cosmic Microwave Background (CMB). We will find that at observable frequencies ($f \gtrsim 10^{-12}$ Hz), the total cumulative phase shift along any particular line-of-sight in the sky is very large $\delta \gg 1$, typically orders-of-magnitude larger than a single cycle. The result is a phase-profile across the sky that appears totally random. All information contained in the initial phase-profile of the background is completely lost.

The consequences are two-fold. The immediate consequence is that phase-coherent methods have no foreseeable application in mapping the SGWB. The astrophysical background was never expected to exhibit phase coherence anyway, and now in addition we argue that the cosmological background loses any phase-coherence it once had. Only intensity-based mapping techniques [118, 135], which use the square of the detector response h^2 and discard the phase information, are useful for reconstructing SGWBs. The second consequence relates to the characterisation of SGWBs with higher-order statistics [136–139]. The sky-average of the metric strain $\langle h \rangle$ for the SGWB vanishes due to its own phase-incoherence (in the same way the average of a centred random variable vanishes). But moreover, the product of any odd number of h's will have this (random) phase dependence causing their correlators (e.g. the bispectrum $\sim \langle hhh \rangle$) to also vanish. As noted also in [140–142], only observables which are quadratic in h have meaning for a phase-incoherent background.

The rest of this chapter is organised as follows. In the next section, we will derive a standard formula for the phase shift of a GW propagating through the perturbed Friedmann–Lemaître–Robertson–Walker (FLRW) spacetime. Then, we define an angular power spectrum for the phase shift. Finally, with the help of pre-existing software, we illustrate with an example the consequences of this effectively random phase shift on an initially phase-coherent background.

5.1 Line-of-sight phase shift

As a reminder, we are returning to gravity as described purely by general relativity, i.e. the Einstein–Hilbert action. Observations of the homogeneity, isotropy and curvature of the universe suggest that our cosmology is well-described by the flat FLRW metric:

$$g^{(0)}_{\alpha\beta} \mathrm{d}x^\alpha \mathrm{d}x^\beta = a^2(\tau) \left(-\mathrm{d}\tau^2 + \mathrm{d}\mathbf{x}^2 \right) \tag{5.1}$$

where τ is the conformal time coordinate and $a(\tau)$ is the scale factor. The evolution of the scale factor is determined by the dominant component of energy density of the universe at that time. It will actually drop out of our calculation of the phase shift, the important point being only that the background metric is conformally flat.

On top of this background, we introduce two types of perturbations: scalar and tensor. Once again, their origin is not strictly important to the following discussion, but the standard picture is that the scalar perturbations were seeded by quantum fluctuations of the so-called "inflaton" field which drove inflation in the early universe. They are parametrised as

$$g^{(1)}_{\alpha\beta}\mathrm{d}x^\alpha \mathrm{d}x^\beta = -2a^2(\tau)\left(\Phi(\tau,\mathbf{x})\mathrm{d}\tau^2 + \Psi(\tau,\mathbf{x})\mathrm{d}\mathbf{x}^2\right). \tag{5.2}$$

We consider these perturbations part of the background (in the sense that we are not interested in their dynamics) and write the background metric as $g_{\alpha\beta} = g^{(0)}_{\alpha\beta} + g^{(1)}_{\alpha\beta}$. The tensor perturbations, $h_{\alpha\beta}(\tau,\mathbf{x})$, represent the gravitational waves seeded by whatever primordial means. We ignore the backreaction of these waves on the background spacetime metric. The total metric is then $g_{\alpha\beta} + h_{\alpha\beta}$.

To leading order, the scalar and tensor perturbations evolve independently. To subleading order, however, the scalar perturbations leave an imprint on the amplitude, frequency and phase of the GWs, as calculated in [143]. Over the course of the history of the universe, all three aspects of the wave are modified by the intervening matter between emission and detection. The amplitude and frequency both carry interesting information about these line-of-sight effects. Indeed, the scalar perturbations of the cosmological metric introduce an angular dependence to the intensity (squared amplitude) of the SGWB, which has been discussed already in [144, 145]. The phase shift, on the other hand, is so large as to override any interesting information (e.g. initial coherence) several times over. We will reproduce the calculation of [143] for this phase shift below.

We work in transverse-traceless gauge:

$$h \equiv g^{\alpha\beta}h_{\alpha\beta} = 0, \tag{5.3a}$$

$$\nabla_\alpha h^{\alpha\beta} = 0, \tag{5.3b}$$

so that the linearised Einstein equations for the metric perturbations are

$$\nabla_\alpha \nabla^\alpha h_{\mu\nu} - 2R^\alpha{}_{\mu\nu\beta} h^\beta{}_\alpha - R_{\alpha\mu} h^\alpha{}_\nu - R_{\alpha\nu} h^\alpha{}_\mu = 0. \tag{5.4}$$

We write the metric perturbation tensor as

$$h_{\alpha\beta} \equiv A_{\alpha\beta}\, e^{i\varphi} \equiv \mathcal{A}\, e_{\alpha\beta}\, e^{i\varphi}, \tag{5.5}$$

where $e_{\alpha\beta}$ is the unit-normalised polarisation tensor ($e_{\alpha\beta}e^{\alpha\beta} = 1$) and $\mathcal{A}$ and φ are real functions corresponding to the amplitude and phase of the GW. The GW wavevector can be identified as

$$k_\alpha = \partial_\alpha \varphi, \tag{5.6}$$

and so

$$\nabla_\alpha \nabla^\alpha h_{\mu\nu} = \left[-k_\alpha k^\alpha A_{\mu\nu} + i\left(2k^\alpha \nabla_\alpha A_{\mu\nu} + \nabla_\alpha k^\alpha A_{\mu\nu}\right) + \nabla_\alpha \nabla^\alpha A_{\mu\nu}\right] e^{i\varphi}. \tag{5.7}$$

At the level of the *un*perturbed FLRW background metric $g^{(0)}_{\alpha\beta}$, we may follow Isaacson's geometric optics approach [146, 147], which is equivalent to the high-frequency/eikonal approximation used in previous chapters. We will use a superscript (0) to indicate quantities at this zeroth-order in scalar perturbations, so $k^{(0)}_\alpha$ is the wavevector of a GW propagating through a perfectly homogeneous FLRW spacetime. The underlying assumption of Isaacson's approach is that the GW varies on scales much shorter than the curvature of the spacetime so that the geometry may be treated as locally flat. On our cosmological background, this amounts to the requirement that $\epsilon \equiv H/\omega \ll 1$ where $\omega = k^{(0)}_\tau$ is the wave frequency and $H = a'/a^2$ is the Hubble parameter. In this sense, both $k^{(0)}_\alpha$ and $\nabla_\alpha k^{(0)}_\beta$ are $\mathcal{O}(\epsilon^{-1})$ while the amplitude is treated as $\mathcal{O}(\epsilon^0)$. At the same time, the energy is not so large as to warrant consideration of the GW's backreaction on the geometry.

The linearised Einstein equations (5.4) can then be studied order-by-order in ϵ. For our purposes, all that is relevant is the lowest order, $\mathcal{O}(\epsilon^{-2})$-equation[1], which is the requirement that $k^{(0)}_\alpha k^{(0)\alpha} = 0$. In other words, the GW follows a null geodesic $x^{(0)\alpha}(l)$ with affine parameter l

[1] We will really only need this $\mathcal{O}(\epsilon^{-2})$ behaviour to describe the phase shift. The next order gives an equation for the amplitude $\mathcal{A}$ of the GW. After some rearranging, and using the fact that $e_{\mu\nu}e^{\mu\nu} = 1$ (and consequently $e^{\mu\nu}\nabla_\alpha e_{\mu\nu} = 0$), the $\mathcal{O}(\epsilon^{-1})$-equation amounts to

$$2k^\alpha \nabla_\alpha \ln \mathcal{A} + \nabla_\alpha k^\alpha = 0. \tag{5.8}$$

such that

$$\frac{\mathrm{d}x^{(0)\alpha}}{\mathrm{d}l} = k^{(0)\alpha}. \tag{5.9}$$

The phase shift along this geodesic is determined by the linear-order correction to the wavevector:

$$\frac{\mathrm{d}}{\mathrm{d}l}\delta\varphi = \frac{\mathrm{d}x^{\alpha}}{\mathrm{d}l}\frac{\partial}{\partial x^{\alpha}}\delta\varphi = k^{(0)\alpha}k^{(1)}_{\alpha}. \tag{5.10}$$

The wavevector, in turn, is determined by the geodesic equation:

$$\frac{\mathrm{d}k^{\mu}}{\mathrm{d}l} + \Gamma^{\mu}_{\alpha\beta}k^{\alpha}k^{\beta} = 0. \tag{5.11}$$

The Christoffel symbols for the perturbed FLRW metric are

$$\Gamma^{\tau}_{\tau\tau} = \frac{a'}{a} + \Phi', \tag{5.12a}$$

$$\Gamma^{\tau}_{\tau i} = \partial_i\Phi, \tag{5.12b}$$

$$\Gamma^{\tau}_{ij} = \left[\frac{a'}{a}(1 - 2\Phi - 2\Psi) - \Psi'\right]\delta_{ij}, \tag{5.12c}$$

$$\Gamma^{i}_{\tau\tau} = \partial_i\Phi, \tag{5.12d}$$

$$\Gamma^{i}_{\tau k} = \left[\frac{a'}{a} - \Psi'\right]\delta_{ik}, \tag{5.12e}$$

$$\Gamma^{i}_{kl} = \partial_i\Psi\delta_{kl} - \partial_k\Psi\delta_{il} - \partial_l\Psi\delta_{ik}, \tag{5.12f}$$

where prime denotes a derivative with respect to τ and ∂_i is a derivative with respect to the Cartesian coordinate x^i. Our conventions for the zeroth-order wavevector are

$$k^{(0)}_{\mu} = \omega(1, \hat{\mathbf{n}}) \qquad \text{and} \qquad k^{(0)\mu} = \frac{\omega}{a^2}(-1, \hat{\mathbf{n}}), \tag{5.13}$$

where ω is the frequency of the GW at emission and $\hat{\mathbf{n}}$ is the unit vector in its direction of travel.

The geodesic equations at first order are given by

$$\frac{\mathrm{d}k^{(1)\tau}}{\mathrm{d}l} + \frac{2\omega a'}{a^3}\left(\hat{\mathbf{n}}\cdot\mathbf{k}^{(1)} - k^{(1)\tau}\right) = \frac{2\omega}{a^2}\frac{\mathrm{d}\Phi}{\mathrm{d}l} + \frac{\omega^2}{a^6}\frac{\partial}{\partial\tau}\left[a^2(\Phi + \Psi)\right], \tag{5.14a}$$

$$\frac{\mathrm{d}\mathbf{k}^{(1)}}{\mathrm{d}l} - \frac{2\omega a'}{a^3}\left(\mathbf{k}^{(1)} - k^{(1)\tau}\hat{\mathbf{n}}\right) = \frac{2\omega}{a^2}\frac{\mathrm{d}\Psi}{\mathrm{d}l}\hat{\mathbf{n}} - \frac{\omega^2}{a^6}\boldsymbol{\nabla}\left[a^2(\Phi + \Psi)\right]. \tag{5.14b}$$

A second consequence of the $\mathcal{O}(\epsilon^{-1})$-equation is that the polarisation tensor is parallel-transported along the null geodesic: $k^{\alpha}\nabla_{\alpha}e_{\mu\nu} = 0$, which is a standard result for high-frequency GWs.

Taking the dot product of the second equation with $\hat{\mathbf{n}}$, then adding it to the first gives the simple result

$$\frac{\mathrm{d}k^{(1)\tau}}{\mathrm{d}l} + \hat{\mathbf{n}} \cdot \frac{\mathrm{d}\mathbf{k}^{(1)}}{\mathrm{d}l} = \omega \frac{\mathrm{d}}{\mathrm{d}l} \frac{\Phi + \Psi}{a^2}. \tag{5.15}$$

Returning to our expression for the phase shift in terms of the linear wavevector (5.10), we have

$$\begin{aligned} \frac{\mathrm{d}}{\mathrm{d}l}\delta\varphi &= k^{(0)}_{\alpha} k^{(1)\alpha} \\ &= \omega(k^{(1)\tau} + \hat{\mathbf{n}} \cdot \mathbf{k}^{(1)}) \\ &= \frac{\omega^2}{a^2}(\Phi + \Psi). \end{aligned} \tag{5.16}$$

The phase shift can be expressed as a simple line-of-sight (l.o.s) integral in conformal time τ as

$$\delta\varphi(\hat{\mathbf{n}}) = \omega \int_{\text{l.o.s}} [\Phi(\tau, \mathbf{x}) + \Psi(\tau, \mathbf{x})] \, \mathrm{d}\tau. \tag{5.17}$$

The integral should be understood to run from conformal time at emission τ_e to observation τ_o and follow the null trajectory $\mathbf{x} = (\tau_o - \tau)\hat{\mathbf{n}}$. The cosmological time delay is related to the phase shift as $\Delta T = \delta\varphi/\omega$ and represents the extra distance travelled by the GW due to gravitational wells along its path.

There are two things to note here. The first is that the phase shift will be different for each direction in the sky, and so waves which were initially in-sync will receive different phase shifts depending on their direction of origin. In principle, there is some angular correlation between scalar perturbations as evidenced by the correlations of temperature anisotropies in the CMB [148]. Naïvely, one might expect those correlations to survive in the phase shifts. However, the second thing to note is that the phase shift is very large for frequencies typical of primordial GWs, much larger than a single wave cycle. We will quantify just how large in the next section. The result is that the apparent phase at observation is effectively randomised, and all possible correlations (from initial coherence or inherited from large scale structure) is completely washed out.

5.2 Decoherence on the sky

The phase shift is determined by the combination

$$\Phi_W = \frac{\Phi + \Psi}{2} \tag{5.18}$$

known as the Weyl potential. The information contained in the phase shift correlator is captured by its angular power spectrum $C_l^{\delta\varphi}$ [149],

$$C_l^{\delta\varphi} = \frac{8}{\pi}\omega^2 \int_0^\infty dk k^2 P_W(k) |\Delta_{W,l}(k, \tau_o)|^2, \tag{5.19}$$

where $P_W(k)$ is the primordial power spectrum of the Weyl potential,

$$\langle \Phi_W^0(\mathbf{k}) \Phi_W^{0*}(\mathbf{k}') \rangle = (2\pi)^3 \delta^{(3)}(\mathbf{k} - \mathbf{k}') P_W(k), \tag{5.20}$$

$\Phi_W(\tau, \mathbf{k})$ is the potential in Fourier space, Φ_W^0 is its stochastic primordial value and $\Delta_{W,l}(k, \tau_o)$ is its angular transfer function,

$$\Delta_{W,l}(k, \tau_o) = \int_{\tau_e}^{\tau_o} \mathrm{d}\tau j_l[k(\tau_o - \tau)] \frac{\Phi_W(\tau, k)}{\Phi_W^0(k)}, \tag{5.21}$$

where $j_l(x)$ are spherical Bessel functions. The transfer function is constructed so that it is not stochastic and is independent of direction on the sky. It simply translates the initial stochastic distribution (as captured by the power spectrum) from inflation to today. In [3] we use the best-fit Λ-Cold-Dark-Matter (ΛCDM) cosmology to compute Φ_W with CAMB[2] [150]. A typical angular power spectrum is plotted for various emission times in figure 5.1. (All figures in this chapter come from [3].) The emission time is given in terms of its redshift, $z = 1/a - 1$, which is monotonically decreasing over the course of cosmic history. The convention is that redshift $z = 0$ corresponds to the present (as does scale factor $a = 1$) and it increases into the past. The angular power spectrum for the phase shift converges by $z_e \sim 1000$, which is to say that the situation doesn't change much for earlier emission dates. The source in these plots has a frequency $f(= \omega/2\pi) = 10^{-9}$ Hz, characteristic of the pulsar timing array (PTA) band in which the NANOGrav experiment operates [151].

A measure of the typical phase shift is given by the one-point correlator (or root mean squared

[2] https://camb.info/

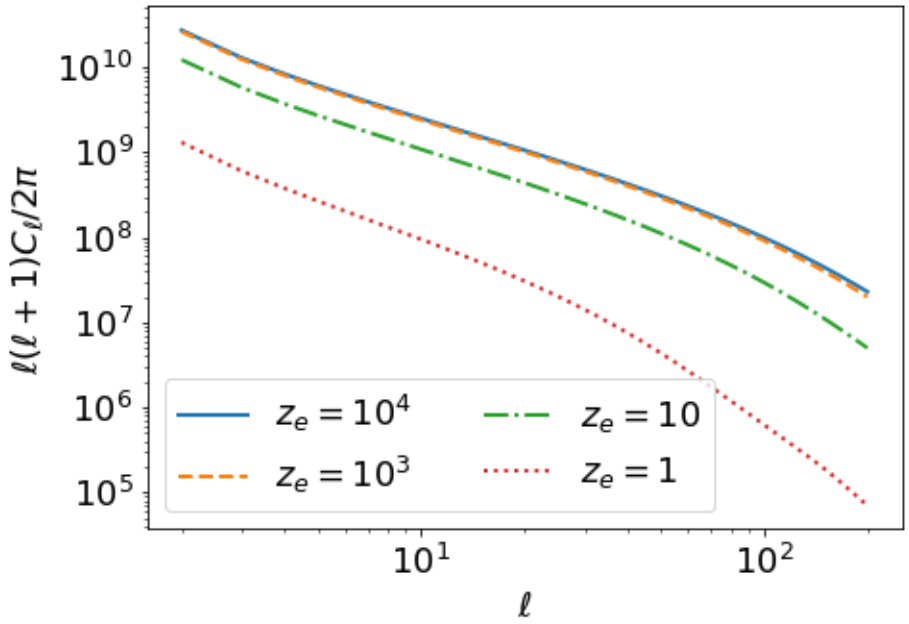

Figure 5.1: The phase shift angular power spectrum $C_l^{\delta\varphi}$ for GW sources at various emission redshifts $z_e = 1/a_e - 1$ with a frequency $f = 10^{-9}$ Hz. The spectrum converges by $z_e \sim 1000$. Image from [3].

(rms) value),

$$\delta\varphi^2_{\rm rms} \equiv \langle \delta\varphi^2(\hat{\mathbf{n}}) \rangle = \sum_{l=1}^{\infty} \frac{2l+1}{4\pi} C_l^{\delta\varphi}, \tag{5.22}$$

where the angular brackets denote sky-averaging (over the direction $\hat{\mathbf{n}}$). At high redshifts $z \gtrsim 1000$, the rms time delay $\Delta T_{\rm rms} = \delta\varphi_{\rm rms}/\omega$ (which is not frequency dependent) is roughly $\Delta T_{\rm rms} = 0.8$ Mpc, in agreement with estimates for the magnitude of the same effect on CMB photons [152]. At nanoHertz frequencies, this translates to an expected phase shift of $\delta\varphi \sim 10^6$ which, as promised, is very large indeed. A realisation of $\delta\varphi$ for an emission redshift $z_e = 1000$ at a frequency of $f = 10^{-9}$ Hz is shown in figure 5.2. Modulo 2π, these massive phase shifts become completely randomised. In fact, for any source at a redshift $z_e \gtrsim 0.01$, the expected cosmological phase shift only approaches $\mathcal{O}(1)$ for frequencies below 10^{-12} Hz. Meanwhile, for any reasonable frequencies within the bands of our current and planned array of detectors, the phase shift is too large to be treated perturbatively and cannot be expected to transmit useful information about the SGWB. We will see an explicit "worked example" of this next.

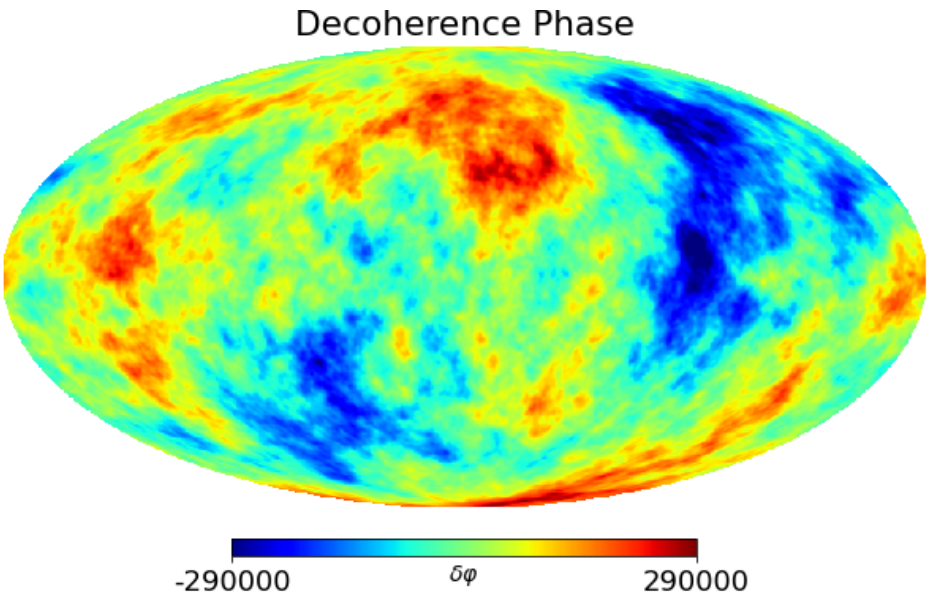

Figure 5.2: A realisation of the phase shift $\delta\varphi$ across the sky for a SGWB emitted at redshift $z_e = 1000$ at a frequency 1 nHz. Along any line of sight, the phase shift is typically orders of magnitude larger than a single cycle, $\delta\varphi \gg 2\pi$. Image from [3].

5.3 Consequences for signal estimation

The sky maps in figure 5.3 illustrate the decoherence process for an originally coherent SGWB. A detailed description of each image follows, but in summary: The top line is an example of a SGWB at emission. The middle line represents the same SGWB after propagating through the universe and experiencing phase decoherence. The last line is a "smoothed" version of the middle line, meant to imitate the effect of estimators which effectively average the strain signal from detectors over the sky.

Top line: In 4-dimensions, GWs have two polarisations: h_+ and $h_\times$. Both are modelled as spin-2 realisations of a constant l^2C_l power spectrum of equal amplitude for both grad and curl modes[3] [153]. The leftmost images on the top line of figure 5.3 show the real and imaginary components of the h_+-component of the strain. The maps are normalised to unit variance. The third image shows the corresponding phase colour-coded in the range $[-\pi, \pi)$. The angular correlations of the SGWB are visible in the phase of the original signal. The last image on the right shows the intensity of original background $I = (|h_+|^2 + |h_\times|^2)/2$, also with visible angular correlations.

Middle line: The same background after propagating through the perturbed FLRW universe.

[3] https://healpix.jpl.nasa.gov/

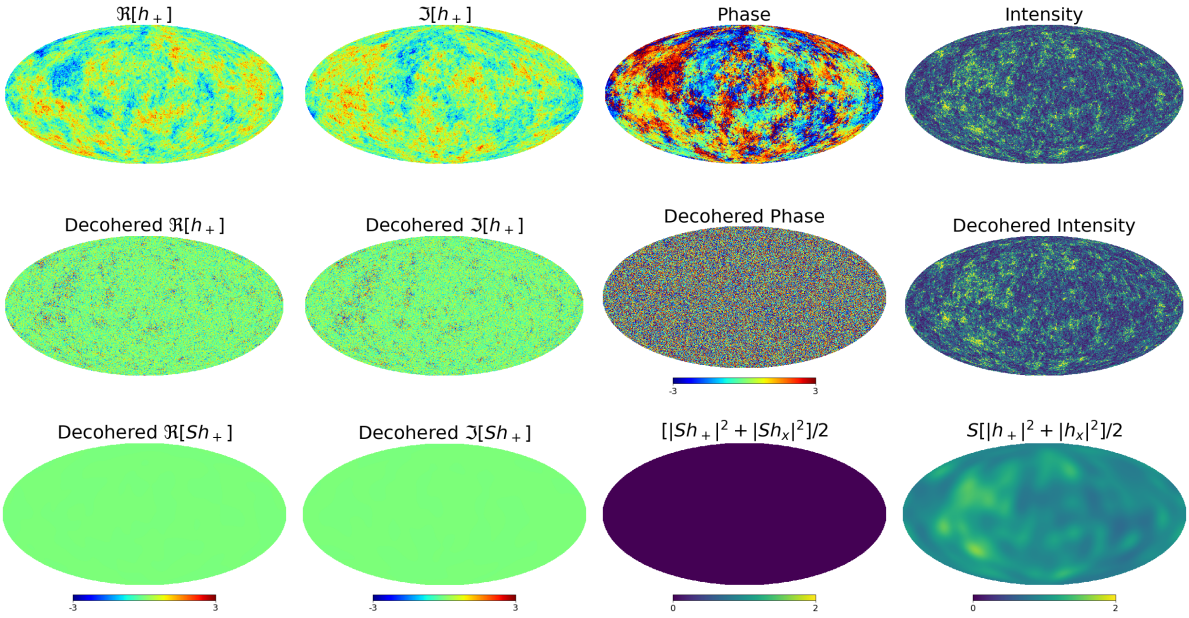

Figure 5.3: An illustration of the decoherence process for an originally coherent SGWB. The top line contains sky maps of the SGWB at emission — the real and imaginary components of its h_+-polarisation, the phase of this polarisation and the total intensity $I = (|h_+|^2 + |h_\times|^2)/2$. All four show initial angular correlations. The middle line shows the same background after undergoing phase decoherence by the scalar perturbations in the FLRW universe. The correlations have been wiped from the linear strain and phase maps but remain in the intensity. The bottom line represents a "smoothing" of the signal to imitate the effect of finite resolution detectors. Only the quadratic estimator for the signal (rightmost map) retains any of the original correlation. Details of how the maps were generated are provided in the main text. Images from [3].

We ignore corrections to the amplitude of the waves, which are truly perturbative in nature and have been considered elsewhere [144, 145]. The difference in the first three images comes from the addition of a phase shift $\delta\varphi$, as represented in figure 5.2. Across the sky, both the real and imaginary components of h_+ have been rotated randomly and the phase has lost all semblance of coherence. The intensity, on the other hand, is unaffected and retains its correlations.

Bottom line: The finite resolution of our detectors completely erases even the white noise which remains in the phase signal. Small patches of the sky are averaged over in estimators which produce SGWB maps. In the bottom line of figure 5.3, the maps from the middle line have been smoothed by a Gaussian kernel of full-width-half-maximum of ~ 20 degrees as a proxy for the limited resolution of observations. Any remaining structure in the linear maps for h_+ are completely washed out. Likewise, if one tries to estimate the intensity from these smoothed maps (third image), all correlation is lost. Information can only be recovered through incoherent reconstruction methods which are based on cross-correlation of the data (order h^2) and discards any phase information from the outset. The result is an estimate for the intensity of the underlying signal which does not vanish in the ensemble limit (fourth image). The original correlations, now smeared by finite resolution, are still visible in this map.

5.4 Chapter summary

Many inflationary models predict the existence of a cosmological gravitational wave background, and detecting such a background could be a window into the early universe. It seems likely that a primordial SGWB would be phase-coherent at generation, raising the possibility of applying phase-coherent mapping methods (which are already very useful in the case of point-like sources such as binary mergers). However, in this chapter, we argued that any initial coherence is spoiled by a cosmological phase shift due to inhomogeneties in the universe.

We calculated the phase shift $\delta\varphi$ along any given line-of-sight $\hat{\mathbf{n}}$ in an FLRW metric with scalar perturbations, Φ and Ψ. The result for a wave of frequency ω was

$$\delta\varphi(\hat{\mathbf{n}}) = \omega \int_{\text{l.o.s}} [\Phi(\tau, \mathbf{x}) + \Psi(\tau, \mathbf{x})]\, \mathrm{d}\tau, \tag{5.23}$$

where τ is conformal time. We showed that the typical phase shift is very large for detectable frequencies, $\delta\varphi \sim 10^6$ in the nanoHertz band, and varying across the sky. When added to the original profile of the SGWB, the result is a completely randomised phase which harbors none of

the initial coherence. The process from emission to detection is illustrated in figure 5.3.

The consequence is that odd-correlators (including the linear strain map $\sim h$ or the bispectrum $\langle hhh \rangle$) of the observed SGWB signal will vanish due to their randomised phase dependence. Only quadratic observables (such as the intensity) transmit meaningful information about the primordial SGWB and only incoherent mapping methods produce a faithful representation of the SGWB.

Chapter 6

Discussion

In this thesis we explored what the phase shift of scattered GWs can teach us about gravity. In chapters 2 – 4, we used the phase shift (more specifically, the associated time delay) as a diagnostic for the causality of the underlying EFT. We saw how demanding a weak positivity condition for the time delay could, in principle, constrain certain EFT parameters. We studied the GB operator (the leading non-trivial correction to GR in vacuum) in depth since its potential to violate causality has come under scrutiny in recent years. We found that, in practice, the GB operator does not violate our notion of causality as long as $|c_{\rm GB}| \lesssim \mathcal{O}(1)$, as expected from naturalness considerations. In chapter 5, we demonstrated that the very large phase shift induced over cosmological timescales can destroy the phase coherence of a primordial SGWB. We used an angular power spectrum to quantify this effect.

The first portion of this thesis ties in to efforts to constrain EFT coefficients in the IR based on physical assumptions about the UV. In our case, we assumed that any reasonable theory of quantum gravity would be causal and that this causality would manifest as luminal GW propagation. We saw that within the leading-order EFT of gravity in vacuum, the propagation of GWs is modified by the presence of the GB operator. We studied this effect on both BH and pp-wave spacetimes, with the latter representing a multi-BH configuration via an Aichelburg–Sexl boost. In both cases, it is unavoidable that at least one polarisation of low-energy GWs will enjoy superluminal speeds as a result. However, we argued that low-energy superluminality alone was not enough to declare acausality. Instead, we calculated the scattering time delay experienced by GWs in these curved spacetimes and again found that some waves will undergo a time advance compared to the geometry of the background.

We discussed two viewpoints on how to relate the scattering time delay to causality. One

perspective is that causality should be defined relative to the asymptotic spacetime — which is Minkowski in the spacetimes we study. This "asymptotic causality" simply requires weak positivity of the net time delay so that information cannot travel faster than it would have on the flat asymptotic region. From this point of view, there would be no issue with a large EFT time advance $|\Delta T_{\rm EFT}|$, so long as it is not larger than the GR time delay $|\Delta T_{\rm GR}|$. We argued in favour of the stronger condition, dubbed "IR causality", which requires the weak positivity of the EFT time delay itself. From this point of view, any (resolvable) gain over the GR time delay represents a violation of causality. The UV modes are assumed (1) to experience the GR delay and (2) to be luminal, thus cementing the GR timescale on the curved background as the relevant reference scale, and not the flat asymptotics. To support our claim that IR causality is the better criteria, we showed that it correctly reproduces the known gravitational positivity bound for the Goldstone boson.

Regardless of the specific criteria used, it is crucial to remember that it should only be applied within the EFT's regime of validity. Any truncated EFT is guaranteed to break down at high enough energies or small enough distances where microscopic degrees of freedom must come into play. We defined the EFT regime of validity by a set of bounds on the parameters of the background spacetime and the probing GW. These bounds emerge by demanding that the EFT asymptotic series expansion is under control. Pragmatically, it can also be seen that specific higher-dimension operators would come to dominate outside the limits set by these bounds. It is only sensible to question the causal properties of the GB operator within the parameter space where it dominates. Doing so, we found that the EFT time advance generated by the GB operator is unresolvable on both the BH and pp-wave spacetimes studied, so long as $|c_{\rm GB}| \lesssim \mathcal{O}(1)$.

An added subtlety in the case of the pp-wave spacetime is that the scattering process is only well-defined for a finite amount of time. As a consequence, we only had to worry about the biggest time advance that can be reasonably generated within that time-frame. We demonstrated various methods for calculating that time-frame on some representative spacetimes. In the limit in which the probe GW can be treated as a point particle, the classical argument is simply that scattering in the transverse directions will bring the probe dangerously close to the source pp-wave after a finite amount of time. It may seem like this effect can be negated by a special "balancing" configuration of sources. However, by promoting the probe to a quantum particle we showed that its wavepacket diffusion will spoil the balance and we return to the previous

scenario.

It is expected that for any EFT derived as the low-energy expansion of a consistent UV theory (e.g. the Euler–Heisenberg expansion of QED), any apparent superluminality could be shown to be unresolvable within that EFT's regime of validity. Flipped on its head, this statement means that any genuinely resolvable EFT time advance indicates a bad choice of Wilson coefficients, ones which could not possibly correspond to a good UV theory. In this sense, low-energy causality is a viable method for possibly constraining large swathes of the EFT parameter space. The framework developed in [1, 2] can be applied to generic gravitational EFTs, and the constraints produced may be tested in future generations of GW and cosmological experiments.

Since the publication of [1], further work has been done on the application of causality to EFTs. In [39], the authors obtain interesting constraints on scalar EFTs by applying IR causality. They find that, for now, positivity bounds provide the tighter constraints. However, this does not preclude the possibility that a more general analysis on a broader (less symmetric) class of backgrounds could shape up the causality bounds.

The second portion of this thesis relates to the cosmological phenomenon of a gravitational wave background. A primordial SGWB may have been generated during the inflationary period in the early universe. It has been argued that such a background could be phase-coherent at origin — that is, there could have been non-trivial angular correlations in its phase profile. Unfortunately, between emission and detection, the GWs comprising this background each undergo a series of scattering events induced by the scalar perturbations to the FLRW metric. The result is adding an effectively random phase shift, thus thoroughly scrambling the original phase information.

The immediate consequence is that phase-coherent mapping methods will be ineffective at mapping the SGWB. It had already been noted that the astrophysical background would be incoherent by default, and now we have shown that the coherence of a primordial background will be wiped out before detection. The second consequence is that odd-correlators (e.g. the bispectrum) are expected to vanish due to their residual phase dependence. Thus only statistics based on even-correlators can be used to characterise the SGWB. Work is ongoing within the LISA and NANOGrav collaborations to develop accurate mapping methods and tools for statistical analysis of the SGWB if/when it is detected in the future.

Appendix A

Asymptotic time delay in a central potential

Throughout this thesis we encounter several spherically symmetric scattering problems — the scalar fields of chapter 2, the Goldstone boson of section 4.2 and GWs scattering off a BH in section 4.3. (Of course, the first two examples are specifically chosen to have spherical symmetry in analogy with the third.) Particles propagating through these fields obey a wave equation of the form

$$\frac{\mathrm{d}^2\chi}{\mathrm{d}r^2} + W(r)\chi(r) = 0, \tag{A.1}$$

where $W(r) \sim \omega^2 - V(r)$ is the difference between the kinetic and potential energy, roughly speaking. There is such an equation describing the motion of each partial wave χ_l in the spherical harmonic expansion described for (e.g.) GWs in appendices B.2 – B.4. Unless otherwise specified, we omit the partial wave label. In this appendix, we use the Wentzel–Kramers–Brillouin (WKB) approximation to identify the asymptotic phase shift experienced by waves scattering through a central potential described by $W(r)$[1]. From the phase shift, we may then calculate the asymptotic time delay.

[1] We will analyse the equation in the standard radial coordinate $r \in [0, \infty)$. It is well known that changing to Langer coordinates $r = e^{\rho}$, and thus mapping the source from the origin to $-\infty$, improves the form of the WKB solution at low energies [58]. In our notation, when combined with a field redefinition of the form $\chi \to e^{\frac{\rho}{2}}\chi$, it has the effect of mapping $W \to e^{2\rho}W - \frac{1}{4}$. However, later in the process of calculating the time delay, we will be making a high-energy approximation anyway and thus negate any effect the change in coordinates would have had.

A.1 The WKB approximation

The WKB approximation amounts to the assumption that the solution varies (spatially) at a much slower rate than the background field generating the potential. The derivation below is due to [154]. To begin with, we insert a bookkeeping parameter ϵ to track the derivatives of the wave solution

$$\epsilon^2 \frac{\mathrm{d}^2\chi}{\mathrm{d}r^2} + W(r)\chi(r) = 0, \tag{A.2}$$

and at the end we will set $\epsilon = 1$. The WKB ansatz for the solution is

$$\chi(r) = \exp\left[\frac{1}{\delta}\sum_{n=0}^{\infty}\delta^n S_n(r)\right]. \tag{A.3}$$

Inserting this ansatz into (A.2) gives

$$\epsilon^2\left[\frac{1}{\delta}\sum_{n=0}^{\infty}\delta^n S_n'' + \frac{1}{\delta^2}\sum_{m,n=0}^{\infty}\delta^{m+n}S_m' S_n'\right] + W = 0 \tag{A.4}$$

where prime denotes derivative with respect to the radial coordinate r. To leading order as $\delta \to 0$, this equation reads

$$\frac{\epsilon^2}{\delta^2}S_0'^2 = -W \tag{A.5}$$

Since the RHS depends on neither ϵ nor δ, we must have $\delta = \epsilon$ and thus

$$S_0(r) = \pm\int^r \mathrm{d}\tilde{r}\sqrt{-W(\tilde{r})}. \tag{A.6}$$

At subleading order in ϵ we have

$$2S_0'S_1' + S_0'' = 0. \tag{A.7}$$

Upon substituting the solution for S_0, this equation can be solved for $S_1 = -\frac{1}{4}\ln|W| + c$. We will stop at this order with WKB solution (setting $\epsilon = 1$)

$$\chi(r) = \frac{c_+}{|W|^{\frac{1}{4}}}\exp\left[\int^r \mathrm{d}\tilde{r}\sqrt{-W(\tilde{r})}\right] + \frac{c_-}{|W|^{\frac{1}{4}}}\exp\left[-\int^r \mathrm{d}\tilde{r}\sqrt{-W(\tilde{r})}\right]. \tag{A.8}$$

This solution is valid away from any region where $W = 0$. However, the scattering problems we deal with will all have a turning point $r = r_t$ where the kinetic and potential energy are equal

and thus

$$W(r_t) = 0. \tag{A.9}$$

On either side of this turning point, the WKB solution (A.8) is valid, but at the turning point we must use a different approximation to patch the two solutions together smoothly.

Below the turning point

First, below the turning point $r < r_t$ we have a classically forbidden region where $W(r < r_t) < 0$. In this region, we choose the decaying branch of (A.8):

$$\chi_{\text{below}}(r < r_t) \approx \frac{\bar{\chi}}{(-W(r))^{\frac{1}{4}}} \exp\left[-\int_r^{r_t} \mathrm{d}\tilde{r}\sqrt{-W(\tilde{r})}\right] \tag{A.10}$$

where $\bar{\chi}$ is some constant determining the amplitude.

Near the turning point

Close to the turning point, we expand the function W in its linear Taylor series

$$W(r) \approx (r - r_t)\left.\frac{\mathrm{d}W}{\mathrm{d}r}\right|_{r=r_t} \tag{A.11}$$

and define the (in our case, positive) constant

$$\alpha^3 = \left.\frac{\mathrm{d}W}{\mathrm{d}r}\right|_{r=r_t} \tag{A.12}$$

so that the wave equation takes the form

$$\frac{\mathrm{d}^2\chi}{\mathrm{d}r^2} \approx -\alpha^3(r - r_t)\chi(r). \tag{A.13}$$

Changing variables to $z = -\alpha(r - r_t)$ puts the above equation in the form of an Airy equation

$$\frac{\mathrm{d}^2\chi}{\mathrm{d}z^2} = z\chi(z). \tag{A.14}$$

The solutions to the Airy equation are the so-called Airy functions

$$\chi_{\text{near}}(z) = a\mathrm{Ai}(z) + b\mathrm{Bi}(z) \tag{A.15}$$

whose asymptotic behaviour is known,

$$\mathrm{Ai}(z) \sim \begin{cases} \dfrac{1}{2\sqrt{\pi} z^{\frac{1}{4}}} \exp\left[-\dfrac{2}{3} z^{\frac{3}{2}}\right] & z \gg 0 \\ \dfrac{1}{\sqrt{\pi}(-z)^{\frac{1}{4}}} \sin\left[\dfrac{2}{3}(-z)^{\frac{3}{2}} + \dfrac{\pi}{4}\right] & z \ll 0 \end{cases} \tag{A.16a}$$

$$\mathrm{Bi}(z) \sim \begin{cases} \dfrac{1}{\sqrt{\pi} z^{\frac{1}{4}}} \exp\left[\dfrac{2}{3} z^{\frac{3}{2}}\right] & z \gg 0 \\ \dfrac{1}{\sqrt{\pi}(-z)^{\frac{1}{4}}} \cos\left[\dfrac{2}{3}(-z)^{\frac{3}{2}} + \dfrac{\pi}{4}\right] & z \ll 0 \end{cases} \tag{A.16b}$$

To determine the constants a and b, we must match the near-turning-point solution (A.15) to the below-turning-point solution (A.10). Evaluating the below-turning-point solution as $r \nearrow r_t$, and rewriting it in terms of $z = -\alpha(r - r_t)$, we find

$$\begin{aligned} \chi_{\mathrm{below}}(r \nearrow r_t) &\approx \frac{\bar{\chi}}{(-\alpha^3(r - r_t))^{\frac{1}{4}}} \exp\left[-\int_r^{r_t} \mathrm{d}\tilde{r} \sqrt{-\alpha^3(\tilde{r} - r_t)}\right] \\ &\approx \frac{\bar{\chi}}{\sqrt{\alpha}} \frac{1}{z^{\frac{1}{4}}} \exp\left[-\frac{2}{3} z^{\frac{3}{2}}\right]. \end{aligned} \tag{A.17}$$

Comparing this with the asymptotic behaviour of the Airy functions at $z \gg 0$, we see that we need

$$a = 2\sqrt{\frac{\pi}{\alpha}} \bar{\chi}, \qquad b = 0, \tag{A.18}$$

for the below- and near-turning-point solutions to connect smoothly.

Above the turning point

Above the turning point, where $W(r > r_t)$ is positive, the WKB solution is oscillatory

$$\chi_{\mathrm{above}}(r > r_t) \approx \frac{c_+}{W^{\frac{1}{4}}} \exp\left[i \int_{r_t}^{r} \mathrm{d}\tilde{r} \sqrt{W(\tilde{r})}\right] + \frac{c_-}{W^{\frac{1}{4}}} \exp\left[-i \int_{r_t}^{r} \mathrm{d}\tilde{r} \sqrt{W(\tilde{r})}\right]. \tag{A.19}$$

The constants $c_\pm$ must be determined by matching onto the near-turning-point solution as $r \searrow r_t$. Again, in terms of $z = -\alpha(r - r_t)$, we have

$$\chi_{\mathrm{above}}(r \searrow r_t) \approx \frac{c_+}{\sqrt{\alpha}} \frac{1}{(-z)^{\frac{1}{4}}} \exp\left[\frac{2i}{3}(-z)^{\frac{3}{2}}\right] + \frac{c_-}{\sqrt{\alpha}} \frac{1}{(-z)^{\frac{1}{4}}} \exp\left[-\frac{2i}{3}(-z)^{\frac{3}{2}}\right]. \tag{A.20}$$

Comparing this with the $z \ll 0$ asymptotic form of the near-turning-point solution (A.15), and the required choice of a and b (A.18) for matching with the below-turning-point solution, gives us the "WKB connection formula":

$$c_+ = 2\bar{\chi}\frac{e^{\frac{i\pi}{4}}}{2i}, \qquad c_- = -2\bar{\chi}\frac{e^{-\frac{i\pi}{4}}}{2i}. \tag{A.21}$$

Note that dependence on the constant α has dropped out.

The upshot of this derivation is that in the classically allowed region of interest, the WKB solution to (A.1) is

$$\chi_{\text{above}}(r > r_t) \approx \frac{2\bar{\chi}}{W^{\frac{1}{4}}} \sin\left[\int_{r_t}^{r} \mathrm{d}\tilde{r}\sqrt{W(\tilde{r})} + \frac{\pi}{4}\right]. \tag{A.22}$$

A.2 Asymptotic phase shift in the eikonal limit

The solution to the spherically symmetric Schrödinger problem has known asymptotic form, for each partial wave l. Temporarily reinstating the partial wave label, it is

$$\chi_l \overset{r\to\infty}{\sim} \left(e^{2i\delta_l}e^{i\omega r} + e^{i\pi l}e^{i\pi(D-2)/2}e^{-i\omega r}\right), \tag{A.23}$$

where δ_l is the l-dependent asymptotic phase shift. In a vacuum Minkowski spacetime, the phase shift is zero, by definition. The phase shift due to the source $W_l(r)$ can be identified by matching the solution calculated in the previous section (A.22) with this asymptotic form to find

$$\delta_l(\omega) = \int_{r_t}^{\infty}\left(\sqrt{W_l(r)} - \omega\right)\mathrm{d}r - \omega r_t + \frac{\pi}{2}\left(l + \frac{D-3}{2}\right), \tag{A.24}$$

where both $W_l(r)$ and the turning point r_t are implicitly dependent on ω and l.

To make progress, we will split W into two parts: there is a part which would be present in a Minkowski vacuum (due to coordinate choice) and there is a part due to the source of the external field (Galileon, Goldstone or gravitational). Sufficiently far away from the source, in a weak field limit, we may treat the source term as a perturbation to the coordinate term and thereby isolate the phase shift due to the source. First, we calculate that term which is present even when the source is "switched off" due to the coordinate choice and show how the phase shift vanishes in this case.

In vacuum Minkowski spacetime

In a Minkowski vacuum, a scalar perturbation ϕ (specifically, some partial wave ϕ_l of the scalar perturbation) experiences an apparent potential simply due to the spherical coordinates. Its equation of motion is

$$\nabla^2\phi = 0 \implies \frac{\partial^2\phi}{\partial r^2} + \frac{(D-2)}{r}\frac{\partial\phi}{\partial r} + \left(\omega^2 - \frac{\kappa_S^2}{r^2}\right)\phi = 0 \tag{A.25}$$

where $-\kappa_S^2$ is the scalar eigenvalue of the Laplace–Beltrami operator on the $(D-2)$-sphere and takes discrete values

$$\kappa_S^2 = l(l+D-3), \quad l = 0, 1, 2, \ldots. \tag{A.26}$$

Rescaling the field as $\phi = r^{-\frac{D-2}{2}}\chi$ puts the equation in the form of (A.1) with

$$W_{\text{coord}}(r) = \omega^2 - \frac{1}{r^2}\left(l + \frac{D-3}{2}\right)^2 + \frac{1}{4r^2}. \tag{A.27}$$

The subscript "coord" indicates that the non-zero effective potential is due to the spherical coordinate choice. By convention, we define the impact parameter as

$$b = \frac{1}{\omega}\left(l + \frac{D-3}{2}\right). \tag{A.28}$$

At high-l (or high frequencies), the impact parameter represents a good approximation to the turning point. Had we worked in Langer coordinates $r = e^\rho$ [58] instead of the traditional radial coordinate, the turning point for the corresponding Langer field $\chi_L = e^{-\frac{\rho}{2}}\chi$ would be exactly equal to the impact parameter at all l. In those improved coordinates, where the WKB approximation does well even at low-l, we would see the exact vanishing of the phase shift of the Langer field in vacuum Minkowski spacetime. As it is, for the sake of sticking to one coordinate system, we will satisfy ourselves with the high-energy regime where

$$W_{\text{coord}}(r) \approx \omega^2\left(1 - \frac{b^2}{r^2}\right) + \mathcal{O}\left(\frac{l^0}{r^2}\right) \tag{A.29}$$

and $r_t \approx b$. At high energies, the phase shift is thus

$$\delta \approx \omega\int_b^\infty \left(\sqrt{1 - \frac{b^2}{r^2}} - 1\right)\mathrm{d}r - \omega b + \frac{\pi}{2}\omega b = 0, \tag{A.30}$$

i.e. the phase shift of a wave perturbation in vacuum Minkowski spacetime vanishes, as promised.

With a source

In the suitable weak field limit — which will depend on the scenario — we may write

$$W(r) = W_{\text{coord}}(r) + W_{\text{source}}(r) \tag{A.31}$$

and treat the source as a small correction term. The turning point $W(r_t) = 0$ depends on the source as

$$\omega^2 b^2 = \omega^2 r_t^2 + r_t^2 W_{\text{source}}(r_t) \tag{A.32}$$

and thus expanding the integral term in (A.24) is not straightforward. The solution, coming from appendix C of [36], is to use the relationship between b and r_t to write (in the high-energy limit)

$$W_{\text{coord}} \approx \omega^2 \left(1 - \frac{r_t^2}{r^2}\right) - \frac{r_t^2}{r^2} W_{\text{source}}(r_t) \tag{A.33}$$

so that, to linear order in W_{source}, the phase shift is

$$\begin{aligned} \delta \approx & \int_{r_t}^{\infty} \left(\sqrt{\omega^2 \left(1 - \frac{r_t^2}{r^2}\right)} - \omega \right) \mathrm{d}r - \omega r_t + \frac{\pi}{2}\omega b \\ & + \frac{1}{2} \int_{r_t}^{\infty} \frac{1}{\sqrt{\omega^2 \left(1 - r_t^2/r^2\right)}} \left(W_{\text{source}}(r) - \frac{r_t^2}{r^2} W_{\text{source}}(r_t) \right) \mathrm{d}r. \end{aligned} \tag{A.34}$$

Performing the integrals (where the integrand is explicit) gives

$$\delta = \frac{\pi}{2}\omega(b - r_t) - \frac{\pi}{4\omega} r_t W_{\text{source}}(r_t) + \frac{1}{2\omega} \int_{r_t}^{\infty} \frac{W_{\text{source}}(r)}{\sqrt{1 - r_t^2/r^2}} \mathrm{d}r. \tag{A.35}$$

Now note that from (A.32) we can recognise the difference between the impact parameter and the turning point as a linear order term,

$$b - r_t = \frac{r_t^2}{\omega^2} \frac{W_{\text{source}}(r_t)}{b + r_t} \approx \frac{b}{2\omega^2} W_{\text{source}}(b). \tag{A.36}$$

In terms linear in W_{source}, the turning point r_t may be replaced with the impact parameter b without affecting this order in the expansion. The resulting phase shift is

$$\delta = \frac{1}{2\omega}\int_b^\infty \mathrm{d}r \frac{W_{\text{source}}(r)}{\sqrt{1-b^2/r^2}}. \tag{A.37}$$

This is the main result of this appendix and is referred to several times throughout the main text.

A.3 Time delay from phase shift

The phase shift depends on three parameters: the conserved energy ω, the impact parameter b and the partial wave number l (though this last one is hidden in W_{source}). These three parameters are not all independent and are related by (A.28). There are thus two reasonable definitions of time delay: one at fixed impact parameter

$$\Delta T_b = 2\left.\frac{\partial\delta}{\partial\omega}\right|_b, \tag{A.38}$$

and one at fixed partial wave number

$$\Delta T_l = 2\left.\frac{\partial\delta}{\partial\omega}\right|_l. \tag{A.39}$$

The two are very similar, differing usually in numerical factors. In this thesis, we will use the latter definition ΔT_l for the time delay as it is best suited to the spherically symmetric problem. Both get used in the literature — in particular, [31] considers the fixed-b time delay.

The factor of 2 appearing in the formulae for time delay accounts for the fact that the definition of δ in (A.24) only captures half the total journey, from the turning point r_t to $+\infty$ rather than from $-\infty$ to $+\infty$ as intended.

A.4 Example: Shapiro time delay

To see the above formalism in action, we will calculate the time delay due to a D-dimensional Schwarzschild black hole in GR (i.e. without any EFT corrections). This is famously known as the Shapiro time delay, the fourth classical test of GR. Consider the Schwrazschild black hole metric

$$\mathrm{d}s^2 = -f(r)\mathrm{d}t^2 + \frac{1}{f(r)}\mathrm{d}r^2 + r^2\mathrm{d}\Omega_{D-2}^2, \tag{A.40}$$

where $\mathrm{d}\Omega_{D-2}^2$ is the line element on the $(D-2)$-sphere and

$$f(r) = 1 - \left(\frac{r_g}{r}\right)^{D-3}. \tag{A.41}$$

The Schwarzschild radius is r_g and the weak field limit in this case corresponds to passing far away from the black hole so that $r_g/r \ll 1$. In vacuum, the BH potential experienced by any massless particle is the same and can be obtained from (e.g.) the Goldstone scalar calculations, (4.20) with $B^2 = A^{-2} = f$ and $c = 0$, or the high-energy, weak-field, GR ($c_{\rm GB} = 0$) limit of (4.45). At leading order in ω, we have

$$W = \underbrace{\omega^2\left(1 - \frac{b^2}{r^2}\right)}_{W_{\rm coord}} + \underbrace{\omega^2\left(\frac{r_g}{r}\right)^{D-3}\left(2 - \frac{b^2}{r^2}\right)}_{W_{\rm BH}}, \tag{A.42}$$

with $W_{\rm BH}$ the stand-in for $W_{\rm source}$. The phase shift due to the BH source according to (A.37) is thus

$$\begin{aligned}
\delta_{\rm BH} &= \frac{\omega r_g^{D-3}}{2}\int_b^\infty \mathrm{d}r \frac{1}{r^{D-3}}\frac{2 - b^2/r^2}{\sqrt{1 - b^2/r^2}} \\
&= \frac{\sqrt{\pi}\Gamma\left(\frac{D}{2}\right)}{2(D-4)\Gamma\left(\frac{D-1}{2}\right)}\frac{\omega r_g^{D-3}}{b^{D-4}} \\
&= \frac{(D-2)\sqrt{\pi}\Gamma\left(\frac{D-4}{2}\right)}{4(D-3)\Gamma\left(\frac{D-3}{2}\right)}\frac{\omega r_g^{D-3}}{b^{D-4}}
\end{aligned} \tag{A.43}$$

where we have used a property of the gamma function, $\Gamma(n+1) = n\Gamma(n)$, to move from the second to last line. At a fixed-l, the impact parameter must be replaced with (A.28) so that $\delta_{\rm BH} \propto \omega^{D-3}$ and the D-dimensional Shapiro time delay is

$$\Delta T_{\rm BH} = \frac{(D-2)\sqrt{\pi}}{2}\frac{\Gamma\left(\frac{D-4}{2}\right)}{\Gamma\left(\frac{D-3}{2}\right)}\left(\frac{r_g}{r}\right)^{D-3} b. \tag{A.44}$$

Appendix B

The Schwarzschild metric and its master equations

B.1 Background metric

The general spherically symmetric solution to Lovelock gravity was found in [76, 79, 155]; the latter of these also proved Birkhoff's theorem for Lovelock gravity, i.e. that such solutions are static. For our purposes, we are interested in the Schwarzschild-like solution to just EGB theory. To this end, consider the general spherically symmetric, static metric ansatz

$$\mathrm{d}s^2 = -f(r)\mathrm{d}t^2 + g(r)\mathrm{d}r^2 + r^2\mathrm{d}\Omega_{D-2}^2 \tag{B.1}$$

which has non-zero Riemann tensor components

$$R_{trtr} = \frac{2ff''g - f'^2g - ff'g'}{4fg}, \tag{B.2a}$$

$$R_{tatb} = \frac{f'}{2rg}g_{ab}, \tag{B.2b}$$

$$R_{rarb} = \frac{g'}{2rg}g_{ab}, \tag{B.2c}$$

$$R_{abcd} = \frac{g-1}{r^2g}\left(g_{ac}g_{bd} - g_{ad}g_{bc}\right). \tag{B.2d}$$

As a reminder, the indices $\{a, b, c, \dots\}$ label directions on the $(D-2)$-sphere and $g_{ab} = r^2\gamma_{ab}$ where γ_{ab} is the metric on the $(D-2)$-sphere. Prime indicates a derivative with respect to the

radial coordinate r. The non-zero Ricci tensor components are

$$R_{tt} = \frac{2ff''g - f'^2g - ff'g'}{4fg^2} + (D-2)\frac{f'}{2rg}, \tag{B.3a}$$

$$R_{rr} = \frac{-2ff''g + f'^2g + ff'g'}{4f^2g} + (D-2)\frac{g'}{2rg}, \tag{B.3b}$$

$$R_{ab} = \left(\frac{fg' - f'g}{2rfg^2} + (D-3)\frac{g-1}{r^2g}\right) g_{ab}, \tag{B.3c}$$

and the Ricci scalar is

$$R = \frac{-2ff'' + f'^2g + ff'g'}{2f^2g^2} + (D-2)\frac{fg' - f'g}{rfg^2} + (D-2)(D-3)\frac{g-1}{r^2g}. \tag{B.4}$$

In terms of this ansatz, the GB operator is easily calculated:

$$\begin{aligned} R^2_{\mathrm{GB}} = (D-2)(D-3)\Bigg[&\frac{(g-1)(-2ff''g + f'^2g + ff'g')}{r^2f^2g^3} - 2\frac{f'g'}{r^2fg^3} \\ &+ (D-4)(D-5)\frac{(g-1)^2}{r^4g^2} + 2(D-4)\frac{(g-1)(fg' - f'g)}{r^3fg^3}\Bigg]. \end{aligned} \tag{B.5}$$

The metric (B.1) should be a solution to the EGB equations (3.5). To find the ordinary differential equations (ODEs) governing the behaviour of $f(r)$ and $g(r)$, we substitute the above ansatz directly into the EGB action (3.4) and demand that it is stationary with respect to variations in these functions[1]. The result is two first order ODEs:

$$\begin{aligned} 0 = g'&\left(1 + 4(D-3)(D-4)\frac{c_{\mathrm{GB}}}{\Lambda^2}\frac{g-1}{r^2g}\right) \\ &+ (D-3)\frac{g(g-1)}{r}\left(1 + 2(D-4)(D-5)\frac{c_{\mathrm{GB}}}{\Lambda^2}\frac{g-1}{r^2g}\right), \end{aligned} \tag{B.6a}$$

$$\begin{aligned} 0 = f'&\left(1 + 4(D-3)(D-4)\frac{c_{\mathrm{GB}}}{\Lambda^2}\frac{g-1}{r^2g}\right) \\ &- (D-3)\frac{f(g-1)}{r}\left(1 + 2(D-4)(D-5)\frac{c_{\mathrm{GB}}}{\Lambda^2}\frac{g-1}{r^2g}\right). \end{aligned} \tag{B.6b}$$

Combining these two equations gives

$$\frac{f'}{f} = -\frac{g'}{g}, \tag{B.7}$$

and the condition that the solution be asymptotically flat (i.e. $g(r\to\infty) = f(r\to\infty) = 1$) fixes

$$g = \frac{1}{f}. \tag{B.8}$$

[1]The VariationalMethods package of Mathematica was used to perform this calculation.

To find the solution for $f(r)$, consider the ansatz

$$f(r) = 1 - r^2\psi(r). \tag{B.9}$$

Now, the equation for $\psi(r)$ can be written in the form

$$2(D-3)(D-4)\frac{c_{\rm GB}}{\Lambda^2}(\psi^2)' + \psi' = -\frac{D-1}{r}\left(2(D-3)(D-4)\frac{c_{\rm GB}}{\Lambda^2}\psi^2 + \psi\right), \tag{B.10}$$

so that the solution obeys the functional equation

$$2(D-3)(D-4)\frac{c_{\rm GB}}{\Lambda^2}\psi^2 + \psi = \frac{r_g^{D-3}}{r^{D-1}}, \tag{B.11}$$

where the integration constant has been chosen appropriately.

Finally, since we are working in the context of an EFT expansion, the function $\psi(r)$ can be solved for perturbatively in powers of Λ^{-1} by plugging the GR ($c_{\rm GB} = 0$) solution, $\psi(r) = r_g^{D-3}/r^{D-1}$, back into the first term on the left-hand side of (B.11) to obtain (3.8).

B.2 Tensor modes

Over the next three subappendices, we derive the tensor/vector/scalar master variables respectively and calculate their master equations. For each mode, we first outline how the calculation was done explicitly in $D = 5$-dimensions, with the help of Mathematica. The results in general D-dimensions come courtesy of Dotti and Gleisir [77, 78].

Following similar notation to [87], the tensor-type metric perturbations are expanded in terms of tensor spherical harmonics $\mathbb{T}_{ab}$ on S^{D-2}, which satisfy

$$\left(\hat{\Delta}_{D-2} + \kappa_T^2\right)\mathbb{T}_{ab} = 0, \tag{B.12a}$$

$$\mathbb{T}^a{}_a = 0, \quad \hat{D}_a\mathbb{T}^a{}_b = 0, \tag{B.12b}$$

where $-\kappa_T^2$ is the eigenvalue of $\hat{\Delta}_{D-2}$ acting on the tensor $\mathbb{T}_{ab}$, and takes discrete values:

$$\kappa_T^2 = \ell(\ell + D - 3) - 2, \quad \ell = 1, 2, \ldots. \tag{B.13}$$

All mode numbers (e.g. ℓ) that could label $\mathbb{T}_{ab}$ have been suppressed. For each such tensor, the

tensor-type metric perturbations can be written at each ℓ as

$$h_{AB} = 0, \quad h_{Aa} = 0, \quad h_{ab} = 2r^2 H_T \mathbb{T}_{ab}. \tag{B.14}$$

It is clear that the only tensor-mode freedom is in the function $H_T \equiv H_T(t, r)$. The dynamics of H_T are governed by the perturbation equation $\delta\mathcal{E}_{ab} = 0$.

B.2.1 5-dimensions

The *xTras* package for *xAct* [156, 157] in Mathematica was used to find the first perturbation of $\mathcal{E}^{\alpha}{}_{\beta}$ (3.5) in terms of $h_{\alpha\beta}$ and its derivatives. The package *Ricci.m* [158] was used to calculate the background Riemann/Ricci tensors etc. explicitly in coordinates in 5-dimensions. Simple methods were developed to turn covariant derivatives into coordinate expressions in Mathematica. The result is 15 differential equations for H_T and the components of $\mathbb{T}_{ab}$. The transverse-traceless constraints and the eigenvalue equation for the spherical harmonics (B.12) were implemented by hand to remove all dependence on $\mathbb{T}_{ab}$. This leaves just one independent equation for the function H_T coming from any of the ab-equations $\delta\mathcal{E}^{a}{}_{b} = 0$,

$$\begin{aligned} 0 = &\left(1 - 8c_{\rm GB}\mu\left(\frac{r_g}{r}\right)^2 rf'\right)\left(-\frac{\partial^2 H_T}{\partial t^2} + \frac{\partial^2 H_T}{\partial r^2}\right) \\ &+ \left(\frac{3f}{r}(f + rf') + 16c_{\rm GB}\mu\left(\frac{r_g}{r}\right)^2\left(\frac{f^2}{r}(1-f) - \frac{ff'}{2}(2f - rf')\right)\right)\frac{\partial H_T}{\partial_r} \\ &- \frac{f}{r^2}\left(\kappa_T^2 + 2\right)\left(1 + 16c_{\rm GB}\mu\left(\frac{r_g}{r}\right)^2(1-f)\right)H_T. \end{aligned} \tag{B.15}$$

We always work only to linear order in μ, the leading order in the EFT. Finally, to bring this equation into the appropriate form we rescale H_T,

$$\Phi_T = r^{3/2}\left(1 - 4c_{\rm GB}\mu\left(\frac{r_g}{r}\right)^4\right)H_T. \tag{B.16}$$

The master equation for Φ_T is then

$$\Box_2\Phi_T - \frac{V_T}{f}\Phi_T = 0. \tag{B.17}$$

where the potential in 5-dimensions is identified as

$$\frac{V_T}{f} = \frac{1}{r^2}\left[\kappa_T^2 + \frac{11}{4} + \frac{9}{4}\left(\frac{r_g}{r}\right)^2 + c_{\rm GB}\mu\left(\frac{r_g}{r}\right)^4\left(32\kappa_T^2 + 32 + 31\left(\frac{r_g}{r}\right)^2\right)\right]. \tag{B.18}$$

B.2.2 Arbitrary dimensions

In general $D \geq 5$-dimensions, the tensor master variable and master equation in this EFT can be obtained from the results of [77] by expanding to linear order in the GB parameter they call "α" $\equiv 4c_{\rm GB}/\Lambda^2$. As in 5-dimensions, the master variable is related to the function H_T by a simple rescaling:

$$\Phi_T = r^{(D-2)/2}\left(1 - 4(D-4)c_{\rm GB}\mu\left(\frac{r_g}{r}\right)^{D-1}\right)H_T. \tag{B.19}$$

The master equation is then of the form (4.54) where, to linear order in μ, the potential for this master variable is

$$\begin{aligned}\frac{V_T}{f} = \frac{1}{r^2}\Bigg[&\kappa_T^2\left(1 + 8(D-1)c_{\rm GB}\mu\left(\frac{r_g}{r}\right)^{D-1}\right)\\ &+ \frac{D(D-6)+16}{4}\left(1 - \frac{32(D-1)(D-6)}{D(D-6)+16}c_{\rm GB}\mu\left(\frac{r_g}{r}\right)^{D-1}\right)\\ &+ \frac{(D-2)^2}{4}\left(\frac{r_g}{r}\right)^{D-3}\left(1 - \frac{6(D-4)(D^2-7D+4)}{D-2}c_{\rm GB}\mu\left(\frac{r_g}{r}\right)^{D-1}\right)\Bigg].\end{aligned} \tag{B.20}$$

B.3 Vector modes

The vector-type metric perturbations are expanded in terms of transverse vector spherical harmonics $\mathbb{V}_a$ on S^{D-2}, which satisfy

$$\left(\hat{\Delta}_{D-2} + \kappa_V^2\right)\mathbb{V}_a = 0, \tag{B.21a}$$

$$\hat{D}_a\mathbb{V}^a = 0, \tag{B.21b}$$

where $-\kappa_V^2$ is the eigenvalue of $\hat{\Delta}_{D-2}$ acting on the vector $\mathbb{V}_a$ and takes discrete values[2]:

$$\kappa_V^2 = \ell(\ell + D - 3) - 1, \quad \ell = 1, 2, \ldots. \tag{B.22}$$

All mode numbers (i.e. ℓ) that could label $\mathbb{V}_a$ have been suppressed. For each vector, the vector-type metric perturbations can be written at each ℓ as

$$h_{AB} = 0, \quad h_{Aa} = r f_A \mathbb{V}_a, \quad h_{ab} = 2r^2 H_T \mathbb{V}_{ab}, \tag{B.23}$$

[2]The $\ell = 1$ vector harmonic corresponds to rotational perturbations of the BH and not a dynamical degree of freedom.

where

$$\mathbb{V}_{ab} = -\frac{1}{2\kappa_V}\left(\hat{D}_a\mathbb{V}_b + \hat{D}_b\mathbb{V}_a\right). \tag{B.24}$$

Identifying the master variable for vectors is a more involved process than it was for tensors because of the non-trivial h_{Aa} components.

B.3.1 5-dimensions

As with the tensor modes, a combination of the *xTras* [156] and *Ricci.m* [158] packages were used to render the equations $\delta\mathcal{E}^{\alpha}{}_{\beta} = 0$ explicitly in coordinates for $D = 5$ in Mathematica. The transverse condition and eigenvalue equations (B.21) for the vector spherical harmonics were implemented by hand to make explicit the structure of the harmonic expansion in the perturbation equations. In particular, we have that $\delta\mathcal{E}_{AB}$ is identically zero due to the vectors being transverse. The other equations are

$$\begin{aligned}
\delta\mathcal{E}^{t}{}_{a} = \frac{r\mathbb{V}_a}{2}\Bigg[& \left(1 - 4c_{\rm GB}\mu\left(\frac{r_g}{r}\right)^2(rf' + r^2f'')\right)\partial_r^2 f_t \\
& + \left(3 + 4c_{\rm GB}\mu\left(\frac{r_g}{r}\right)^2(4(1-f) - 3rf' - r^2f'')\right)\frac{\partial_r f_t}{r} \\
& - \Bigg((\kappa_V^2 - 2)\left(1 + 4c_{\rm GB}\mu\left(\frac{r_g}{r}\right)^2(2(1-f) - rf')\right) \\
& \quad + f\left(3 + 4c_{\rm GB}\mu\left(\frac{r_g}{r}\right)^2(7 - 4f - 3rf' - r^2f'')\right)\Bigg)\frac{f_t}{r^2 f} \\
& - \left(4 + 8c_{\rm GB}\mu\left(\frac{r_g}{r}\right)^2(2(1-f) - 2rf' + r^2f'')\right)\frac{\partial_t f_r}{r} \\
& - \left(1 - 4c_{\rm GB}\mu\left(\frac{r_g}{r}\right)^2(rf' + r^2f'')\right)\partial_t\partial_r f_r \\
& - (\kappa_V^2 - 2)\left(1 + 4c_{\rm GB}\mu\left(\frac{r_g}{r}\right)^2(2(1-f) - rf')\right)\frac{\partial_t H_T}{rf}\Bigg],
\end{aligned} \tag{B.25a}$$

$$\begin{aligned}
\delta\mathcal{E}^{r}{}_{a} = \frac{r\mathbb{V}_a}{2}\Bigg[& \left(1 - 4c_{\rm GB}\mu\left(\frac{r_g}{r}\right)^2(rf' + r^2f'')\right)\left(\partial_t^2 f_r - \partial_t\partial_r f_t + \frac{\partial_t f_t}{r}\right) \\
& + \frac{f}{r^2}(\kappa_V^2 - 2)\left(1 + 4c_{\rm GB}\mu\left(\frac{r_g}{r}\right)^2(2(1-f) - rf')\right)(f_r + r\partial_r H_T)\Bigg],
\end{aligned} \tag{B.25b}$$

$$\begin{aligned}\delta\mathcal{E}^a{}_b = \hat{D}^a\mathbb{V}_b\Bigg[&\left(rf' - 8c_{\rm GB}\mu\left(\frac{r_g}{r}\right)^2(2f^2 + r^2f'^2)\right)\left(\frac{f_r}{r^2} + \frac{\partial_r H_T}{r}\right)\\ &+ 2f\left(1 + 4c_{\rm GB}\mu\left(\frac{r_g}{r}\right)^2(2 - rf')\right)\frac{f_r}{r^2}\\ &+ f\left(3 + 16c_{\rm GB}\mu\left(\frac{r_g}{r}\right)^2(1 - rf')\right)\frac{\partial_r H_T}{r}\\ &+ \left(1 - 8c_{\rm GB}\mu\left(\frac{r_g}{r}\right)^2 rf'\right)\left(f\frac{\partial_r f_r}{r} + f\partial_r^2 H_T - \frac{\partial_t f_t}{rf} - \frac{\partial_t^2 H_T}{f}\right)\Bigg].\end{aligned} \tag{B.25c}$$

From the initial parametrisation, we then construct the variables

$$F_A = f_A + rD_A H_T. \tag{B.26}$$

Substituting the f_A for F_A and the background solution for $f(r)$ in the perturbation equations has the effect of removing H_T from the equations altogether.

$$\begin{aligned}\delta\mathcal{E}^t{}_a = \frac{r\mathbb{V}_a}{2}\Bigg[&\left(1 + 8c_{\rm GB}\mu\left(\frac{r_g}{r}\right)^4\right)\partial_r^2 F_t + \left(3 + 8c_{\rm GB}\mu\left(\frac{r_g}{r}\right)^4\right)\frac{\partial_r F_t}{r}\\ &- \left((\kappa_V^2 + 1)\frac{1 - 3\left(\frac{r_g}{r}\right)^3}{1 - \left(\frac{r_g}{r}\right)^2} + 2c_{\rm GB}\mu\left(\frac{r_g}{r}\right)^4\left((\kappa_V^2 - 2)\frac{\left(\frac{r_g}{r}\right)^2}{\left(1 - \left(\frac{r_g}{r}\right)^2\right)^2} - 4\right)\right)\frac{F_t}{r^2}\\ &- \left(1 - 8c_{\rm GB}\mu\left(\frac{r_g}{r}\right)^4\right)\partial_t\partial_r F_r - \left(4 + 4c_{\rm GB}\mu\left(\frac{r_g}{r}\right)^4\right)\frac{\partial_t F_r}{r}\Bigg]\end{aligned} \tag{B.27a}$$

$$\begin{aligned}\delta\mathcal{E}^r{}_a = \frac{r\mathbb{V}_a}{2}\Bigg[&\left(1 + 8c_{\rm GB}\mu\left(\frac{r_g}{r}\right)^4\right)\left(\partial_t^2 F - r - \partial_t\partial_r F_t + \frac{\partial_t F_t}{r}\right)\\ &+ (\kappa_V^2 - 2)\left(1 - \left(\frac{r_g}{r}\right)^2 + 2c_{\rm GB}\mu\left(\frac{r_g}{r}\right)^6\right)\frac{F_r}{r^2}\Bigg]\end{aligned} \tag{B.27b}$$

$$\begin{aligned}\delta\mathcal{E}^a{}_b = \hat{D}^a\mathbb{V}_b\Bigg[&- \left(1 - 4c_{\rm GB}\mu\left(\frac{r_g}{r}\right)^2\left(4 - 5\left(\frac{r_g}{r}\right)^2\right)\right)\frac{\partial_r F_r}{r} + \left(2 + 48c_{\rm GB}\mu\left(\frac{r_g}{r}\right)^6\right)\frac{F_r}{r^2}\\ &- \left(1 + 4c_{\rm GB}\mu\left(\frac{r_g}{r}\right)^2\left(4 - 3\left(\frac{r_g}{r}\right)^2\right)\right)\frac{\partial_t F_t}{r}\Bigg]\end{aligned} \tag{B.27c}$$

The last of these, $\delta\mathcal{E}^a{}_b = 0$ (B.27c), may be rearranged to get $\partial_t F_t$ in terms of F_r and its r-derivative. Substituting this into $\delta\mathcal{E}^r{}_a = 0$ (B.27b) gives one second order partial differential equation (PDE) for $F_r(t, r)$. The remaining equation $\delta\mathcal{E}^t{}_a = 0$ is automatically inferred from the other two. The master variable is then related to F_r as

$$\Phi_V = r^{1/2}\left(1 - 4c_{\rm GB}\mu\left(\frac{r_g}{r}\right)^4\right)f(r)F_r, \tag{B.28}$$

such that the equation for F_r becomes the master equation

$$\Box_2 \Phi_V - \frac{V_V}{f}\Phi_V = 0. \tag{B.29}$$

The vector potential in $D = 5$-dimensions is

$$\begin{aligned}\frac{V_V}{f} = \frac{1}{r^2}\Bigg[\kappa_V^2\left(1 - 16c_{\rm GB}\mu\left(\frac{r_g}{r}\right)^4\right) + \frac{7}{4}\left(1 + \frac{640}{7}c_{\rm GB}\mu\left(\frac{r_g}{r}\right)^4\right) \\ - \frac{27}{4}\left(\frac{r_g}{r}\right)^2\left(1 + \frac{760}{27}c_{\rm GB}\mu\left(\frac{r_g}{r}\right)^4\right)\Bigg].\end{aligned} \tag{B.30}$$

B.3.2 Arbitrary dimensions

To find the vector master variable in D-dimensions, we begin by defining the gauge invariant variables[3]

$$F_A = f_A + \frac{r}{\kappa_V} D_A H_T. \tag{B.31}$$

as per [87] and [78]. The master variable Φ_V is directly related to F_r as [78]

$$\Phi_V = r^{(D-6)/2}\left(1 - 4(D-4)c_{\rm GB}\mu\left(\frac{r_g}{r}\right)^{D-1}\right) f(r) F_r, \tag{B.32}$$

and its potential is

$$\begin{aligned}\frac{V_V}{f} = \frac{1}{r^2}\Bigg[&\kappa_V^2\left(1 - 4(D-1)(D-4)c_{\rm GB}\mu\left(\frac{r_g}{r}\right)^{D-1}\right) \\ &+ \frac{D(D-6)+12}{4}\left(1 + 16\frac{(D-1)(D-4)(3D-5)}{D(D-6)+12}c_{\rm GB}\mu\left(\frac{r_g}{r}\right)^{D-1}\right) \\ &- \frac{3(D-2)^2}{4}\left(\frac{r_g}{r}\right)^{D-3}\left(1 - \frac{2(D-4)\left[5D^3 - 57D^2 + 134D - 88\right]}{3(D-2)^2}c_{\rm GB}\mu\left(\frac{r_g}{r}\right)^{D-1}\right)\Bigg].\end{aligned} \tag{B.33}$$

B.4 Scalar modes

The scalar-type metric perturbations are expanded in terms of scalar spherical harmonics $\mathbb{S}$ on S^{D-2}, which satisfy

$$\left(\hat{\Delta}_{D-2} + \kappa_S^2\right)\mathbb{S} = 0, \tag{B.34}$$

[3]Note this definition for F_A in D-dimensions differs from the corresponding definition in 5d by a factor of κ_V, which was omitted in the 5d case for computational ease in Mathematica.

where κ_S^2 is the eigenvalue of $\hat{\Delta}_{D-2}$ acting on the scalar $\mathbb{S}$ and takes discrete values[4]:

$$\kappa_S^2 = \ell(\ell + D - 3), \quad l = 0, 1, 2, \dots . \tag{B.35}$$

All mode numbers (e.g. ℓ) that could label $\mathbb{S}$ have been suppressed, as before. For each ℓ, the scalar-type metric perturbations can be written as

$$h_{AB} = f_{AB}\mathbb{S}, \quad h_{Aa} = r f_A \mathbb{S}_a, \quad h_{ab} = 2r^2 \left(H_L \gamma_{ab}\mathbb{S} + H_T \mathbb{S}_{ab}\right), \tag{B.36}$$

where

$$\mathbb{S}_a = -\frac{1}{\kappa_S}\hat{D}_a\mathbb{S}, \tag{B.37a}$$

$$\mathbb{S}_{ab} = \frac{1}{\kappa_S^2}\hat{D}_a\hat{D}_b\mathbb{S} + \frac{1}{D-2}\gamma_{ab}\mathbb{S}. \tag{B.37b}$$

B.4.1 5-dimensions

The equations describing scalar perturbations are long and unwieldy. As such, this section is largely schematic with explicit equations provided only for the end result. Once again, a combination of the *xTras* [156] and *Ricci.m* [158] packages were used to render the equations $\delta\mathcal{E}^{\alpha}{}_{\beta} = 0$ explicitly in coordinates for $D = 5$ in Mathematica. There is no transverse/traceless condition for the scalars, but still the eigenvalue equation (B.34) must be implemented to render apparent the structure of the harmonic expansion. There are seven coupled equations for the seven variables appearing in the parametrisation of the scalar modes (B.36),

$$\begin{aligned}
\delta\mathcal{E}^{A}{}_{B} &\propto \mathbb{S} && \rightarrow \quad 3 \text{ equations}, \\
\delta\mathcal{E}^{A}{}_{a} &\propto \hat{D}_a\mathbb{S} && \rightarrow \quad 2 \text{ equations}, \\
\delta\mathcal{E}^{a}{}_{b} &\propto \hat{D}^a\hat{D}_b\mathbb{S} \quad (a \neq b) && \rightarrow \quad 1 \text{ equation},
\end{aligned}$$

and 1 equation from the diagonal components $\delta\mathcal{E}^{a}{}_{a}$ (no sum), which has complicated dependence on $\hat{D}^a\hat{D}_b\mathbb{S}$ and the metric.

As for the vectors, a stepping stone towards identifying the master variables in terms of the

[4]The $\ell = 0$ scalar harmonic corresponds to a shift in the BH mass, while the $\ell = 1$ scalar harmonic turns out to be pure gauge [87], so neither are dynamical.

functions in (B.36) is constructing the following gauge-invariant quantities:

$$F = H_L + \frac{1}{3}H_T + \frac{1}{r}D^A r X_A, \tag{B.38a}$$

$$F_{AB} = f_{AB} + D_A X_B + D_B X_A, \tag{B.38b}$$

$$X_A = \frac{r}{\kappa_S}\left(f_A + \frac{r}{\kappa_S}D_A H_T\right). \tag{B.38c}$$

Making this field redefinition, and using the explicit background solution for $f(r)$, removes dependence on $\{H_T, f_A\}$ from the equations. This leaves just four variables $\{F, F_{AB}\}$. The equation $\delta\mathcal{E}^a{}_b = 0$ can be rearranged to obtain F_{tt} in terms of F and F_{rr} and their derivatives. The equation $\delta\mathcal{E}^t{}_r = 0$ can be rearranged to obtain F_{tr} in terms of F and F_{rr} and their derivatives. The equations $\delta\mathcal{E}^r{}_r = 0$, $\delta\mathcal{E}^t{}_t = 0$ and $\delta\mathcal{E}^r{}_a = 0$, may then be massaged to give F_{rr} in terms of F and its derivatives. This leaves us with fives PDEs for one function $F(t, r)$. Furthermore, it can be shown that $\delta\mathcal{E}^r{}_r$ is proportional to $\delta\mathcal{E}^t{}_t$ and $\delta\mathcal{E}^t{}_a$ is proportional to its t-derivative. Thus, we are down to three equations: $\delta\mathcal{E}^t{}_t = 0$, $\delta\mathcal{E}^r{}_a = 0$ and $\delta\mathcal{E}^a{}_a = 0$ (no sum).

The master variable must be related to F. To identify it, we need to find a change of variables of the form

$$F(t, r) = \alpha(r)\Phi_S(t, r) + \beta(r)\partial_r\Phi_S(t, r) \tag{B.39}$$

such that a second order PDE for Φ_S of the form

$$\partial_t^2\Phi_S = A(r)\Phi_S + B(r)\partial_r\Phi_S + C(r)\partial_r^2\Phi_S \tag{B.40}$$

consistently implies all of the above three equations for F are simultaneously satisfied. We have the freedom to choose $B(r)$ by rescaling Φ_S accordingly, so we choose $B(r) = f(r)f'(r)$, to mimic the derivative structure of $\Box_2\Phi_S$. We use (B.40) to eliminate $\partial_t^2\Phi_S$ (and some derivatives thereof) from the remaining three perturbation equations. Then, demanding that the 5th order terms (in particular, the coefficient of $\partial_t^2\partial_r^3\Phi_S$) should vanish from $\delta\mathcal{E}^r{}_a$ allows us to solve for $C(r) = f(r)^2$. Demanding that the 4th order terms should vanish allows us to solve for $\beta(r)$:

$$\beta = \frac{1}{r^{1/2}}\left(1 - \left(\frac{r_g}{r}\right)^2 + 4c_{\rm GB}\mu\left(\frac{r_g}{r}\right)^4\right). \tag{B.41}$$

Demanding that the 3rd order terms should vanish allows us to solve for $A(r)$ in terms of $\alpha(r)$ and $\alpha'(r)$. Finally, demanding that the 2nd and 1st order terms vanish (separately) allows us to

solve for $\alpha(r)$,

$$\begin{aligned}\alpha = \frac{1}{6r^{1/2}H}\left[2\kappa_S^4 - 3\kappa_S^2 - 9 + 9(\kappa_S^2-5)\left(\frac{r_g}{r}\right)^2 + 54\left(\frac{r_g}{r}\right)^4\right] \\ + \frac{2}{3}c_{\rm GB}\mu\left(\frac{r_g}{r}\right)^4\frac{r^{1/2}}{H^2}\Bigg[(\kappa_S^2-3)^2(2\kappa_S^2-69) + 12(8\kappa_S^4-81\kappa_S^2+171)\left(\frac{r_g}{r}\right)^2 \\ + 36(14\kappa_S^2-69)\left(\frac{r_g}{r}\right)^4 + 864\left(\frac{r_g}{r}\right)^6\Bigg],\end{aligned} \tag{B.42}$$

where

$$H \equiv H(r) = \kappa_S^2 - 3 + 6\left(\frac{r_g}{r}\right)^2. \tag{B.43}$$

The scalar master variable now satisfies the master equation

$$\Box_2\Phi_S - \frac{V_S}{f}\Phi_S = 0, \tag{B.44}$$

where the potential is $-A(r)$ and given by

$$\begin{aligned}\frac{V_S}{f} = \frac{1}{4r^2H^2}\Bigg[(\kappa_S^2-3)^2(4\kappa_S^2+3) + 9(\kappa_S^4-18\kappa_S^2+45)\left(\frac{r_g}{r}\right)^2 \\ + 12(13\kappa_S^2-42)\left(\frac{r_g}{r}\right)^4 + 324\left(\frac{r_g}{r}\right)^6\Bigg] \\ + c_{\rm GB}\mu\left(\frac{r_g}{r}\right)^4\frac{1}{r^2H^3}\Bigg[-32(\kappa_S^2-3)^3(\kappa_S^2+9) \\ + 15(\kappa_S^2-3)^2(\kappa_S^2-195)\left(\frac{r_g}{r}\right)^2 \\ + 162(7\kappa_S^4-106\kappa_S^2+255)\left(\frac{r_g}{r}\right)^4 \\ + 108(47\kappa_S^2-269)\left(\frac{r_g}{r}\right)^6 + 6696\left(\frac{r_g}{r}\right)^8\Bigg].\end{aligned} \tag{B.45}$$

Only one perturbation equation ($\delta\mathcal{E}^r{}_a = 0$) was used to derive the master equation, but it was checked that the other two ($\delta\mathcal{E}^t{}_t = 0$ and $\delta\mathcal{E}^a{}_a = 0$) are also satisfied.

B.4.2 Arbitrary dimensions

For the scalar master equation in D-dimensions, we use the results of [82] for Lovelock theory and set only the GB coefficient ("a_2") to be nonzero[5]. They work in a gauge in which $f_A = 0$ and $H_T = 0$. Note, with this choice of gauge, the functions $F(r)$ and $H_L(r)$ are equal (B.38a).

[5]The previously referenced [78] also derives the scalar master variable but does not provide an explicit expression for the potential.

The master variable Φ_S is directly related to H_L via a change of variables of the form

$$H_L = \alpha(r)\Phi_S + \beta(r)\partial_r\Phi_S, \tag{B.46}$$

such that all components of the perturbed EGB equations (3.18) are automatically satisfied when Φ_S obeys the master equation (3.28). To leading order in μ, we need [82]

$$\begin{aligned}
\alpha(r) = \frac{1}{4(D-2)r^{\frac{D-2}{2}}H}\Bigg[&2\left(\kappa_S^2-(D-2)\right)\left(2\kappa_S^2+(D-2)(D-4)\right)\\
&+\left(6(D-2)\kappa_S^2-(D-2)^2(D-5D+10)\right)\left(\frac{r_g}{r}\right)^{D-3}\\
&+(D-1)(D-2)^3\left(\frac{r_g}{r}\right)^{2(D-3)}\Bigg]\\
+\frac{(D-4)c_{\rm GB}\mu}{4(D-2)r^{\frac{D-2}{2}}H^2}\left(\frac{r_g}{r}\right)^{D-1}&\Bigg[8\left(\kappa_S^2-(D-2)\right)^2\left(2\kappa_S^2-(D-2)(2D^2-7D+8)\right)\\
&+4(D-2)(5D^2-17D+24)\left(\kappa_S^2-(D-2)\right)\kappa_S^2\left(\frac{r_g}{r}\right)^{D-3}\\
&-4(D-2)^2(13D^2-43D+42)\left(\kappa_S^2-(D-2)\right)\left(\frac{r_g}{r}\right)^{D-3}\\
&+16(D-1)(D-2)^2(3-2D)\kappa_S^2\left(\frac{r_g}{r}\right)^{2(D-3)}\\
&+2(D-1)(D-2)^3(3D^2+7D-18)\left(\frac{r_g}{r}\right)^{2(D-3)}\\
&-(D-1)^2(D-2)^3(D^2-11D+14)\left(\frac{r_g}{r}\right)^{3(D-3)}\Bigg]
\end{aligned} \tag{B.47}$$

where

$$H \equiv H(r) = \kappa_S^2 - D + 2 + \frac{(D-1)(D-2)}{2}\left(\frac{r_g}{r}\right)^{D-3}, \tag{B.48}$$

and

$$\beta(r) = \frac{1}{r^{\frac{D-4}{2}}}\left[1-\left(\frac{r_g}{r}\right)^{D-3}+4(D-4)c_{\rm GB}\mu\left(\frac{r_g}{r}\right)^{D-1}\left(1+\frac{D-5}{2}\left(\frac{r_g}{r}\right)^{D-3}\right)\right]. \tag{B.49}$$

The scalar potential is

$$\frac{V_S}{f} = \frac{1}{16r^2H^2}\mathcal{V}^{\rm GR} + \frac{D-4}{16H^3r^2}c_{\rm GB}\mu\left(\frac{r_g}{r}\right)^{D-1}\mathcal{V}^{\rm GB}, \tag{B.50}$$

where the contribution from GR is given by

$$\begin{aligned}\mathcal{V}^{\rm GR} = & \, 4\left(\kappa_S^2-(D-2)\right)^2\left(4\kappa_S^2+(D-2)(D-4)\right)\\ & -12(D-2)\left(\kappa_S^2-(D-2)\right)\left[(D-6)\kappa_S^2+(D-2)(D^2-6D+10)\right]\left(\frac{r_g}{r}\right)^{D-3}\\ & +4(D-1)(D-2)(2D^2-11D+18)\kappa_S^2\left(\frac{r_g}{r}\right)^{2(D-3)}\\ & +(D-1)(D-2)^2(D^3-19D^2+78D-96)\left(\frac{r_g}{r}\right)^{2(D-3)}\\ & +(D-1)^2(D-2)^4\left(\frac{r_g}{r}\right)^{3(D-3)},\end{aligned} \tag{B.51}$$

and that from the GB term by

$$\begin{aligned}\mathcal{V}^{\rm GB} = & -128(D-1)\left(\kappa_S^2-(D-2)\right)^3\left(\kappa_S^2+(D-2)^2\right)\\ & +8(D-2)\left(\kappa_S^2-(D-2)\right)^2(21D^2-131D+140)\kappa_S^2\left(\frac{r_g}{r}\right)^{D-3}\\ & +8(D-2)^2(8D^3-125D^2+347D-260)\left(\kappa_S^2-(D-2)\right)^2\left(\frac{r_g}{r}\right)^{D-3}\\ & -36(D-1)(D-2)^2(D-3)(D-12)\left(\kappa_S^2-(D-2)\right)\kappa_S^2\left(\frac{r_g}{r}\right)^{2(D-3)}\\ & +12(D-1)(D-2)^3(3D^2-77D+140)\left(\kappa_S^2-(D-2)\right)\left(\frac{r_g}{r}\right)^{2(D-3)}\\ & -2(D-1)^2(D-2)^2(9D^3-97D^2+226D-112)\kappa_S^2\left(\frac{r_g}{r}\right)^{3(D-3)}\\ & +2(D-1)^2(D-2)^3(9D^3-113D^2+258D-128)\left(\frac{r_g}{r}\right)^{3(D-3)}\\ & -(D-1)^3(D-2)^3(3D^3-27D^2+54D-32)\left(\frac{r_g}{r}\right)^{4(D-3)}.\end{aligned} \tag{B.52}$$

B.5 Higher-dimension operators

At the end of section 3.3.1, we gave an explicit example of an operator in a generic EFT expansion whose sub-dominance to the GB operator reproduced an EFT validity requirement. In this appendix, we motivate our choice of dimension-8 operator above a dimension-4 or -6 operator. We also derive its leading-in-κ_T contribution to the effective potential by tracking the highest-derivative terms and perturbatively replacing them with the lower-order equations.

B.5.1 Dimension-4 operators

It transpires that dimension-4 and -6 operators do not produce higher-derivative terms in the tensor master equation due to the symmetry of the background and the transverse-traceless condition of tensor perturbations. Higher-derivatives are necessary to produce non-trivial energy bounds. Rather than explicitly calculating perturbations of such terms in this next and the

section, we will just outline why they lack higher-derivatives.

The dimension-4 operators which we neglect

$$\mathcal{L}_{\rm D4} \sim \frac{R^2}{\Lambda^2}, \frac{R_{\alpha\beta}^2}{\Lambda^2}, \tag{B.53}$$

are suppressed in vacuum so enter the EFT equations of motion at $\mathcal{O}(\mu^2)$. By dimensional analysis, they may introduce terms of the schematic form

$$\nabla^4 h, \quad R\nabla^2 h, \quad R^4 h. \tag{B.54}$$

Of these, obviously only the first has the potential for fourth-derivatives. It may appear in the equation $\delta\mathcal{E}_{\alpha\beta} = 0$ as

$$\nabla^4 h \quad \rightarrow \quad \Box^2 h_{\alpha\beta}, \quad \Box\nabla_\alpha\nabla^\sigma h_{\sigma\beta}, \quad \Box\nabla_\alpha\nabla_\beta h^\sigma{}_\sigma. \tag{B.55}$$

The last term vanishes because tensor modes are traceless $h^\sigma{}_\sigma = 0$, and the middle term vanishes becasue tensor modes are transverse $\nabla^\sigma h_{\sigma\beta} = 0$. In all three possibilities, we are forced to contract at least two covariant derivatives. Using the leading GR equations, $\Box h_{\alpha\beta} \approx 0$, we see that the first term is doubly suppressed and so doesn't contribute until a higher order.

B.5.2 Dimension-6 operators

Similarly, the dimension-6 operators $\mathcal{L}_{\rm D6} \sim R^3/\Lambda^4$ (not listed here), produce terms in the equation of motion of the form

$$\nabla^6 h, \quad R\nabla^4 h, \quad R^2\nabla^2 h, \quad R^3 h. \tag{B.56}$$

Of these, only the first two have a chance of introducing truly higher-derivative terms. The first term unavoidably has at least two "boxes" $\nabla^6 h \sim \Box^2\nabla_\bullet\nabla^\bullet h_\bullet{}^\bullet$, meaning it is again suppressed upon substitution of the lower-order equations. Furthermore, due to the transverse-traceless nature of the tensor-type perturbations and symmetries of the Riemann tensor, the only possible non-trivial contraction of the second kind that could appear in $\delta\mathcal{E}_{\alpha\beta}$ is

$$\nabla^4 h \quad \rightarrow \quad R^{\sigma\rho\kappa\lambda}\nabla_\alpha\nabla_\beta\nabla_\sigma\nabla_\kappa h_{\rho\lambda}. \tag{B.57}$$

Since $h_{AB} = h_{Aa} = 0$ for tensor-type perturbations, and using the Riemann components in (3.9), we find

$$\begin{aligned} R^{\sigma a \kappa b}\nabla_\alpha\nabla_\beta\nabla_\sigma\nabla_\kappa h_{ab} &= R^{AaBb}\nabla_\alpha\nabla_\beta\nabla_A\nabla_B h_{ab} + R^{cadb}\nabla_\alpha\nabla_\beta\nabla_c\nabla_d h_{ab} \\ &= -\frac{f'}{2r}g^{AB}g^{ab}\nabla_\alpha\nabla_\beta\nabla_A\nabla_B h_{ab} + \frac{1-f}{r^2}\left(g^{cd}g^{ab} - g^{cb}g^{ad}\right)\nabla_\alpha\nabla_\beta\nabla_c\nabla_d h_{ab} \\ &= 0 \end{aligned} \tag{B.58}$$

that this term also vanishes for transverse-traceless tensors.

B.5.3 Dimension-8 operator

We will now show that the dimension-8 operator included in (3.55) does lead to genuine higher derivatives in the perturbation equation. The modified Einstein equations for this theory are

$$\mathcal{E}_{\alpha\beta} \coloneqq G_{\alpha\beta} + 2\frac{c_{\rm GB}}{\Lambda^2}B_{\alpha\beta} + 2\frac{c_{\rm R4}}{\Lambda^6}D_{\alpha\beta} = 0, \tag{B.59}$$

where

$$D_{\alpha\beta} = -\frac{1}{2}g_{\alpha\beta}(R^4) + 4(R^4)_{\alpha\sigma\beta}{}^{\sigma} + 8\nabla_\sigma\nabla_\rho(R^3)_{\alpha}{}^{\sigma}{}_{\beta}{}^{\rho}. \tag{B.60}$$

The only term in the perturbed tensor $\delta D_{\alpha\beta}$ with four derivatives acting on the metric perturbation is

$$\delta D_{\alpha\beta} = -16R_{\alpha\sigma\mu\kappa}R_{\beta\rho\nu\lambda}\nabla^\rho\nabla^\sigma\nabla^\kappa\nabla^\lambda h^{\mu\nu} + \dots \tag{B.61}$$

where $\dots$ stands for trivially lower derivative terms for reasons similar to the previous two sections. (This was checked using the *xTras* [156] package for *xAct* [157].) The four-derivative contribution to the $\delta\mathcal{E}_{ab}$-equation for tensor modes ($h_{AB} = h_{Aa} = 0$) is

$$\begin{aligned} \delta D_{ab} =& -16R_{a\sigma c\kappa}R_{b\rho d\lambda}\nabla^\rho\nabla^\sigma\nabla^\kappa\nabla^\lambda h^{cd} + \dots \\ =& -16\left[\left(\frac{f'}{2r}\right)^2\partial_A\partial^A\partial_B\partial^B - \frac{(1-f)f'}{r^3}\partial_A\partial^A\partial_c\partial^c + \left(\frac{1-f}{r^2}\right)^2\partial_c\partial^c\partial_d\partial^d\right]h_{ab} + \dots \\ =& -16\frac{r_g^{2D-6}}{r^{2D-2}}\left[\frac{(D-3)^2}{4} + (D-3) + 1\right]\partial_c\partial^c\partial_d\partial^d h_{ab} + \dots + \mathcal{O}(\mu) \\ =& -4(D-1)^2\frac{r_g^{2D-6}}{r^{2D+2}}\hat{\Delta}^2_{D-2}h_{ab} + \dots + \mathcal{O}(\mu). \end{aligned} \tag{B.62}$$

In going from the first to second line, we have isolated just the full four-derivative terms out of the covariant derivative expression. In going from the second to third line, we have used the lower-order GR equation $\Box \approx 0$ to replace $\partial_A \partial^A \to -\partial_c \partial^c + \dots$ up to leading order in μ.

This term appears in the perturbation equations as

$$\begin{aligned} 0 = \delta\mathcal{E}_{ab} &= \delta G_{ab} + 2\frac{c_{\rm GB}}{\Lambda^2}\delta B_{ab} + 2\frac{c_{\rm R4}}{\Lambda^6}\delta D_{ab} \\ &= -\frac{1}{2}\Box h_{ab} + 2\frac{c_{\rm GB}}{\Lambda^2}\delta B_{ab} - 8(D-1)^2\frac{c_{\rm R4}}{\Lambda^6}\frac{r_g^{2D-6}}{r^{2D+2}}\hat{\Delta}^2_{D-2}h_{ab} + \dots \end{aligned} \tag{B.63}$$

and since the metric perturbations are simply related to the tensor master variable by a rescaling $h_{ab} \propto \Phi_T \mathbb{T}_{ab}$ which cannot change the derivative structure, we can simply read off the contribution to the potential

$$\frac{V_T^{\rm R4}}{f} = -16(D-1)^2 c_{\rm R4}\mu^3 \left(\frac{r_g}{r}\right)^{2D}\frac{\kappa_T^4}{r^2} + \dots \tag{B.64}$$

to leading order in κ_T.

Appendix C

The pp-wave metric and its master equations

C.1 Explicit field equations

In lightcone gauge $h_{v\alpha} = 0$, the left-hand-side of the EFT field equations for the metric perturbations (3.18) on the pp-wave background are explicitly given by

$$-2\delta\mathcal{E}_{vv} = \partial_v^2 h_{ii}, \tag{C.1a}$$

$$-2\delta\mathcal{E}_{vu} = -\tilde{\Box}h_{ii} + \partial_v\partial_u h_{ii} + \partial_i(\partial_v h_{iu} + \partial_j h_{ij}), \tag{C.1b}$$

$$-2\delta\mathcal{E}_{vi} = \partial_v\partial_i h_{jj} - \partial_v(\partial_v h_{iu} + \partial_j h_{ij}), \tag{C.1c}$$

$$\begin{aligned}-2\delta\mathcal{E}_{uu} = {}& \tilde{\Box}h_{uu} - 2\partial_u(\partial_v h_{uu} + \partial_i h_{iu}) + \partial_i H\partial_v h_{iu} - \partial_j(\partial_i H h_{ij}) + \partial_u^2 h_{ii} - H\tilde{\Box}h_{ii} \\ & + \frac{1}{2}\partial_j H\partial_j h_{ii} - \frac{1}{2}\partial_u H\partial_v h_{ii} + H\partial_i(\partial_v h_{iu} + \partial_j h_{ij}) + H\partial_v(\partial_v h_{uu} + \partial_i h_{iu}) \\ & + \frac{4c_{\rm GB}}{\Lambda^2}\partial_i\partial_j H(\partial_v\partial_i h_{ju} - \partial_v\partial_j h_{iu} + \partial_k\partial_k h_{ij} - \partial_i\partial_k h_{jk} - \partial_j\partial_k h_{ik} + \partial_i\partial_j h_{kk}),\end{aligned} \tag{C.1d}$$

$$\begin{aligned}-2\delta\mathcal{E}_{ui} = {}& \tilde{\Box}h_{ui} + \partial_j H\partial_v h_{ij} - \partial_i(\partial_v h_{uu} + \partial_j h_{ju}) - \partial_u(\partial_v h_{iu} + \partial_j h_{ij}) \\ & + \partial_i\partial_u h_{jj} - \frac{1}{2}\partial_i H\partial_v h_{jj} \\ & - \frac{4c_{\rm GB}}{\Lambda^2}\partial_v\left[\partial_i\partial_j H(\partial_j h_{kk} - \partial_k h_{jk}) + \partial_j\partial_k H(\partial_i h_{jk} - \partial_j h_{ik})\right],\end{aligned} \tag{C.1e}$$

$$
\begin{aligned}
-2\delta\mathcal{E}_{ij} = {} & \tilde{\Box}h_{ij} - \partial_i(\partial_v h_{ju} + \partial_k h_{jk}) - \partial_j(\partial_v h_{iu} + \partial_k h_{ik}) + \partial_i\partial_j h_{kk} - \delta_{ij}\tilde{\Box}h_{kk} \\
& + \delta_{ij}\partial_k(\partial_v h_{ku} + \partial_l h_{kl}) + \delta_{ij}\partial_v(\partial_v h_{uu} + \partial_k h_{ku}) \\
& + \frac{4c_{\mathrm{GB}}}{\Lambda^2}\partial_v^2(\partial_i\partial_j H h_{kk} - \partial_i\partial_k H h_{jk} - \partial_j\partial_k H h_{ik} + \delta_{ij}\partial_k\partial_l H h_{kl}).
\end{aligned} \tag{C.1f}
$$

These equations are satisfied with the constraints (3.36) – (3.38) and the equation of motion for h_{ij} (3.39).

C.2 Master variables in balancing source background

Identifying the master variables for the metric perturbations on the point-source background was a straightforward procedure described in the main text above equation (3.42). When a second source is introduced (to "balance" the first as discussed in section 4.4.1), spherical symmetry is lost and the previous decomposition is no longer suitable. Without loss of generality, assume the two sources are aligned along the z-axis. Then, we can write the transverse-space metric in cylindrical coordinates as:

$$
\delta_{ij}\mathrm{d}x^i\mathrm{d}x^j = \mathrm{d}z^2 + \mathrm{d}r^2 + r^2\mathrm{d}\Omega_{d-2}^2. \tag{C.2}
$$

For this appendix only, γ_{ab} will refer to the metric on the $(d-2) = (D-4)$-dimensional sphere. In these coordinates, the harmonic condition on the metric function is

$$
\frac{\partial^2}{\partial z^2}H(u,r,z) = -\frac{\partial^2}{\partial r^2}H(u,r,z) - (d-2)\frac{1}{r}\frac{\partial}{\partial r}H(u,r,z). \tag{C.3}
$$

While most of the components of the metric perturbations — h_{rr}, h_{rz}, h_{zz}, h_{ra}, h_{za} and the diagonal components of h_{ab} — are coupled in a complicated way via (3.39), it happens that the off-diagonal components of h_{ab} are completely decoupled from the rest and evolve independently. These account for $(D-5)(D-4)/2$ of the total $D(D-3)/2$ propagating modes. Their equation of motion is

$$
\tilde{\Box}h_{ab} - 8\frac{c_{\mathrm{GB}}}{\Lambda^2}\frac{\partial_r H}{r}\partial_v^2 h_{ab} = 0, \quad a \neq b \tag{C.4}
$$

which has the same format as the equations for the modes in the spherically-symmetric background (3.42). From this, it is clear that the estimates for the time delay used throughout section 4.4.1 apply equally well to the balancing source background.

C.3 Higher-dimension EFT field equations

In section 3.3.2, we show that control over the higher-dimension EFT action (3.65) amounts to exactly the regime of validity found by generic arguments (3.64). In this appendix, we provide the field equations for that action and also identify the tensor-type master variable and its master equation.

The background equation is

$$\mathcal{E}_{\alpha\beta} \coloneqq G_{\alpha\beta} + 2\frac{c_{\rm GB}}{\Lambda^2}B_{\alpha\beta} + 2\frac{c_{\rm R3}}{\Lambda^4}C_{\alpha\beta} + 2\frac{c_{\rm R4}}{\Lambda^6}D_{\alpha\beta} = 0, \tag{C.5}$$

where

$$B_{\alpha\beta} = 4R_{\sigma\alpha\beta\rho}R^{\sigma\rho} + 2R_{\alpha}{}^{\sigma\rho\kappa}R_{\beta\sigma\rho\kappa} - 4R_{\alpha\sigma}R_{\beta}{}^{\sigma} + 2RR_{\alpha\beta} - \frac{1}{2}R^2_{\rm GB}\,g_{\alpha\beta}, \tag{C.6}$$

$$C_{\alpha\beta} = -\frac{1}{2}g_{\alpha\beta}(R^3) + 3(R^3)_{\alpha\sigma\beta}{}^{\sigma} + 6\nabla_\sigma\nabla_\rho(R^2)_{\alpha}{}^{\sigma}{}_{\beta}{}^{\rho}, \tag{C.7}$$

$$D_{\alpha\beta} = -\frac{1}{2}g_{\alpha\beta}(R^4) + 4(R^4)_{\alpha\sigma\beta}{}^{\sigma} + 8\nabla_\sigma\nabla_\rho(R^3)_{\alpha}{}^{\sigma}{}_{\beta}{}^{\rho}, \tag{C.8}$$

and

$$(R^n)_{\alpha\beta\sigma\rho} = R_{\alpha\beta\gamma\delta}R^{\gamma\delta\bullet\bullet}\ldots R^{\bullet\bullet\kappa\lambda}R_{\kappa\lambda\sigma\rho}, \tag{C.9}$$

$$(R^n) = (R^n)_{\alpha\beta}{}^{\alpha\beta}. \tag{C.10}$$

The vacuum pp-wave metric (3.10) is again a solution to (C.5).

In lightcone gauge, the presence of the R^3-operator modifies the v-component perturbation equations

$$-2\delta\mathcal{E}_{vv} = \partial_v^2 h_{ii}, \tag{C.11a}$$

$$\begin{aligned}-2\delta\mathcal{E}_{vu} = &-\tilde{\Box}_v^2 h_{ii} + \partial_v\partial_u h_{ii} + \partial_i(\partial_v h_{iu} + \partial_j h_{ij}) \\ &- 12\frac{c_{\rm R3}}{\Lambda^4}\partial_v^2\partial_i\left[\partial_i\partial_j H(\partial_v h_{ju} + \partial_k h_{jk}) + \partial_i\partial_j\partial_k H h_{jk}\right],\end{aligned} \tag{C.11b}$$

$$\begin{aligned}-2\delta\mathcal{E}_{vi} = &\partial_v\partial_i h_{jj} - \partial_v(\partial_v h_{iu} + \partial_j h_{ij}) \\ &+ 12\frac{c_{\rm R3}}{\Lambda^4}\partial_v^3\left[\partial_i\partial_j H(\partial_v h_{ju} + \partial_k h_{jk}) + \partial_i\partial_j\partial_k H h_{jk}\right],\end{aligned} \tag{C.11c}$$

such that, while the traceless condition $h_{ii} = 0$ is unchanged, the second constraint equation (3.37) becomes

$$\partial_v h_{iu} + \partial_j h_{ij} = 12\frac{c_{\rm R3}}{\Lambda^4}\partial_v^2\left[\partial_i\partial_j H(\partial_v h_{ju} + \partial_k h_{jk}) + \partial_i\partial_j\partial_k H h_{jk}\right]. \tag{C.12}$$

The $\delta\mathcal{E}_{ij}$ is also modified by both new operators

$$\begin{aligned}
-2\delta\mathcal{E}_{ij} = {}& \tilde{\Box}h_{ij} - \partial_i(\partial_v h_{ju} + \partial_k h_{jk}) - \partial_j(\partial_v h_{iu} + \partial_k h_{ik}) + \partial_i\partial_j h_{kk} - \delta_{ij}\tilde{\Box}h_{kk} \\
&+ \delta_{ij}\partial_k(\partial_v h_{ku} + \partial_l h_{kl}) + \delta_{ij}\partial_v(\partial_v h_{uu} + \partial_k h_{ku}) \\
&+ \frac{4c_{\rm GB}}{\Lambda^2}\partial_v^2(\partial_i\partial_j H h_{kk} - \partial_i\partial_k H h_{jk} - \partial_j\partial_k H h_{ik} + \delta_{ij}\partial_k\partial_l H h_{kl}) \\
&-12\frac{c_{\rm R3}}{\Lambda^4}\partial_v^2\left[\partial_i\partial_k H\tilde{\Box}h_{jk} + \partial_i\partial_k H\tilde{\Box}h_{jk} + \partial_u\partial_i\partial_k H\partial_v h_{jk} + \partial_u\partial_j\partial_k H\partial_v h_{ik}\right. \\
&\qquad - \partial_i\partial_k H\partial_j(\partial_v h_{ku} + \partial_l h_{kl}) - \partial_j\partial_k H\partial_i(\partial_v h_{ku} + \partial_l h_{kl}) \\
&\qquad \left.-\partial_i\partial_k\partial_l H(\partial_j h_{kl} - \partial_k h_{jl}) - \partial_j\partial_k\partial_l H(\partial_i h_{kl} - \partial_k h_{il})\right] \\
&+ 16\frac{c_{\rm R4}}{\Lambda^6}\partial_i\partial_k H\partial_j\partial_l H\partial_v^4 h_{kl}
\end{aligned} \tag{C.13}$$

The final constraint will again come from the trace of this equation. However, the process is complicated by the presence of the R^3-operator. In EGB theory, the second constraint (3.37) allowed us to exactly remove the h_{iu} components which appeared in the ij-equation. But now, the h_{iu} components also appear on the right hand side of (C.12). As a result, they may only be replaced perturbatively in inverse powers of the cut-off inside $\delta\mathcal{E}_{ij}$. Up to corrections of $\mathcal{O}(\Lambda^{-8})$, the third constraint equation is

$$\begin{aligned}
\partial_v h_{uu} + \partial_i h_{iu} = {}& -4\frac{d-2}{d}\frac{c_{\rm GB}}{\Lambda^2}\partial_i\partial_j H\partial_v h_{ij} \\
&+ \frac{24}{d}\frac{c_{\rm R3}}{\Lambda^4}\partial_v\left[\partial_i\partial_j H\tilde{\Box}h_{ij} + \partial_u\partial_i\partial_j H\partial_v h_{ij} - \frac{d-2}{2}\partial_i\partial_j\partial_k H\partial_i h_{jk}\right] \\
&- \frac{16}{d}\frac{c_{\rm R4}}{\Lambda^6}\partial_i\partial_j H\partial_i\partial_k H\partial_v^3 h_{jk}.
\end{aligned} \tag{C.14}$$

As before, we see that the dynamical degrees of freedom contained within the metric perturbations are in the transverse directions h_{ij}. Applying the three constraint equations, their equation of motion becomes (up to corrections of $\mathcal{O}(\Lambda^{-8})$):

$$\tilde{\Box}h_{ij} - 8\frac{c_{\rm GB}}{\Lambda^2}\partial_v^2 X_{ij} - 24\frac{c_{\rm R3}}{\Lambda^4}\partial_v^2 Y_{ij} - 16\frac{c_{\rm R4}}{\Lambda^6}\partial_v^4 Z_{ij} = 0, \tag{C.15}$$

where

$$X_{ij} = \frac{1}{2}\left(h_{ik}\partial_j\partial_k H + h_{jk}\partial_i\partial_k H\right) - \frac{1}{d}\delta_{ij}h_{kl}\partial_k\partial_l H, \tag{C.16}$$

$$\begin{aligned} Y_{ij} = {} & \frac{1}{2}\left(\tilde{\Box}h_{ik}\partial_j\partial_k H + \tilde{\Box}h_{jk}\partial_i\partial_k H\right) - \frac{1}{d}\delta_{ij}\tilde{\Box}h_{kl}\partial_k\partial_l H \\ & + \frac{1}{2}\left(\partial_v h_{ik}\partial_u\partial_j\partial_k H + \partial_v h_{jk}\partial_u\partial_i\partial_k H\right) - \frac{1}{d}\delta_{ij}\partial_v h_{kl}\partial_u\partial_k\partial_l H \\ & + \frac{1}{2}\left(\partial_l h_{ik}\partial_j\partial_k\partial_l H + \partial_l h_{jk}\partial_i\partial_k\partial_l H\right) - \frac{1}{d}\delta_{ij}\partial_m h_{kl}\partial_k\partial_l\partial_m H \\ & + h_{kl}\partial_i\partial_j\partial_k\partial_l H, \end{aligned} \tag{C.17}$$

$$Z_{ij} = -h_{kl}\partial_i\partial_k H\partial_j\partial_l H + \frac{1}{d}\delta_{ij}h_{lm}\partial_k\partial_l H\partial_k\partial_m H. \tag{C.18}$$

Tensor modes

The perturbation equations (C.15) couple all components of h_{ij} in a non-trivial fashion when $c_{\mathrm{R3}} \neq 0$. Even in the point source case, the master variable identification used in section 3.2.2 for EGB theory no longer works when the R^3-operator is included in the EFT. For illustrative purposes, we will just consider the spherically symmetric point source case. Due to the symmetry, we may perform a scalar-vector-tensor decomposition with each type of perturbation (scalar, vector or tensor) evolving independently of the other types. The simplest of them are the tensor modes, which are parameterised by

$$h_{rr} = h_{ra} = 0, \quad h_{ab} = r^2\Phi_T\mathbb{T}_{ab}, \tag{C.19}$$

where $\mathbb{T}_{ab}$ is a tensor spherical harmonic on the $(d-1)$-sphere and satisfies

$$\left(\hat{\Delta}_{d-1} + \kappa_T^2\right)\mathbb{T}_{ab} = 0, \tag{C.20a}$$

$$\mathbb{T}^a{}_a = 0, \quad \hat{D}^a\mathbb{T}_{ab} = 0. \tag{C.20b}$$

There is one tensor mode Φ_T for each tensor spherical harmonic on the $(d-1)$-sphere. They all share a master equation, which can be derived from the ab-components of (C.15),

$$\begin{aligned} 0 = {} & \tilde{\Box}\Phi_T - \frac{\kappa_T^2+2}{r^2}\Phi_T - 8\frac{c_{\mathrm{GB}}}{\Lambda^2}\frac{\partial_r H}{r}\partial_v^2\Phi_T + 24\frac{c_{\mathrm{R3}}}{\Lambda^4}\partial_v^2\left[d\frac{\partial_r H}{r^2}\left(\partial_r\Phi_T + \frac{\Phi_T}{r}\right)\right. \\ & \left. - \frac{\partial_u\partial_r H}{r}\partial_v\Phi_T\right] + 16\frac{c_{\mathrm{R4}} - 12c_{\mathrm{GB}}c_{\mathrm{R3}}}{\Lambda^6}\left(\frac{\partial_r H}{r}\right)^2\partial_v^4\Phi_T. \end{aligned} \tag{C.21}$$

In arriving at this equation, the $\tilde{\Box} h_{ab}$ terms present in Y_{ab} have been replaced perturbatively using the lower-order equation of motion, giving rise to the cross term $\propto c_{\rm GB} c_{\rm R3}$. Once again, this equation is valid up to corrections of order $\mathcal{O}(\Lambda^{-8})$.

Appendix D

Quantum arguments on the pp-wave spacetime

D.1 EFT validity bound on wavefunction spread

At the end of section 4.4.1, we discuss how a generic initial quantum state has a non-zero spread σ in transverse space and thus cannot be perfectly balanced at an unstable equilibrium point. As a state in a low-energy EFT, this spread is in fact bounded below by Λ^{-1}. To demonstrate this, we must initially bound a Lorentz-invariant quantity dependent on σ (as we did for $H(u,r)$, k_v and b in section 3.3.2). The spread in momentum space is inversely related to the spread in real space, $|\Delta\mathbf{k}| \sim \sigma^{-1}$, so we would like to bound the dot product of two opposing wavevectors $\mathbf{k}^{\pm} = \mathbf{k^0} \pm \Delta\mathbf{k}$, where $\mathbf{k^0}$ is some central momentum. But to construct a scalar quantity, they must first be embedded in D-vectors on the full D-dimensional pp-wave spacetime

$$\left(k_\alpha^\pm\right) = \left(k_u^\pm, k_v^\pm, \mathbf{k}^\pm\right) \tag{D.1}$$

with the condition that $k^\pm$ is null due to the GR equations of motion,

$$g^{\alpha\beta}k_\alpha^\pm k_\beta^\pm = 0 \quad \Longrightarrow \quad k_u^\pm = \frac{H(k_v^\pm)^2 - \mathbf{k}^{\pm 2}}{2k_v^\pm}. \tag{D.2}$$

For a fixed "mass" $k_v^+ = k_v^- = k_v$, the dot product reduces simply to

$$k^+ \cdot k^- = -2\Delta\mathbf{k}^2. \tag{D.3}$$

With the Lorentz-invariant bound $k^+ \cdot k^- \ll \Lambda^2$, we get the desired result $|\Delta \mathbf{k}| \ll \Lambda$, or $\sigma\Lambda \gg 1$.

D.2 Expectation values for time delay in perturbation theory

In section 4.4.3 we define a quantum time delay operator $\widehat{\Delta T}$ and calculate its expectation value for a representative in-state with wavefunction (4.79). In this appendix, we provide details of that calculation. We will deal with both the point source case and balancing source case simultaneously. In order to accommodate this, the location of the point source $\mathbf{x} = -\mathbf{b}$ is shifted relative to the discussion of sections 3.1.2 and 4.4.1. The GR potential is thus

$$V(u, \mathbf{x}) = -\frac{k_v j(u)}{2}\left(\frac{\Theta_{\text{bal}}}{|\mathbf{x}-\mathbf{b}|^{d-2}} + \frac{1}{|\mathbf{x}+\mathbf{b}|^{d-2}}\right) \tag{D.4}$$

or, expressed as a Fourier transform,

$$V(u, \mathbf{x}) = -\frac{2\pi^{\frac{d}{2}}}{\Gamma\left(\frac{d-2}{2}\right)} k_v j(u) \int \frac{\mathrm{d}^d q}{(2\pi)^d} \frac{\left(e^{i\mathbf{q}\cdot\mathbf{b}} + \Theta_{\text{bal}} e^{-i\mathbf{q}\cdot\mathbf{b}}\right)}{\mathbf{q}^2} e^{i\mathbf{q}\cdot\mathbf{x}}. \tag{D.5}$$

The interaction picture potential is related to this Schrödinger potential via a shift in the space coordinate (4.89), i.e.

$$\hat{V}_I(u) = -\frac{2\pi^{\frac{d}{2}}}{\Gamma\left(\frac{d-2}{2}\right)} k_v j(u) \int \frac{\mathrm{d}^d q}{(2\pi)^d} \frac{e^{i\mathbf{q}\cdot\mathbf{b}} + \Theta_{\text{bal}} e^{-i\mathbf{q}\cdot\mathbf{b}}}{\mathbf{q}^2} e^{i\mathbf{q}\cdot\left(\hat{\mathbf{x}} + \frac{u}{k_v}\hat{\mathbf{k}}\right)}. \tag{D.6}$$

Applying the Zassenhaus formula for operators in the exponential and inserting a complete set of momentum states and a complete set of position states appropriately, we arrive at

$$\begin{aligned}\hat{V}_I(u) = -\frac{2\pi^{\frac{d}{2}}}{\Gamma\left(\frac{d-2}{2}\right)} k_v j(u) \int \frac{\mathrm{d}^d q}{(2\pi)^d} \int \frac{\mathrm{d}^d k}{(2\pi)^d} \int \mathrm{d}^d x \frac{e^{i\mathbf{q}\cdot\mathbf{b}} + \Theta_{\text{bal}} e^{-i\mathbf{q}\cdot\mathbf{b}}}{\mathbf{q}^2} \\ \exp\left[i\mathbf{x}\cdot(\mathbf{q}+\mathbf{k}) + \frac{iu}{k_v}\mathbf{q}\cdot\left(\frac{\mathbf{q}}{2}+\mathbf{k}\right)\right] |\mathbf{x}\rangle \langle \mathbf{k}|.\end{aligned} \tag{D.7}$$

Roughly speaking, the n-th order time delay expectation value is the expectation value of n-powers of $\hat{V}_I$ over the state

$$|\Phi_0\rangle = \frac{1}{(2\pi\sigma^2)^{d/4}} \int \mathrm{d}^d x \exp\left[-\frac{\mathbf{x}^2}{4\sigma^2}\right] |\mathbf{x}\rangle. \tag{D.8}$$

Additionally, in (4.95) the k_v-derivatives of (4.91) have been replaced in favour of u-derivatives by noting that

$$\begin{aligned}\frac{\partial \hat{V}_I(u)}{\partial k_v} = -\frac{2\pi^{\frac{d}{2}}}{\Gamma\left(\frac{d-2}{2}\right)} j(u) \int \frac{\mathrm{d}^d q}{(2\pi)^d} \int \frac{\mathrm{d}^d k}{(2\pi)^d} \int \mathrm{d}^d x \frac{e^{i\mathbf{q}\cdot\mathbf{b}} + \Theta_{\text{bal}} e^{-i\mathbf{q}\cdot\mathbf{b}}}{\mathbf{q}^2} \\ \left(1 - u\frac{\partial}{\partial u}\right) \exp\left[i\mathbf{x}\cdot(\mathbf{q}+\mathbf{k}) + \frac{iu}{k_v}\mathbf{q}\cdot\left(\frac{\mathbf{q}}{2}+\mathbf{k}\right)\right] |\mathbf{x}\rangle \langle\mathbf{k}| \,.\end{aligned} \tag{D.9}$$

Lastly, the Heaviside θ-functions in (4.95) simply capture the different limits of the nested integrals in the S-matrix expansion (4.90).

D.3 Expressions for $a^{(n)}$ and $\tilde{a}^{(n)}$

The expressions (4.107) give the parameter dependence of the first three orders of the Wigner–Smith time delay expanded in 1) S-matrix perturbation theory, 2) small Gaussian width, and 3) early times. Four dimensionless numbers $\{a^{(2)}, \tilde{a}^{(2)}, a^{(3)}, \tilde{a}^{(3)}\}$ feature in these equations and are given below in terms of integrals, where $\hat{\mathbf{b}} = \mathbf{b}/b$ is the unit vector in the direction of $\mathbf{b}$.

$$\begin{aligned}a^{(2)} = &-2\left(-\frac{2\pi^{\frac{d}{2}}}{\Gamma\left(\frac{d-2}{2}\right)}\right)^2 \int_0^1 \mathrm{d}w_1 \mathrm{d}w_2 \Theta(w_1 - w_2) \int \frac{\mathrm{d}^d p_1}{(2\pi)^d} \frac{\mathrm{d}^d p_2}{(2\pi)^d} \\ &\frac{e^{i\mathbf{p}_1\cdot\hat{\mathbf{b}}} + \Theta_{\text{bal}} e^{-i\mathbf{p}_1\cdot\hat{\mathbf{b}}}}{\mathbf{p}_1^2} \frac{e^{i\mathbf{p}_2\cdot\hat{\mathbf{b}}} + \Theta_{\text{bal}} e^{-i\mathbf{p}_2\cdot\hat{\mathbf{b}}}}{\mathbf{p}_2^2} (\mathbf{p}_1 + \mathbf{p}_2)^2 (w_1 - w_2) \mathbf{p}_1 \cdot \mathbf{p}_2\end{aligned} \tag{D.10a}$$

$$\begin{aligned}\tilde{a}^{(2)} = &-2\left(-\frac{2\pi^{\frac{d}{2}}}{\Gamma\left(\frac{d-2}{2}\right)}\right)^2 \int_0^1 \mathrm{d}w_1 \mathrm{d}w_2 \Theta(w_1 - w_2) \int \frac{\mathrm{d}^d p_1}{(2\pi)^d} \frac{\mathrm{d}^d p_2}{(2\pi)^d} \\ &\frac{e^{i\mathbf{p}_1\cdot\hat{\mathbf{b}}} + \Theta_{\text{bal}} e^{-i\mathbf{p}_1\cdot\hat{\mathbf{b}}}}{\mathbf{p}_1^2} \frac{e^{i\mathbf{p}_2\cdot\hat{\mathbf{b}}} + \Theta_{\text{bal}} e^{-i\mathbf{p}_2\cdot\hat{\mathbf{b}}}}{\mathbf{p}_2^2} (w_1\mathbf{p}_1 + w_2\mathbf{p}_2)^2 (w_1 - w_2) \mathbf{p}_1 \cdot \mathbf{p}_2\end{aligned} \tag{D.10b}$$

$$\begin{aligned}a^{(3)} = &2\left(-\frac{2\pi^{\frac{d}{2}}}{\Gamma\left(\frac{d-2}{2}\right)}\right)^3 \int_0^1 \mathrm{d}w_1 \mathrm{d}w_2 \mathrm{d}w_3 \int \frac{\mathrm{d}^d p_1}{(2\pi)^d} \frac{\mathrm{d}^d p_2}{(2\pi)^d} \frac{\mathrm{d}^d p_3}{(2\pi)^d} \\ &\frac{e^{i\mathbf{p}_1\cdot\hat{\mathbf{b}}} + \Theta_{\text{bal}} e^{-i\mathbf{p}_1\cdot\hat{\mathbf{b}}}}{\mathbf{p}_1^2} \frac{e^{i\mathbf{p}_2\cdot\hat{\mathbf{b}}} + \Theta_{\text{bal}} e^{-i\mathbf{p}_2\cdot\hat{\mathbf{b}}}}{\mathbf{p}_2^2} \frac{e^{i\mathbf{p}_3\cdot\hat{\mathbf{b}}} + \Theta_{\text{bal}} e^{-i\mathbf{p}_3\cdot\hat{\mathbf{b}}}}{\mathbf{p}_3^2} (\mathbf{p}_1 + \mathbf{p}_2 + \mathbf{p}_3)^2 \\ &(2\Theta(w_1 - w_2)\Theta(w_2 - w_3) - \Theta(w_2 - w_1)\Theta(w_2 - w_3))\end{aligned} \tag{D.10c}$$

$$\begin{aligned}\tilde{a}^{(3)} =& 2\left(-\frac{2\pi^{\frac{d}{2}}}{\Gamma\left(\frac{d-2}{2}\right)}\right)^3 \int_0^1 \mathrm{d}w_1 \mathrm{d}w_2 \mathrm{d}w_3 \int \frac{\mathrm{d}^d p_1}{(2\pi)^d} \frac{\mathrm{d}^d p_2}{(2\pi)^d} \frac{\mathrm{d}^d p_3}{(2\pi)^d} \\ & \frac{e^{i\mathbf{p}_1\cdot\hat{\mathbf{b}}} + \Theta_{\mathrm{bal}} e^{-i\mathbf{p}_1\cdot\hat{\mathbf{b}}}}{\mathbf{p}_1^2} \frac{e^{i\mathbf{p}_2\cdot\hat{\mathbf{b}}} + \Theta_{\mathrm{bal}} e^{-i\mathbf{p}_2\cdot\hat{\mathbf{b}}}}{\mathbf{p}_2^2} \frac{e^{i\mathbf{p}_3\cdot\hat{\mathbf{b}}} + \Theta_{\mathrm{bal}} e^{-i\mathbf{p}_3\cdot\hat{\mathbf{b}}}}{\mathbf{p}_3^2} \left(w_1\mathbf{p}_1 + w_2\mathbf{p}_2 + w_3\mathbf{p}_3\right)^2 \\ & \left(2\Theta(w_1 - w_2)\Theta(w_2 - w_3) - \Theta(w_2 - w_1)\Theta(w_2 - w_3)\right)\end{aligned} \tag{D.10d}$$

Bibliography

[1] C. Y. R. Chen, C. de Rham, A. Margalit and A. J. Tolley, *A cautionary case of casual causality*, *JHEP* **03** (2022) 025, [2112.05031].

[2] C. Y. R. Chen, C. de Rham, A. Margalit and A. J. Tolley, *Surfin' pp-waves with Good Vibrations: Causality in the presence of stacked shockwaves*, 2309.04534.

[3] A. Margalit, C. R. Contaldi and M. Pieroni, *Phase decoherence of gravitational wave backgrounds*, *Phys. Rev. D* **102** (2020) 083506, [2004.01727].

[4] A. Einstein, *The Foundations of the General Theory of Relativity*, *Annalen der Physik* **49** (1916) 769–822.

[5] LIGO Scientific Collaboration and Virgo Collaboration collaboration, B. P. Abbott, R. Abbott, T. D. Abbott, M. R. Abernathy, F. Acernese, K. Ackley et al., *Observation of Gravitational Waves from a Binary Black Hole Merger*, *Phys. Rev. Lett.* **116** (Feb, 2016) 061102, [1602.03837].

[6] J. F. Donoghue, *General relativity as an effective field theory: The leading quantum corrections*, *Phys. Rev. D* **50** (1994) 3874–3888, [gr-qc/9405057].

[7] J. F. Donoghue, *Introduction to the Effective Field Theory Description of Gravity*, in *Advanced School on Effective Theories*, 6, 1995. gr-qc/9512024.

[8] C. P. Burgess, *Quantum Gravity in Everyday Life: General Relativity as an Effective Field Theory*, *Living Rev. Rel.* **7** (2004) 5–56, [gr-qc/0311082].

[9] J. F. Donoghue, *The effective field theory treatment of quantum gravity*, *AIP Conf. Proc.* **1483** (2012) 73–94, [1209.3511].

[10] S. Weinberg, *Phenomenological Lagrangians*, *Physica A* **96** (1979) 327–340.

[11] W. Buchmuller and D. Wyler, *Effective Lagrangian Analysis of New Interactions and Flavor Conservation*, *Nucl. Phys. B* **268** (1986) 621–653.

[12] C. N. Leung, S. T. Love and S. Rao, *Low-Energy Manifestations of a New Interaction Scale: Operator Analysis*, *Z. Phys. C* **31** (1986) 433.

[13] A. Adams, N. Arkani-Hamed, S. Dubovsky, A. Nicolis and R. Rattazzi, *Causality, analyticity and an IR obstruction to UV completion*, *JHEP* **10** (2006) 014, [hep-th/0602178].

[14] S. A. Melville, *Constraining low energy effective field theories via high energy axioms*. PhD thesis, Imperial Coll., London, 2019. 10.25560/78765.

[15] C. de Rham, S. Kundu, M. Reece, A. J. Tolley and S.-Y. Zhou, *Snowmass White Paper: UV Constraints on IR Physics*, in *Snowmass 2021*, 3, 2022. 2203.06805.

[16] T. N. Pham and T. N. Truong, *Evaluation of the Derivative Quartic Terms of the Meson Chiral Lagrangian From Forward Dispersion Relation*, *Phys. Rev. D* **31** (1985) 3027.

[17] B. Ananthanarayan, D. Toublan and G. Wanders, *Consistency of the chiral pion pion scattering amplitudes with axiomatic constraints*, *Phys. Rev. D* **51** (1995) 1093–1100, [hep-ph/9410302].

[18] L. Vecchi, *Causal versus analytic constraints on anomalous quartic gauge couplings*, *JHEP* **11** (2007) 054, [0704.1900].

[19] A. Nicolis, R. Rattazzi and E. Trincherini, *Energy's and amplitudes' positivity*, *JHEP* **05** (2010) 095, [0912.4258].

[20] B. Bellazzini, C. Cheung and G. N. Remmen, *Quantum Gravity Constraints from Unitarity and Analyticity*, *Phys. Rev. D* **93** (2016) 064076, [1509.00851].

[21] B. Bellazzini, *Softness and amplitudes' positivity for spinning particles*, *JHEP* **02** (2017) 034, [1605.06111].

[22] C. de Rham, S. Melville, A. J. Tolley and S.-Y. Zhou, *Positivity bounds for scalar field theories*, *Phys. Rev. D* **96** (2017) 081702, [1702.06134].

[23] C. de Rham, S. Melville, A. J. Tolley and S.-Y. Zhou, *UV complete me: Positivity Bounds for Particles with Spin*, *JHEP* **03** (2018) 011, [1706.02712].

[24] B. Bellazzini, J. Elias Miró, R. Rattazzi, M. Riembau and F. Riva, *Positive moments for scattering amplitudes*, *Phys. Rev. D* **104** (2021) 036006, [2011.00037].

[25] A. J. Tolley, Z.-Y. Wang and S.-Y. Zhou, *New positivity bounds from full crossing symmetry*, *JHEP* **05** (2021) 255, [2011.02400].

[26] S. Caron-Huot and V. Van Duong, *Extremal Effective Field Theories*, *JHEP* **05** (2021) 280, [2011.02957].

[27] N. Arkani-Hamed, T.-C. Huang and Y.-t. Huang, *The EFT-Hedron*, *JHEP* **05** (2021) 259, [2012.15849].

[28] A. Sinha and A. Zahed, *Crossing Symmetric Dispersion Relations in Quantum Field Theories*, *Phys. Rev. Lett.* **126** (2021) 181601, [2012.04877].

[29] Z.-Z. Du, C. Zhang and S.-Y. Zhou, *Triple crossing positivity bounds for multi-field theories*, *JHEP* **12** (2021) 115, [2111.01169].

[30] G. N. Remmen and N. L. Rodd, *Consistency of the Standard Model Effective Field Theory*, *JHEP* **12** (2019) 032, [1908.09845].

[31] X. O. Camanho, J. D. Edelstein, J. Maldacena and A. Zhiboedov, *Causality Constraints on Corrections to the Graviton Three-Point Coupling*, *JHEP* **02** (2016) 020, [1407.5597].

[32] K. Hinterbichler, A. Joyce and R. A. Rosen, *Massive Spin-2 Scattering and Asymptotic Superluminality*, *JHEP* **03** (2018) 051, [1708.05716].

[33] J. Bonifacio, K. Hinterbichler, A. Joyce and R. A. Rosen, *Massive and Massless Spin-2 Scattering and Asymptotic Superluminality*, *JHEP* **06** (2018) 075, [1712.10020].

[34] K. Hinterbichler, A. Joyce and R. A. Rosen, *Eikonal scattering and asymptotic superluminality of massless higher spin fields*, *Phys. Rev. D* **97** (2018) 125019, [1712.10021].

[35] C. de Rham and A. J. Tolley, *Speed of gravity*, *Phys. Rev. D* **101** (2020) 063518, [1909.00881].

[36] C. de Rham and A. J. Tolley, *Causality in curved spacetimes: The speed of light and gravity*, *Phys. Rev. D* **102** (2020) 084048, [2007.01847].

[37] M. Accettulli Huber, A. Brandhuber, S. De Angelis and G. Travaglini, *Eikonal phase matrix, deflection angle and time delay in effective field theories of gravity*, *Phys. Rev. D* **102** (2020) 046014, [2006.02375].

[38] C. de Rham, A. J. Tolley and J. Zhang, *Causality Constraints on Gravitational Effective Field Theories*, *Phys. Rev. Lett.* **128** (2022) 131102, [2112.05054].

[39] M. Carrillo Gonzalez, C. de Rham, V. Pozsgay and A. J. Tolley, *Causal effective field theories*, *Phys. Rev. D* **106** (2022) 105018, [2207.03491].

[40] N. Brunner, V. Scarani, M. Wegmüller, M. Legré and N. Gisin, *Direct Measurement of Superluminal Group Velocity and Signal Velocity in an Optical Fiber*, *Phys. Rev. Lett.* **93** (Nov, 2004) 203902.

[41] L. Brillouin, *Wave propagation and group velocity*, vol. 8. Academic Press, New York, London, 1960.

[42] P. Milonni, *Fast Light, Slow Light and Left-Handed Light*. Taylor & Francis, Boca Raton, 2004, https://doi.org/10.1201/9780367801557.

[43] I. T. Drummond and S. J. Hathrell, *QED Vacuum Polarization in a Background Gravitational Field and Its Effect on the Velocity of Photons*, *Phys. Rev. D* **22** (1980) 343.

[44] T. J. Hollowood and G. M. Shore, *Causality and Micro-Causality in Curved Spacetime*, *Phys. Lett. B* **655** (2007) 67–74, [0707.2302].

[45] T. J. Hollowood and G. M. Shore, *The Refractive Index of Curved Spacetime: The Fate of Causality in QED*, *Nucl. Phys. B* **795** (2008) 138–171, [0707.2303].

[46] T. J. Hollowood and G. M. Shore, *The Causal Structure of QED in Curved Spacetime: Analyticity and the Refractive Index*, *JHEP* **12** (2008) 091, [0806.1019].

[47] T. J. Hollowood, G. M. Shore and R. J. Stanley, *The Refractive Index of Curved Spacetime II: QED, Penrose Limits and Black Holes*, *JHEP* **08** (2009) 089, [0905.0771].

[48] T. J. Hollowood and G. M. Shore, *The Effect of Gravitational Tidal Forces on Vacuum Polarization: How to Undress a Photon*, *Phys. Lett. B* **691** (2010) 279–284, [1006.0145].

[49] T. J. Hollowood and G. M. Shore, *'Superluminal' Photon Propagation in QED in Curved Spacetime is Dispersive and Causal*, 1006.1238.

[50] T. J. Hollowood and G. M. Shore, *The Effect of Gravitational Tidal Forces on Renormalized Quantum Fields*, *JHEP* **02** (2012) 120, [1111.3174].

[51] T. J. Hollowood and G. M. Shore, *The Unbearable Beingness of Light, Dressing and Undressing Photons in Black Hole Spacetimes*, *Int. J. Mod. Phys. D* **21** (2012) 1241003, [1205.3291].

[52] T. J. Hollowood and G. M. Shore, *Causality Violation, Gravitational Shockwaves and UV Completion*, *JHEP* **03** (2016) 129, [1512.04952].

[53] J. Ghiglieri, G. Jackson, M. Laine and Y. Zhu, *Gravitational wave background from Standard Model physics: Complete leading order*, *JHEP* **07** (2020) 092, [2004.11392].

[54] NANOGrav collaboration, G. Agazie et al., *The NANOGrav 15-year Data Set: Evidence for a Gravitational-Wave Background*, 2306.16213.

[55] NANOGrav collaboration, A. Afzal et al., *The NANOGrav 15-year Data Set: Search for Signals from New Physics*, 2306.16219.

[56] C. Caprini et al., *Detecting gravitational waves from cosmological phase transitions with LISA: an update*, *JCAP* **03** (2020) 024, [1910.13125].

[57] C. de Rham and S. Melville, *Gravitational Rainbows: LIGO and Dark Energy at its Cutoff*, *Phys. Rev. Lett.* **121** (2018) 221101, [1806.09417].

[58] R. E. Langer, *On the Connection Formulas and the Solutions of the Wave Equation*, *Phys. Rev.* **51** (Apr, 1937) 669–676.

[59] L. Eisenbud, *The formal properties of nuclear collisions*. PhD thesis, Princeton U., 1948.

[60] E. P. Wigner, *Lower Limit for the Energy Derivative of the Scattering Phase Shift*, *Phys. Rev.* **98** (1955) 145–147.

[61] F. T. Smith, *Lifetime Matrix in Collision Theory*, *Phys. Rev.* **118** (1960) 349–356.

[62] P. A. Martin, *On the Time Delay of Simple Scattering Systems*, *Commun. Math. Phys.* **47** (1976) 221–227.

[63] A. Nicolis, R. Rattazzi and E. Trincherini, *The Galileon as a local modification of gravity*, *Phys. Rev. D* **79** (2009) 064036, [0811.2197].

[64] C. de Rham, M. Fasiello and A. J. Tolley, *Galileon Duality*, *Phys. Lett. B* **733** (2014) 46–51, [1308.2702].

[65] C. de Rham and G. Gabadadze, *Generalization of the Fierz-Pauli Action*, *Phys. Rev. D* **82** (2010) 044020, [1007.0443].

[66] C. de Rham, G. Gabadadze and A. J. Tolley, *Resummation of Massive Gravity*, *Phys. Rev. Lett.* **106** (2011) 231101, [1011.1232].

[67] C. de Rham, *Massive Gravity*, *Living Rev. Rel.* **17** (2014) 7, [1401.4173].

[68] G. L. Goon, K. Hinterbichler and M. Trodden, *Stability and superluminality of spherical DBI galileon solutions*, *Phys. Rev. D* **83** (2011) 085015, [1008.4580].

[69] P. de Fromont, C. de Rham, L. Heisenberg and A. Matas, *Superluminality in the Bi- and Multi- Galileon*, *JHEP* **07** (2013) 067, [1303.0274].

[70] C. de Rham, S. Melville, A. J. Tolley and S.-Y. Zhou, *Massive Galileon Positivity Bounds*, *JHEP* **09** (2017) 072, [1702.08577].

[71] C. M. Will, *The Confrontation between General Relativity and Experiment*, *Living Rev. Rel.* **17** (2014) 4, [1403.7377].

[72] I. G. Avramidi, *Covariant methods for the calculation of the effective action in quantum field theory and investigation of higher derivative quantum gravity.* PhD thesis, Moscow State University, 1986. hep-th/9510140.

[73] I. G. Avramidi, *The Covariant Technique for Calculation of One Loop Effective Action*, *Nucl. Phys. B* **355** (1991) 712–754.

[74] C. de Rham, J. Francfort and J. Zhang, *Black Hole Gravitational Waves in the Effective Field Theory of Gravity*, *Phys. Rev. D* **102** (2020) 024079, [2005.13923].

[75] R. Penrose, *Any Space-Time has a Plane Wave as a Limit*, in *Differential Geometry and Relativity*, pp. 271–275. Springer, Dordrecht, 1976. DOI.

[76] J. T. Wheeler, *Symmetric Solutions to the Gauss–Bonnet Extended Einstein Equations*, *Nucl. Phys. B* **268** (1986) 737–746.

[77] G. Dotti and R. J. Gleiser, *Linear stability of Einstein-Gauss-Bonnet static spacetimes. Part I: Tensor perturbations*, *Phys. Rev. D* **72** (2005) 044018, [gr-qc/0503117].

[78] R. J. Gleiser and G. Dotti, *Linear stability of Einstein-Gauss-Bonnet static spacetimes. Part II: Vector and scalar perturbations*, *Phys. Rev. D* **72** (2005) 124002, [gr-qc/0510069].

[79] B. Whitt, *Spherically symmetric solutions of general second-order gravity*, *Phys. Rev. D* **38** (Nov, 1988) 3000–3007.

[80] T. Takahashi and J. Soda, *Stability of Lovelock Black Holes under Tensor Perturbations*, *Phys. Rev. D* **79** (2009) 104025, [0902.2921].

[81] T. Takahashi and J. Soda, *Instability of Small Lovelock Black Holes in Even-dimensions*, *Phys. Rev. D* **80** (2009) 104021, [0907.0556].

[82] T. Takahashi and J. Soda, *Master Equations for Gravitational Perturbations of Static Lovelock Black Holes in Higher Dimensions*, *Prog. Theor. Phys.* **124** (2010) 911–924, [1008.1385].

[83] P. C. Aichelburg and R. U. Sexl, *On the gravitational field of a massless particle*, *General Relativity and Gravitation* **2** (1971) 303–312.

[84] T. Regge and J. A. Wheeler, *Stability of a Schwarzschild singularity*, *Phys. Rev.* **108** (1957) 1063–1069.

[85] F. J. Zerilli, *Gravitational field of a particle falling in a Schwarzschild geometry analyzed in tensor harmonics*, *Phys. Rev. D* **2** (1970) 2141–2160.

[86] H. Kodama, A. Ishibashi and O. Seto, *Brane world cosmology: Gauge invariant formalism for perturbation*, *Phys. Rev. D* **62** (2000) 064022, [hep-th/0004160].

[87] H. Kodama and A. Ishibashi, *A master equation for gravitational perturbations of maximally symmetric black holes in higher dimensions*, *Prog. Theor. Phys.* **110** (2003) 701–722, [hep-th/0305147].

[88] A. Ishibashi and H. Kodama, *Stability of higher dimensional Schwarzschild black holes*, *Prog. Theor. Phys.* **110** (2003) 901–919, [hep-th/0305185].

[89] A. Higuchi, *Symmetric Tensor Spherical Harmonics on the N Sphere and Their Application to the De Sitter Group SO(N,1)*, *J. Math. Phys.* **28** (1987) 1553.

[90] D. Brecher, J. P. Gregory and P. M. Saffin, *String theory and the classical stability of plane waves*, *Phys. Rev. D* **67** (2003) 045014, [hep-th/0210308].

[91] C. Burrage, C. de Rham, L. Heisenberg and A. J. Tolley, *Chronology Protection in Galileon Models and Massive Gravity*, *JCAP* **07** (2012) 004, [1111.5549].

[92] G. Papallo and H. S. Reall, *Graviton time delay and a speed limit for small black holes in Einstein–Gauss–Bonnet theory*, *JHEP* **11** (2015) 109, [1508.05303].

[93] H. Reall, N. Tanahashi and B. Way, *Causality and Hyperbolicity of Lovelock Theories*, *Class. Quant. Grav.* **31** (2014) 205005, [1406.3379].

[94] K. Benakli, S. Chapman, L. Darmé and Y. Oz, *Superluminal graviton propagation*, *Phys. Rev. D* **94** (2016) 084026, [1512.07245].

[95] T. Andrade, E. Caceres and C. Keeler, *Boundary causality versus hyperbolicity for spherical black holes in Gauss–Bonnet gravity*, *Class. Quant. Grav.* **34** (2017) 135003, [1610.06078].

[96] R. Brustein and Y. Sherf, *Causality Violations in Lovelock Theories*, *Phys. Rev. D* **97** (2018) 084019, [1711.05140].

[97] Y. Sherf, *Hyperbolicity Constraints in Extended Gravity Theories*, *Phys. Scripta* **94** (2019) 085005, [1806.09984].

[98] E. Cáceres, A. S. Misobuchi and J. F. Pedraza, *Constraining higher order gravities with subregion duality*, *JHEP* **11** (2019) 175, [1907.08021].

[99] S. Gao and R. M. Wald, *Theorems on gravitational time delay and related issues*, *Class. Quant. Grav.* **17** (2000) 4999–5008, [gr-qc/0007021].

[100] L. Alberte, C. de Rham, S. Jaitly and A. J. Tolley, *QED positivity bounds*, *Phys. Rev. D* **103** (2021) 125020, [2012.05798].

[101] L. Alberte, C. de Rham, S. Jaitly and A. J. Tolley, *Positivity Bounds and the Massless Spin-2 Pole*, *Phys. Rev. D* **102** (2020) 125023, [2007.12667].

[102] S. Caron-Huot, D. Mazac, L. Rastelli and D. Simmons-Duffin, *Sharp boundaries for the swampland*, *JHEP* **07** (2021) 110, [2102.08951].

[103] L. Alberte, C. de Rham, S. Jaitly and A. J. Tolley, *Reverse Bootstrapping: IR Lessons for UV Physics*, *Phys. Rev. Lett.* **128** (2022) 051602, [2111.09226].

[104] LIGO Scientific collaboration, J. Aasi et al., *Advanced LIGO*, *Class. Quant. Grav.* **32** (2015) 074001, [1411.4547].

[105] VIRGO collaboration, F. Acernese et al., *Advanced Virgo: a second-generation interferometric gravitational wave detector*, *Class. Quant. Grav.* **32** (2015) 024001, [1408.3978].

[106] KAGRA collaboration, K. Somiya, *Detector configuration of KAGRA: The Japanese cryogenic gravitational-wave detector*, *Class. Quant. Grav.* **29** (2012) 124007, [1111.7185].

[107] A. I. Renzini, B. Goncharov, A. C. Jenkins and P. M. Meyers, *Stochastic Gravitational-Wave Backgrounds: Current Detection Efforts and Future Prospects*, *Galaxies* **10** (2022) 34, [2202.00178].

[108] N. Christensen, *Stochastic Gravitational Wave Backgrounds*, *Rept. Prog. Phys.* **82** (2019) 016903, [1811.08797].

[109] A. Buonanno and B. S. Sathyaprakash, *Sources of Gravitational Waves: Theory and Observations*, 1410.7832.

[110] T. Regimbau, *The astrophysical gravitational wave stochastic background*, *Res. Astron. Astrophys.* **11** (2011) 369–390, [1101.2762].

[111] X.-J. Zhu, E. Howell, T. Regimbau, D. Blair and Z.-H. Zhu, *Stochastic Gravitational Wave Background from Coalescing Binary Black Holes*, *Astrophys. J.* **739** (2011) 86, [1104.3565].

[112] P. A. Rosado, *Gravitational wave background from binary systems*, *Phys. Rev. D* **84** (2011) 084004, [1106.5795].

[113] S. Marassi, R. Schneider, G. Corvino, V. Ferrari and S. Portegies Zwart, *Imprint of the merger and ring-down on the gravitational wave background from black hole binaries coalescence*, *Phys. Rev. D* **84** (2011) 124037, [1111.6125].

[114] B. Allen, *The stochastic gravity wave background: sources and detection*, in *Les Houches School of Physics: Astrophysical Sources of Gravitational Radiation*, pp. 373–417, 4, 1996. gr-qc/9604033.

[115] A. C. Jenkins, R. O'Shaughnessy, M. Sakellariadou and D. Wysocki, *Anisotropies in the astrophysical gravitational-wave background: The impact of black hole distributions*, *Phys. Rev. Lett.* **122** (2019) 111101, [1810.13435].

[116] A. C. Jenkins, M. Sakellariadou, T. Regimbau and E. Slezak, *Anisotropies in the astrophysical gravitational-wave background: Predictions for the detection of compact binaries by LIGO and Virgo*, *Phys. Rev. D* **98** (2018) 063501, [1806.01718].

[117] N. J. Cornish, *Mapping the gravitational wave background*, *Class. Quant. Grav.* **18** (2001) 4277–4292, [astro-ph/0105374].

[118] A. I. Renzini and C. R. Contaldi, *Mapping Incoherent Gravitational Wave Backgrounds*, *Mon. Not. Roy. Astron. Soc.* **481** (2018) 4650–4661, [1806.11360].

[119] L. Xiao, A. I. Renzini and A. J. Weinstein, *Model-independent search for anisotropies in stochastic gravitational-wave backgrounds and application to LIGO–Virgo's first three observing runs*, 2211.10010.

[120] P. Binetruy, A. Bohe, C. Caprini and J.-F. Dufaux, *Cosmological Backgrounds of Gravitational Waves and eLISA/NGO: Phase Transitions, Cosmic Strings and Other Sources*, *JCAP* **06** (2012) 027, [1201.0983].

[121] C. Caprini and D. G. Figueroa, *Cosmological Backgrounds of Gravitational Waves*, *Class. Quant. Grav.* **35** (2018) 163001, [1801.04268].

[122] G. Cusin, C. Pitrou and J.-P. Uzan, *The signal of the gravitational wave background and the angular correlation of its energy density*, *Phys. Rev. D* **97** (2018) 123527, [1711.11345].

[123] C. Conneely, A. H. Jaffe and C. M. F. Mingarelli, *On the Amplitude and Stokes Parameters of a Stochastic Gravitational-Wave Background*, *Mon. Not. Roy. Astron. Soc.* **487** (2019) 562–579, [1808.05920].

[124] L. P. Grishchuk and M. V. Sazhin, *Excitation and detection of standing gravitational waves*, *Zhurnal Eksperimentalnoi i Teoreticheskoi Fiziki* **68** (5, 1975) 1569–1582.

[125] C. R. Contaldi and J. Magueijo, *Unsqueezing of standing waves due to inflationary domain structure*, *Phys. Rev. D* **98** (2018) 043523, [1803.03649].

[126] K. Danzmann, T. A. Prince, P. Binetruy, P. Bender, S. Buchman, J. Centrella et al., *LISA: Unveiling a Hidden Universe*, *Tech. Rep.* **2011** (2011) 1–141.

[127] P. Amaro-Seoane, S. Aoudia, S. Babak, P. Binétruy, E. Berti, A. Bohé et al., *eLISA: Astrophysics and cosmology in the milliHertz regime*, 1201.3621.

[128] M. Armano, H. Audley, G. Auger, J. T. Baird, M. Bassan, P. Binetruy et al., *Sub-Femto-g Free Fall for Space-Based Gravitational Wave Observatories: LISA Pathfinder Results*, *Phys. Rev. Lett.* **116** (jun, 2016) 231101.

[129] N. J. Cornish and R. van Haasteren, *Mapping the nano-Hertz gravitational wave sky*, 1406.4511.

[130] J. Gair, J. D. Romano, S. Taylor and C. M. F. Mingarelli, *Mapping gravitational-wave backgrounds using methods from CMB analysis: Application to pulsar timing arrays*, *Phys. Rev. D* **90** (2014) 082001, [1406.4664].

[131] J. D. Romano, S. R. Taylor, N. J. Cornish, J. Gair, C. M. F. Mingarelli and R. van Haasteren, *Phase-coherent mapping of gravitational-wave backgrounds using ground-based laser interferometers*, *Phys. Rev. D* **92** (2015) 042003, [1505.07179].

[132] S. W. Ballmer, *A radiometer for stochastic gravitational waves*, *Class. Quant. Grav.* **23** (2006) S179–S186, [gr-qc/0510096].

[133] R. K. Sachs and A. M. Wolfe, *Perturbations of a Cosmological Model and Angular Variations of the Microwave Background*, *Astrophys. J.* **147** (Jan., 1967) 73.

[134] M. J. Rees and D. W. Sciama, *Large-scale Density Inhomogeneities in the Universe*, *Nature* **217** (1968) 511–516.

[135] A. I. Renzini and C. R. Contaldi, *Gravitational Wave Background Sky Maps from Advanced LIGO O1 Data*, *Phys. Rev. Lett.* **122** (2019) 081102, [1811.12922].

[136] N. Bartolo, V. De Luca, G. Franciolini, A. Lewis, M. Peloso and A. Riotto, *Primordial Black Hole Dark Matter: LISA Serendipity*, *Phys. Rev. Lett.* **122** (2019) 211301, [1810.12218].

[137] N. Bartolo, V. Domcke, D. G. Figueroa, J. García-Bellido, M. Peloso, M. Pieroni et al., *Probing non-Gaussian Stochastic Gravitational Wave Backgrounds with LISA*, *JCAP* **11** (2018) 034, [1806.02819].

[138] M. Tsuneto, A. Ito, T. Noumi and J. Soda, *Searching for Bispectrum of Stochastic Gravitational Waves with Pulsar Timing Arrays*, *JCAP* **03** (2019) 032, [1812.10615].

[139] C. Powell and G. Tasinato, *Probing a stationary non-Gaussian background of stochastic gravitational waves with pulsar timing arrays*, *JCAP* **01** (2020) 017, [1910.04758].

[140] N. Bartolo, D. Bertacca, S. Matarrese, M. Peloso, A. Ricciardone, A. Riotto et al., *Anisotropies and non-Gaussianity of the Cosmological Gravitational Wave Background*, *Phys. Rev. D* **100** (2019) 121501, [1908.00527].

[141] N. Bartolo, D. Bertacca, S. Matarrese, M. Peloso, A. Ricciardone, A. Riotto et al., *Characterizing the cosmological gravitational wave background: Anisotropies and non-Gaussianity*, *Phys. Rev. D* **102** (2020) 023527, [1912.09433].

[142] N. Bartolo, D. Bertacca, V. De Luca, G. Franciolini, S. Matarrese, M. Peloso et al., *Gravitational wave anisotropies from primordial black holes*, *JCAP* **02** (2020) 028, [1909.12619].

[143] P. Laguna, S. L. Larson, D. Spergel and N. Yunes, *Integrated Sachs-Wolfe Effect for Gravitational Radiation*, *Astrophys. J. Lett.* **715** (2010) L12, [0905.1908].

[144] C. R. Contaldi, *Anisotropies of Gravitational Wave Backgrounds: A Line Of Sight Approach*, *Phys. Lett. B* **771** (2017) 9–12, [1609.08168].

[145] G. Cusin, C. Pitrou and J.-P. Uzan, *Anisotropy of the astrophysical gravitational wave background: Analytic expression of the angular power spectrum and correlation with cosmological observations*, *Phys. Rev. D* **96** (2017) 103019, [1704.06184].

[146] R. A. Isaacson, *Gravitational Radiation in the Limit of High Frequency. I. The Linear Approximation and Geometrical Optics*, *Phys. Rev.* **166** (1968) 1263–1271.

[147] R. A. Isaacson, *Gravitational Radiation in the Limit of High Frequency. II. Nonlinear Terms and the Effective Stress Tensor*, *Phys. Rev.* **166** (1968) 1272–1279.

[148] Planck collaboration, Y. Akrami et al., *Planck 2018 results. VII. Isotropy and Statistics of the CMB*, *Astron. Astrophys.* **641** (2020) A7, [1906.02552].

[149] S. Dodelson, *Modern Cosmology*. Academic Press, Amsterdam, 2003.

[150] A. Lewis, A. Challinor and A. Lasenby, *Efficient computation of CMB anisotropies in closed FRW models*, *Astrophys. J.* **538** (2000) 473–476, [astro-ph/9911177].

[151] NANOGrav collaboration, J. M. Cordes and M. A. McLaughlin, *Gravitational Waves, Extreme Astrophysics, and Fundamental Physics with Precision Pulsar Timing*, 1903.08653.

[152] W. Hu and A. Cooray, *Gravitational time delay effects on cosmic microwave background anisotropies*, *Phys. Rev. D* **63** (2001) 023504, [astro-ph/0008001].

[153] A. Stebbins, *Weak lensing on the celestial sphere*, astro-ph/9609149.

[154] C. M. Bender and S. A. Orszag, *Advanced Mathematical Methods for Scientists and Engineers I*. Springer New York, New York, 1999.

[155] J. T. Wheeler, *Symmetric Solutions to the Maximally Gauss–Bonnet Extended Einstein Equations*, *Nucl. Phys. B* **273** (1986) 732–748.

[156] T. Nutma, *xTras : A field-theory inspired xAct package for Mathematica*, *Comput. Phys. Commun.* **185** (2014) 1719–1738, [1308.3493].

[157] J. M. Martín-García et al., *xAct: Efficient tensor computer algebra for Mathematica*, *http://xact.es/*, *Accessed: 22/02/2023* (2002) .

[158] J. M. Lee, *Ricci.m*, *https://sites.math.washington.edu/~lee/Ricci/*, *Accessed: 22/02/2023* .